Author: Waaijer, Mariëtte
Title: The skin as a mirror of the aging process
Issue Date: 2016-10-12

The skin as a mirror of the aging process

Mariëtte Waaijer

ISBN: 978-94-6233-382-6.

Financial support for the publication of this thesis by Unilever PLC, Alrijne Zorggroep and the Nederlandse Vereniging voor Gerontologie (Dutch Society for Gerontology) is gratefully acknowledged.

Printed by Gildeprint
Cover: Narcissus by Caravaggio (ca 1597–1599). The painting can be found in Galleria Nazionale d'Arte Antica, Palazzo Barberini, Rome, Italy.

The skin as a mirror of the aging process

Proefschrift

ter verkrijging van
de graad van Doctor aan de Universiteit Leiden,
op gezag van Rector Magnificus prof.mr. C.J.J.M. Stolker,
volgens besluit van het College voor Promoties
te verdedigen op woensdag 12 oktober 2016
klokke 13.45 uur

door

Mariëtte Eveline Corinne Waaijer
geboren te Delft
in 1988

Promotiecommissie

Promotores:	Prof. dr. R.G.J. Westendorp Prof. dr. A.B. Maier (*University of Melbourne. VU, Amsterdam*)
Overige leden:	Prof. dr. H.J. Tanke Prof. dr. D.I. Boomsma (*VU, Amsterdam*) Dr. M. Demaria (*UMCG, Groningen*)

CONTENTS

General introduction and outline of the thesis

General introduction

The skin is a most crucial organ, but often under-valued in its importance for human health. It is the main organ through which we interact with the outside world, functioning as a sensor of external stimuli and as a barrier to protect our internal milieu from damaging external exposures. Its appearance is not only of cosmetic interest, but reflects the internal physiological state of the body. The skin is connected to the entire body, and many biological processes in the skin span across the body, such as vitamin D metabolism [1], immune responses [2] and thermoregulation [3]. Hence, the process of skin aging is likely to also reflect aging processes occurring in other tissues and is therefore a good model in which we can study the aging process and its impact on human health.

The degree skin has aged is reflected by an individual's perceived age in facial images[4], i.e. how old an individual looks irrespective of their actual calendar age. This measure of facial aging has been strongly linked to systemic aging: already in younger subjects perceived age has been linked to a sharper decline in a composite of biomarkers reflecting aging of several organ systems [11]. In middle-aged to elderly individuals a higher perceived age is associated with indicators of poorer health such as high glucose levels, high blood pressure and carotid atherosclerosis [5-7]. In the elderly a higher perceived age has also been linked to lower survival [8;9]. Other phenotypes indicative of poorer health such as lower cognitive performance and low handgrip strength are also associated with a higher perceived age in elderly persons [9;10].

The appearance of skin is closely related its structural properties- i.e. its histologic and morphological characteristics. The most exterior layer of the skin, the epidermis typically shows atrophy with advanced age. The interface of the epidermis with the layer underneath, the dermis, also flattens with age [12-15]. The dermis itself consists of various cell types, collagen, elastic fibers and extracellular matrix proteins, plus various appendages such as vasculature, glands and hair follicles. At a higher age collagen is less synthesized by fibroblasts, and collagen networks are disorganised and thickened compared to at younger ages [16]. Elastic fibres are found in higher amounts in aged skin and have a larger and less structured appearance [16-18]. These features are found at sun-protected sites but are also evoked to a greater extent by external stressors such as UV damage and smoking [19;20].

Another age related phenomenon that occurs in the skin is cellular senescence – i.e. stable cell cycle arrest. This phenomenon was first described by Hayflick and Moorhead in the form of so-called replicative senescence, observing the limited replicative capacity of cultured fibroblasts. They theorized that this in vitro phenomenon could occur in vivo as well and contributes to the aging process [21;22]. Cellular senescence can be triggered by insults such as genomic damage, oncogenic signals and telomere attrition [23;24]. Next to the occurrence of cellular senescence in vitro, an increasing number of studies report a higher prevalence of senescence in aged tissues of several mammals [25-30]. In human skin higher amounts of senescence-associated markers have been found in older persons compared to young [31-33]. In addition to this presumed age-dependency of cellular senescence, links with age-related disease have been described. For example, senescent cells have been linked to glomerular disease, lung emphysema, Alzheimer's disease and diabetic nephropathy [30;34-36].

Detrimental effects of cellular senescence could be the result of loss of tissue homeostasis with reduced numbers of cells with replicative potential, but could also be the result of factors secreted by senescent cells, i.e. the senescence-associated secretory phenotype (SASP). Amongst these SASP factors are cytokines, proteases and growth factors [37], and there is some evidence that in vitro the SASP adds to inflammation [23] and can have tumorigenic properties in neighbouring cells [38;39]. These clues that cellular senescence might be implicated in the aging process have led to studies investigating its use of as a potential marker for the aging process and its potential for slowing the aging process [40-45].

In this thesis we focus on the skin as a model to study aging, using several methodologies: the appearance of facial skin, histological and morphological characteristics, the presence of cellular senescence in skin biopsies and characteristics of cultured skin fibroblasts. All these skin phenotypes were measured in middle-aged to old participants of the Leiden Longevity Study. The Leiden Longevity Study aimed to determine factors contributing to familial longevity [46]. Families were defined as long-lived if at least two siblings were alive and aged 89 (male) or 91 (female) or older. From these families their middle-aged to old (63 years on average) offspring were asked to participate, as it was hypothesized that a familial propensity for longevity would be (partially) conveyed to these offspring. Their partners were included as age and environmentally matched controls. The offspring of these nonagenarian sibling indeed appear to age at a slower pace when compared to their partners, as indicated by a lower standardized mortality rate [46], a lower prevalence of cardiovascular and metabolic diseases [47], enhanced insulin sensitivity [48] and better cognitive performance [49]. In addition, fibroblasts derived from skin biopsies of these offspring display less cellular senescence upon stress in vitro compared to their partners [50].

From both the offspring and their partners we obtained their perceived ages from facial photographs, and skin biopsies were obtained from the sun-protected upper inner arm to assess histologic morphological characteristics and cellular senescence. The cultured fibroblasts from these biopsies were assessed for different senescence-associated features in vitro. In order to study larger age differences we also made use of fibroblasts strains obtained from 90 year old participants from the Leiden 85-plus Study, a prospective population-based study [51], and young controls (22 years on average) [52].

Aim of the thesis

We aim to study the manner and extent to which the skin reflects the aging process. We will study the appearance of facial skin, histologic morphological characteristics, cellular senescence in skin biopsies and in cultured skin fibroblasts, and their respective associations with age, membership of a long-lived family and health status.

Outline of the thesis

In **Part I** we question whether skin fibroblasts in vitro mirror the aging process. We study the association between several senescence-associated features in cultured fibroblasts (microRNA-663 expression, DNA damage markers) with (1) the age of the donor from who the cultured fibroblasts were derived, (2) membership of a long-lived family (propensity for longevity) and (3) health status (presence of cardiovascular or metabolic diseases). We further study whether different senescence markers are associated in vitro, and whether these markers are associated intra-individually with the senescence-associated protein p16INK4a in situ. **Part II** focusses on phenotypes of the skin biopsies from the Leiden Longevity Study participants, to study whether skin tissue mirrors the aging process. Differences in the exterior appearance of the skin, histologic morphological characteristics and amount of cellular senescence in situ were studied dependent on age, membership of a long-lived family and health status. In addition the interrelations between these skin phenotypes were studied. In **Part III** we aim to further place the phenomenon of cellular senescence in context, firstly recapitulating published work on cellular senescence dependent on age in various human tissues in a systematic review. Secondly we compared its value as potential marker of the aging process to currently used measures of functional capacity.

References

(1) Holick MF. Vitamin D deficiency. *N Engl J Med* 2007;357:266-281.
(2) Di MP, Perera GK, Nestle FO. The multitasking organ: recent insights into skin immune function. *Immunity* 2011;35:857-869.
(3) Charkoudian N. Skin blood flow in adult human thermoregulation: how it works, when it does not, and why. *Mayo Clin Proc* 2003;78:603-612.
(4) Gunn DA, Rexbye H, Griffiths CE et al. Why some women look young for their age. *PLoS One* 2009;4:e8021.
(5) Noordam R, Gunn DA, Tomlin CC et al. High serum glucose levels are associated with a higher perceived age. *Age (Dordr)* 2013;35:189-195.
(6) Gunn DA, de Craen AJ, Dick JL et al. Facial appearance reflects human familial longevity and cardiovascular disease risk in healthy individuals. *J Gerontol A Biol Sci Med Sci* 2013;68:145-152.
(7) Kido M, Kohara K, Miyawaki S, Tabara Y, Igase M, Miki T. Perceived age of facial features is a significant diagnosis criterion for age-related carotid atherosclerosis in Japanese subjects: J-SHIPP study. *Geriatr Gerontol Int* 2012;12:733-740.
(8) Dykiert D, Bates TC, Gow AJ, Penke L, Starr JM, Deary IJ. Predicting mortality from human faces. *Psychosom Med* 2012;74:560-566.
(9) Christensen K, Thinggaard M, McGue M et al. Perceived age as clinically useful biomarker of ageing: cohort study. *BMJ* 2009;339:b5262.
(10) Gunn DA, Larsen LA, Lall JS, Rexbye H, Christensen K. Mortality is Written on the Face. *J Gerontol A Biol Sci Med Sci* 2016;71:72-77.
(11) Belsky DW, Caspi A, Houts R et al. Quantification of biological aging in young adults. *Proc Natl Acad Sci U S A* 2015;112:E4104-E4110.
(12) Fenske NA, Conard CB. Aging skin. *Am Fam Physician* 1988;37:219-230.
(13) Fenske NA, Lober CW. Structural and functional changes of normal aging skin. *J Am Acad Dermatol* 1986;15:571-585.
(14) Kurban RS, Bhawan J. Histologic changes in skin associated with aging. *J Dermatol Surg Oncol* 1990;16:908-914.
(15) Lavker RM, Zheng PS, Dong G. Morphology of aged skin. *Dermatol Clin* 1986;4:379-389.
(16) Baumann L. Skin ageing and its treatment. *J Pathol* 2007;211:241-251.
(17) Robert C, Lesty C, Robert AM. Ageing of the skin: study of elastic fiber network modifications by computerized image analysis. *Gerontology* 1988;34:291-296.
(18) Frances C, Branchet MC, Boisnic S, Lesty CL, Robert L. Elastic fibers in normal human skin. Variations with age: a morphometric analysis. *Arch Gerontol Geriatr* 1990;10:57-67.
(19) Warren R, Gartstein V, Kligman AM, Montagna W, Allendorf RA, Ridder GM. Age, sunlight, and facial skin: a histologic and quantitative study. *J Am Acad Dermatol* 1991;25:751-760.
(20) Just M, Ribera M, Monso E, Lorenzo JC, Ferrandiz C. Effect of smoking on skin elastic fibres: morphometric and immunohistochemical analysis. *Br J Dermatol* 2007;156:85-91.
(21) Hayflick L, Moorhead PS. The serial cultivation of human diploid cell strains. *Exp Cell Res* 1961;25:585-621.
(22) Hayflick L. The limited in vitro lifetime of human diploid cell strains. *Exp Cell Res* 1965;37:614-636.
(23) Campisi J. Aging, cellular senescence, and cancer. *Annu Rev Physiol* 2013;75:685-705.
(24) Campisi J, d'Adda di FF. Cellular senescence: when bad things happen to good cells. *Nat Rev Mol Cell Biol* 2007;8:729-740.
(25) Krishnamurthy J, Torrice C, Ramsey MR et al. Ink4a/Arf expression is a biomarker of aging. *J Clin Invest* 2004;114:1299-1307.
(26) Herbig U, Ferreira M, Condel L, Carey D, Sedivy JM. Cellular senescence in aging primates. *Science* 2006;311:1257.
(27) Jeyapalan JC, Ferreira M, Sedivy JM, Herbig U. Accumulation of senescent cells in mitotic tissue of aging primates. *Mech Ageing Dev* 2007;128:36-44.
(28) Melk A, Schmidt BM, Takeuchi O, Sawitzki B, Rayner DC, Halloran PF. Expression of p16INK4a and other cell cycle regulator and senescence associated genes in aging human kidney. *Kidney Int* 2004;65:510-520.
(29) Liu Y, Sanoff HK, Cho H et al. Expression of p16(INK4a) in peripheral blood T-cells

is a biomarker of human aging. *Aging Cell* 2009;8:439-448.
(30) Bhat R, Crowe EP, Bitto A et al. Astrocyte senescence as a component of Alzheimer's disease. *PLoS One* 2012;7:e45069.
(31) Dimri GP, Lee X, Basile G et al. A biomarker that identifies senescent human cells in culture and in aging skin in vivo. *Proc Natl Acad Sci U S A* 1995;92:9363-9367.
(32) Ressler S, Bartkova J, Niederegger H et al. p16INK4A is a robust in vivo biomarker of cellular aging in human skin. *Aging Cell* 2006;5:379-389.
(33) Kalfalah F, Seggewiss S, Walter R et al. Structural chromosome abnormalities, increased DNA strand breaks and DNA strand break repair deficiency in dermal fibroblasts from old female human donors. *Aging (Albany NY)* 2015;7:110-122.
(34) Sis B, Tasanarong A, Khoshjou F, Dadras F, Solez K, Halloran PF. Accelerated expression of senescence associated cell cycle inhibitor p16INK4A in kidneys with glomerular disease. *Kidney Int* 2007;71:218-226.
(35) Tsuji T, Aoshiba K, Nagai A. Alveolar cell senescence in patients with pulmonary emphysema. *Am J Respir Crit Care Med* 2006;174:886-893.
(36) Verzola D, Gandolfo MT, Gaetani G et al. Accelerated senescence in the kidneys of patients with type 2 diabetic nephropathy. *Am J Physiol Renal Physiol* 2008;295:F1563-F1573.
(37) Coppe JP, Patil CK, Rodier F et al. Senescence-associated secretory phenotypes reveal cell-nonautonomous functions of oncogenic RAS and the p53 tumor suppressor. *PLoS Biol* 2008;6:2853-2868.
(38) Laberge RM, Awad P, Campisi J, Desprez PY. Epithelial-mesenchymal transition induced by senescent fibroblasts. *Cancer Microenviron* 2012;5:39-44.
(39) Parrinello S, Coppe JP, Krtolica A, Campisi J. Stromal-epithelial interactions in aging and cancer: senescent fibroblasts alter epithelial cell differentiation. *J Cell Sci* 2005;118:485-496.
(40) Gingell-Littlejohn M, McGuinness D, McGlynn LM et al. Pre-transplant CDKN2A expression in kidney biopsies predicts renal function and is a future component of donor scoring criteria. *PLoS One* 2013;8:e68133.
(41) Koppelstaetter C, Schratzberger G, Perco P et al. Markers of cellular senescence in zero hour biopsies predict outcome in renal transplantation. *Aging Cell* 2008;7:491-497.
(42) Pustavoitau A, Barodka V, Sharpless NE et al. Role of senescence marker p16INK4a measured in peripheral blood T-lymphocytes in predicting length of hospital stay after coronary artery bypass surgery in older adults. *Experimental Gerontology*. In press.
(43) Baker DJ, Wijshake T, Tchkonia T et al. Clearance of p16Ink4a-positive senescent cells delays ageing-associated disorders. *Nature* 2011;479:232-236.
(44) Zhu Y, Tchkonia T, Pirtskhalava T et al. The Achilles' heel of senescent cells: from transcriptome to senolytic drugs. *Aging Cell* 2015;14:644-658.
(45) Baker DJ, Childs BG, Durik M et al. Naturally occurring p16-positive cells shorten healthy lifespan. *Nature* 2016.
(46) Schoenmaker M, de Craen AJ, de Meijer PH et al. Evidence of genetic enrichment for exceptional survival using a family approach: the Leiden Longevity Study. *Eur J Hum Genet* 2006;14:79-84.
(47) Westendorp RG, van Heemst D, Rozing MP et al. Nonagenarian siblings and their offspring display lower risk of mortality and morbidity than sporadic nonagenarians: The Leiden Longevity Study. *J Am Geriatr Soc* 2009;57:1634-1637.
(48) Wijsman CA, Rozing MP, Streefland TC et al. Familial longevity is marked by enhanced insulin sensitivity. *Aging Cell* 2011;10:114-121.
(49) Stijntjes M, de Craen AJ, van HD et al. Familial longevity is marked by better cognitive performance at middle age: the Leiden Longevity Study. *PLoS One* 2013;8:e57962.
(50) Dekker P, Maier AB, van HD et al. Stress-induced responses of human skin fibroblasts in vitro reflect human longevity. *Aging Cell* 2009;8:595-603.
(51) Bootsma-van der Wiel A, Gussekloo J, de Craen AJ, Van EE, Bloem BR, Westendorp RG. Common chronic diseases and general impairments as determinants of walking disability in the oldest-old population. *J Am Geriatr Soc* 2002;50:1405-1410.
(52) Maier AB, le CS, de Koning-Treurniet C, Blom J, Westendorp RG, van HD. Persistence of high-replicative capacity in cultured fibroblasts from nonagenarians. *Aging Cell* 2007;6:27-33.

Part I

Part I

Do skin fibroblasts in vitro mirror the aging process?

Chapter 1

Chapter 1

MicroRNA-663 induction upon oxidative stress in cultured human fibroblasts depends on the chronological age of the donor

M.E.C. Waaijer*, M.Wieser*, R. Grillari-Voglauer, D. van Heemst, J. Grillari**, A.B. Maier**

* Both authors contributed equally

Biogerontology. 2014 Jun;15(3):269-78

Abstract

MicroRNAs, regulators of messenger RNA translation, have been observed to influence many physiological processes, amongst them the process of aging. Higher levels of microRNA-663 (miR-663) have previously been observed in human dermal fibroblasts subject to both replicative and stress-induced senescence compared to early passage cells. Also, higher levels of miR-663 have been found in memory T-cells and in human fibroblasts derived from older donors compared to younger donors. In previous studies we observed that dermal fibroblasts from donors of different chronological and biological age respond differentially to oxidative stress measured by markers of cellular senescence and apoptosis. In the present study we set out to study the association between miR-663 levels and chronological and biological age. Therefore we tested in a total of 92 human dermal fibroblast strains whether the levels of miR-663 in non-stressed and stressed conditions (fibroblasts were treated with 0.6μM rotenone in stressed conditions) were different in young, middle aged and old donors and whether they were different in middle aged donors dependent on their biological age, as indicated by the propensity for familial longevity. In non-stressed conditions the level of miR-663 did not differ between donors of different age categories and was not dependent on biological age. Levels of miR-663 did not differ dependent on biological age in stressed conditions either. However, for different age categories the level of miR-663 in stressed conditions did differ: the level of miR-663 was higher at higher age categories. Also, the ratio of miR-663 induction upon stress was significantly higher in donors from older age categories. In conclusion, we present evidence for an association of miR-663 upon stress and chronological age.

Introduction

Although widely studied, molecular mechanisms contributing to the process of aging in humans have not yet been fully uncovered. Interestingly, some individuals appear to age slower and healthier than others. This slower rate of aging was previously studied in a unique cohort of Caucasian offspring of long lived families. These offspring were observed to have a lower mortality rate, beneficial glucose and lipid metabolism and preservation of insulin sensitivity when compared with their partners as age and environmentally matched controls [1-3]. Furthermore, the *in vitro* stress response of dermal fibroblasts of these offspring was observed to mimic that of chronologically younger donors (i.e. fewer senescent cells) while the stress response of partners mimicked that of chronologically older donors (i.e. more senescent cells) [4]. These in vitro results are in line with recent findings showing that a higher number of p16INK4a positive cells in human skin is associated with higher biological age ex situ [5]. The importance of senescence in the aging process was previously observed *in vivo* as well, as clearance of p16INK4a positive cells was shown to delay age-related pathologies in mice [6].

MicroRNAs (miRNAs), a class of non-coding RNAs, are important regulators of messenger RNA translation [7]. Thereby, single miRNAs can regulate up to hundreds of mRNA targets and are therefore considered to act similar to transcription factors, modulating multiple physiological processes, amongst others the aging process [8;9]. The level of microRNA-663 (miR-663) was previously found to be higher in replicative senescence [10-12] and in stress-induced senescence [11] in human fibroblasts *in vitro,* as well as in memory T-cells [12]. Furthermore, a higher level of miR-663 in human foreskin fibroblasts from elderly versus young healthy donors was observed [12].

In the present study we investigated the level of miR-663 in human dermal fibroblasts in both non-stressed and stressed conditions, as well as the ratio thereof. We tested if these levels differ between donors of different chronological age categories and between middle aged subjects of a different biological age, namely offspring of nonagenarian siblings (with a propensity for familial longevity) and their middle aged partners.

Methods

Study design

The current study included three age categories consisting of young (n=8), middle aged (N=76) and old donors (N=8) derived from the Leiden 85-plus Study or the Leiden Longevity Study (LLS).

The Leiden 85-plus Study is a prospective population-based study in which all inhabitants aged 85 years of the city of Leiden (The Netherlands) were invited to take part [13]. A biobank was established from fibroblasts cultivated from skin biopsies from 68 of the 275 surviving 90-year-old participants [14] from December 2003 to May 2004. A biobank of fibroblasts from biopsies of 27 young donors (18-25 years) was established from August to November 2006.

In the LLS genetic factors contributing to familial longevity are studied. Middle aged Caucasian offspring from nonagenarian siblings (not related to the subjects of the Leiden 85-plus Study) were included together with their partners as age and environmentally matched controls. There were no selection criteria on health or demographic characteristics. From November 2006 to May 2008, a biobank was established from fibroblasts cultivated from skin biopsies from 150 offspring-partner couples.

The Medical Ethical Committee of the Leiden University Medical Center approved both studies and written informed consent was obtained from all participants.

Characteristics of the donors

Demographic characteristics were available for each donor. Information on medical history was obtained from the participants' treating physicians. Total number of cardiovascular diseases included cases of cerebrovascular accident, myocardial infarction, hypertension and diabetes mellitus.

Culture conditions and experimental set-up

Fibroblast strains were isolated from three (Leiden 85-plus Study) and four (LLS) mm biopsies of the sun unexposed medial side of the upper arm and cultured under predefined, highly standardized conditions as published earlier [14]. Fibroblasts were grown in D-MEM:F-12 (1:1) medium supplemented with 10% fetal calf serum (Bodinco, Alkmaar, the Netherlands, batch no. 162229), 1 mM MEM sodium pyruvate, 10 mM HEPES, 2 mM glutamax I, and antibiotics (100 Units/mL penicillin, 100 μg/mL streptomycin, and 0.25–2.5 μg/mL amphotericin B), all obtained from Gibco, Breda, the Netherlands unless stated otherwise. Fibroblasts were incubated at 37°C with 5% CO_2 and 100% humidity. Trypsin (Sigma, St Louis, MO, USA) was used to split fibroblasts using a 1:4 ratio each time they reached 80-100% confluence. Further experimental procedures have been published earlier as well [15]. In short, on day 0, passage 11 fibroblasts were thawed from frozen stocks and on days 4, 7 and 11, fibroblasts were further passaged in order to multiply fibroblasts. The experiments were started on day 18. Fibroblast strains were seeded at 2300 and 3900 cells/cm^2 for non-stressed and rotenone-stressed cultures respectively. Fibroblast strains were seeded in batches of eight strains per condition. To stress fibroblast strains, medium was supplemented with 0.6 μM rotenone (Sigma, St Louis, MO, USA), known to induce an increase in the intracellular production of ROS at the mitochondrial level [16]. This particular concentration of rotenone was observed to give an stress-induced increase of SAβ-gal and the low percentage of apoptosis, as shown in previously published work [15]. After 72 hours fibroblasts were frozen in pellets from 92 randomly chosen donors (8 young and 8 old donors from the Leiden 85-plus Study and 38 offspring of the LLS together with 38 partners thereof) for RNA extraction.

RNA extraction

Total RNA was extracted by classical phenol–chloroform extraction [17]. In brief, cells were homogenized in 0.5 mL Tri-Reagent by vortexing for 15 seconds, incubated at room temperature for 5 minutes and vortexed again for 15 seconds. 100 μl chloroform (Emsure, Merck KGsA, 64271 Darmstadt, Germany) was added to the samples, which were then vortexed for 15 seconds and incubated at room temperature for 3 minutes. The samples were then centrifuged at 12000xg for 15 minutes at 4°C. After centrifugation the upper aqueous phase was transferred to a RNase-free tube. 1 μl of glycogen (Ambion, 5 mg/ml) and 250 μl of 100% isopropanol were added to this aqueous phase, followed by vortexing and 10 minutes incubation at room temperature. Afterwards the samples were centrifuged at 12000xg for 10 minutes at 4°C. The supernatant was discarded and the RNA pellets were washed with 500 μl 75% ethanol. The samples were centrifuged at 7600xg for 5 minutes at 4°C. After discarding the ethanol the RNA pellets were air-dried for 10 minutes. The RNA was resuspended in 15 μl RNase-free water and dissolved by incubation for 10 minutes at 57°C. To improve the purity of the RNA and decrease possible residing phenol the samples were precipitated again by adding 1.5 μl of natrium acetate (3 M, pH 5.2), 1 μl of glycogen (Ambion, 5 mg/ml) and 18 μl of 100% isopropanol and incubated at -20°C overnight. The samples were then centrifuged at 9300xg for 15 minutes at 4°C and the supernatant removed. The pellets were washed with 500 μl 75% cold ethanol and centrifuged at 7600xg for 5 minutes at 4°C. The ethanol was discarded and the pellets were air-dried for 10 minutes. The pellets were then resuspended with 15 μl RNase-free water and incubated for 10 minutes at 57°C. The RNA concentration was quantified by using NanoDrop (ThermoScientific, Wilmington, USA).

qPCR

cDNA was synthesized from 100 ng of total RNA using the NCode™ VILO™ miRNA cDNA Synthesis Kit (Life technologies, Carlsbad, CA 92008, USA) and was diluted 1:5 with RNAse-free water. qPCR was performed using Sensimix SYBR® Hi-Rox Mastermix

(Bioline) and the Universal qPCR Primer (10 µM) of the NCode™ VILO™miRNA cDNA Synthesis Kit according to the manufacturer's instructions. Forward primers (1 pmol/µl) used were 5'-AGGCGGGGCGCCGCGGGAC for hsa-miR-663 and 5'-CAGGGTCGGGCCTGGTTAGTA for 5S rRNA (serving as a reference gene). The qPCR reactions were performed on a Rotor-Gene Q (Qiagen) thermocycler.

Statistics

Levels of miR-663 in fibroblasts in both non-stressed and stressed conditions were measured by qPCR and normalized to 5S rRNA, which has been used in various studies as a housekeeping gene in various settings and across various species [18-20], by subtracting the mean miR-663 cycling threshold (Ct) of 4 replicates with the mean 5S Ct of 4 replicates. These ΔCt's are hereafter named miR-663 levels in non-stressed and stressed conditions. To calculate the ratio of miR-663 induction upon stress the ΔΔCt method was used. With this ratio the miR-663 level in stressed conditions was related to the miR-663 level in non-stressed conditions. Data are expressed as log2 fold change for this ratio of miR-663 induction upon stress. Donors with a log2 fold change value being 3 standard deviations below or above the mean were excluded in all analyses (N=2, middle aged donors).

Table 1. Characteristics of the donors

	Leiden 85-plus Study		Leiden Longevity Study	
	Young (N=8)	Old (N=8)	Offspring (N=38)	Partners (N=38)
Demographic data				
Female, no.(%)	6 (75.0)	5 (62.5)	19 (50.0)	19 (50.0)
Age, years, mean (SD)	22.3 (1.0)	90.2 (0.5)	63.5 (7.1)	63.4 (7.7)
Anthropometric data, mean (SD)				
Body mass index, kg/m^2	22.5 (2.0)	25.5 (3.7)	26.8 (4.7)[a]	25.8 (3.4)[b]
Co-morbidities, no. (%)				
Myocardial infarction	0 (0.0)	2 (25.0)	0 (0.0)[c]	0 (0.0)[a]
Cerebrovascular accident	0 (0.0)	1 (12.5)	1 (2.8)[a]	2 (5.6)[a]
Hypertension	0 (0.0)	3 (37.5)	9 (25.0)[a]	8 (22.2)[a]
Diabetes mellitus	0 (0.0)	2 (25.0)	2 (5.7)[c]	5 (14.3)[c]
Malignancies	0 (0.0)	1 (12.5)	1 (2.9)[b]	2 (5.9)[d]
Chronic obstructive pulmonary disease	0 (0.0)	1 (12.5)	1 (2.8)[a]	2 (5.7)[c]
Rheumatoid arthritis	0 (0.0)	3 (37.5)	0 (0.0)[a]	0 (0.0)[a]
Intoxications, no. (%)				
Smoking, current	0 (0.0)	1 (12.5)	6 (16.7)[a]	4 (11.1)[a]

SD: standard deviation, no.: number
a: N=36, b:N=37, c: N=35, d: N=34

Differences in levels of miR-663 in non-stressed and stressed conditions and the ratio thereof between young and old donors, and offspring and partners were analyzed with the use of linear mixed models. A linear mixed model differs from a standard regression model in the ability to take intra-individual repeated measurements into account. Further adjustments included potential random batch effects, gender, chronological age (the last in offspring and partner comparison only) and the number of cardiovascular diseases. Since hypertension was previously linked to miR-663 expression [21], the association between miR-663 and chronological age categories was studied as well separately for donors with and donors without cardiovascular diseases. All analyses were performed using SPSS editor software.

Table 2. Levels of microRNA-663 and ratio of induction upon stress dependent on chronological age categories

	Young (N=8)	Middle-aged (N=74)	Old (N=8)	P for trend
Levels of miR-663				
ΔCt non-stressed				
Model 1, estimated mean (SE)	-9.77 (0.35)	-9.65 (0.23)	-9.75 (0.35)	0.95
Model 2, estimated mean (SE)	-9.76 (0.37)	-9.69 (0.23)	-9.83 (0.36)	0.87
ΔCt stressed				
Model 1, estimated mean (SE)	-9.56 (0.35)	-9.53 (0.22)	-8.82 (0.35)	0.04
Model 2, estimated mean (SE)	-9.65 (0.36)	-9.56 (0.22)	-8.78 (0.36)	0.02
Ratio of induction upon stress				
log2 fold change stressed to non-stressed				
Model 1, estimated mean (SE)	0.06 (0.30)	0.27 (0.10)	0.76 (0.30)	0.09
Model 2, estimated mean (SE)	-0.03 (0.30)	0.27 (0.09)	0.92 (0.30)	0.04

SE: standard error, ΔCt: delta cycle threshold. Calculations were made with the ΔΔCt method, in which Ct values of microRNA-663 were normalised to those of a housekeeper gene. Higher ΔCt values indicate higher microRNA-663 expression. The log2 fold change was calculated as miR-663 expression levels in stressed to those in non-stressed conditions. Number of cardiovascular diseases include cerebrovascular accident, myocardial infarction, hypertension and diabetes mellitus. Donors with a datapoint 3 standard deviations below or above the mean were excluded from this analysis. The young donors are aged 21 to 24 years (mean 22 years), the middle-aged donors 44 to 73 years (mean 64 years) and the old donors 90 to 91 years (mean 90 years).
Model 1: adjusted for batch and repeated measurements
Model 2: adjusted for batch, repeated measurements, gender and number of cardiovascular diseases

Results

The present study included human dermal fibroblast strains from 92 donors, consisting of 8 young donors (mean age 22.3 years), 76 middle-aged donors (mean age 63.5 years) of whom

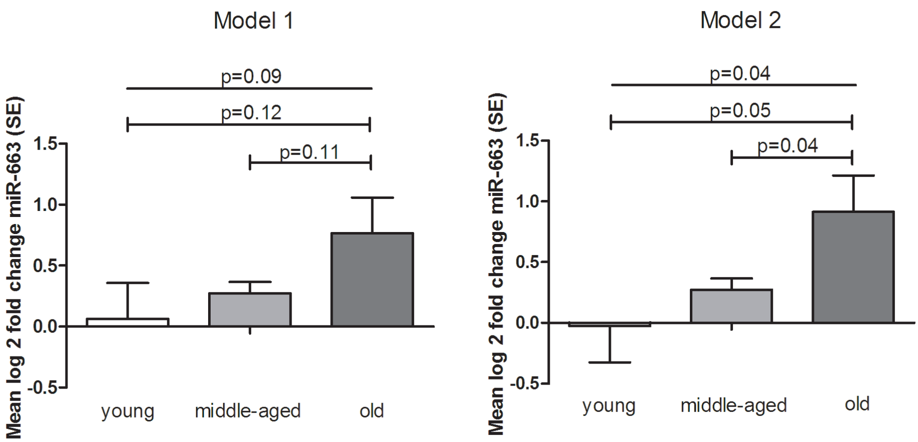

Figure 1. Ratio of microRNA-663 induction upon stress dependent on chronological age categories
SE: standard error, miR-663: microRNA-663. The log2 fold change was calculated with ΔΔCt method as miR-663 expression levels in stressed to those in non-stressed conditions. Number of cardiovascular diseases include cerebrovascular accident, myocardial infarction, hypertension and diabetes mellitus. The middle-aged group consists of both offspring and partners. Donors with a datapoint 3 standard deviations below or above the mean were excluded from this analysis. The young donors are aged 21 to 24 years (mean 22 years), the middle-aged donors 44 to 73 years (mean 64 years) and the old donors 90 to 91 years (mean 90 years).
Model 1: adjusted for batch and repeated measurements
Model 2: adjusted for batch, repeated measurements, gender and number of cardiovascular diseases

38 offspring and 38 partners (mean ages 63.5 and 63.4 years, respectively) and 8 old donors (mean age 90.2 years). The characteristics of donors are summarized in Table 1.

Table 2 shows the levels of miR-663 dependent on chronological age categories. The mean level of miR-663 normalized to 5S RNA in non-stressed conditions did not differ between the three chronological age categories, also after adjustment for gender and cardiovascular diseases. The mean level of miR-663 in stressed conditions was dependent on chronological age categories, showing significantly higher mean levels at higher ages. After adjustment for gender and cardiovascular diseases this association remained statistically significant.
The ratio of miR-663 induction upon stress, expressed as the ratio between miR-663 levels in stressed and non-stressed conditions from each individual, was also higher in higher chronological age categories. This association was significant after adjustment for gender and cardiovascular diseases. The ratio of miR-663 induction upon stress dependent on chronological age categories is visualized in Figure 1.
To disentangle the potential influence of cardiovascular disease on the association between miR-663 induction upon stress and chronological age categories we repeated the analysis

Table 3. Ratio of microRNA-663 induction upon stress dependent on chronological age categories, stratified on cardiovascular diseases

	Young	Middle-aged	Old	P-value
Subjects without CVD, N=57				
ΔCt non-stressed, estimated mean (SE)	-9.86 (0.37)	-9.83 (0.22)	-10.44 (0.58)	0.50
ΔCt stressed, estimated mean (SE)	-9.65 (0.38)	-9.46 (0.23)	-9.01 (0.61)	0.31
Log2 fold change stressed to non-stressed, estimated mean (SE)	0.06 (0.31)	0.39 (0.12)	1.50 (0.58)	0.05
Subjects with one or more CVD, N=26				
ΔCt non-stressed, estimated mean (SE)	n/a	-9.71 (0.29)	-9.60 (0.43)	0.80
ΔCt stressed, estimated mean (SE)	n/a	-9.79 (0.26)	-8.81 (0.41)	0.02
Log2 fold change stressed to non-stressed, estimated mean (SE)	n/a	0.01 (0.17)	0.43 (0.34)	0.27

SE: standard error, CVD: cardiovascular diseases, ΔCt: delta cycle threshold. Calculations were made with the ΔΔCt method, in which Ct values of microRNA-663 were normalised to those of a housekeeper gene. Higher ΔCt values indicate higher microRNA-663 expression. The log2 fold change was calculated as miR-663 expression levels in stressed to those in non-stressed conditions. Number of cardiovascular diseases includes cerebrovascular accident, myocardial infarction, hypertension and diabetes mellitus. Only 5 donors had more than one cardiovascular disease. Donors with a datapoint 3 standard deviations below or above the mean were excluded from this analysis. Adjusted for batch effects, repeated measurements and gender. The young donors are aged 21 to 24 years (mean 22 years), the middle-aged donors 44 to 73 years (mean 64 years) and the old donors 90 to 91 years (mean 90 years).

Table 4. Levels of microRNA-663 and ratio of induction upon stress in offspring of nonagenarian siblings and their partners

	Offspring (N=37)	Partners (N=37)	P-value
Levels of miR-663			
ΔCt non-stressed			
Model 1, estimated mean (SE)	-9.69 (0.24)	-9.65 (0.24)	0.82
Model 2, estimated mean (SE)	-9.73 (0.25)	-9.70 (0.25)	0.87
ΔCt stressed			
Model 1, estimated mean (SE)	-9.59 (0.23)	-9.53 (0.23)	0.70
Model 2, estimated mean (SE)	-9.61 (0.23)	-9.57 (0.24)	0.81
Ratio of induction upon stress			
Log2 fold change stressed to non-stressed			
Model 1, estimated mean (SE)	0.24 (0.13)	0.31 (0.13)	0.70
Model 2, estimated mean (SE)	0.24 (0.14)	0.32 (0.14)	0.67

SE: standard error, ΔCt: delta cycle threshold. Calculations were made with the ΔΔCt method, in which Ct values of microRNA-663 were normalised to those of a housekeeper gene. Higher ΔCt values indicate higher microRNA-663 expression. The log2 fold change was calculated as miR-663 expression levels in stressed to those in non-stressed conditions. Number of cardiovascular diseases include cerebrovascular accident, myocardial infarction, hypertension and diabetes mellitus. Donors with a datapoint 3 standard deviations below or above the mean were excluded from this analysis.
Model 1: adjusted for batch and repeated measurements
Model 2: adjusted for batch, repeated measurements, gender, chronological age and number of cardiovascular diseases

in donors with and in donors without cardiovascular diseases. This stratification on cardiovascular disease did not materially alter the results, however, significance decreased due to the lower sample size (Table 3).

Next we questioned whether the levels of miR-663 in stressed and non-stressed conditions and the ratio of stress induction differed in middle aged offspring from nonagenarian siblings compared to their partners of the same chronological age. As shown in table 4, the offspring and partners did not differ in their mean miR-663 level either in stressed or non-stressed conditions or in their ratio of miR-663 induction upon stress. Adjustment for possible confounders did not change these results.

Discussion

While no differences depending on chronological age categories in non-stressed conditions were observed, mean miR-663 levels in stressed conditions were dependent on chronological age categories, being higher at higher age. Furthermore, the ratio of miR-663 induction upon stress was significantly associated with chronological age categories. No association of miR-663 and biological age was found when comparing middle aged offspring of nonagenarian siblings with their partners.

Single miRNA's can potentially downregulate several mRNA targets, and so far few targets of miR-663 have been validated: renin and ApoE [21], p21 [22], JunB and JunD [23] and TGFβ1 [24]. The exact mechanism by which miR-663 could act in (cellular) aging therefore remains to be elucidated. Previously higher levels of miR-663 in both replicative and stress-induced senescence *in vitro* were observed [10;11]. Furthermore, higher levels of miR-663 were seen in fibroblasts and memory T-cells that were derived from older donors compared to younger donors [12]. We did not find differences in levels of miR-663 dependent on chronological age categories in non-stressed conditions, which could possibly be explained by different age ranges of donors (especially the inclusion of adolescents in comparison to children). Our group has previously shown that fibroblasts from donors of different age have different stress-induced increases in markers of senescence and apoptosis [4]. In line with these findings we showed that fibroblasts from donors of different age categories respond differently in their miR-663 level upon cellular stress *in vitro*.

Stress-induced differences in senescence and apoptosis were also observed in middle aged offspring of nonagenarian siblings and their partners of different biological age [4]. To our knowledge we are the first reporting on levels of miR-663 and miR-663 stress induction dependent on the propensity for familial longevity, and show that both levels of miR-663 and its stress induction are not dependent on this propensity. Another factor that reflects biological age is the presence of age-related pathologies. A possible relation between cardiovascular diseases and miR-663 has been reported in few studies. One study showed that miR-663 levels are lower in kidney tissue form hypertensive donors than in tissue of normotensive donors [21]. MiR-663 has furthermore been (indirectly) related to the process of atherosclerosis [25;26]. Stratification on donors with and without cardiovascular diseases however did not alter our results.

Recently miR-663 was shown to be involved in the induction of ATF4 and the downregulation of VEGF in HUVECs by several unfolded protein response inducers and oxidized lipids, providing a possible mechanism in atherosclerosis [26]. Also another factor in development of atherosclerosis, oscillatory shear stress, was associated with an upregulation of miR-663 in HUVECs [25]. In another study miR-663 levels in tumor tissue were found to be increased with longer ischemia time and evidence was found that miR-663 affected stress response through FOSB [27]. Following TDP-43 depletion an upregulated miR-663 expression and a decrease of epoxide hydrolase, an antagonist of oxidative stress and a possible target of miR-663, were observed too [28]. Levels of miR-663 were observed to be higher in denatured dermis in deep burn wounds compared to normal dermis [29]. In a study on the effect of 4-hydroxynonenal, a lipid peroxidation product affecting cell growth and differentiation, on microRNA expression a significant upregulation of miR-663 was observed [30]. All these examples would support the idea that miR-663 is induced upon various stressors. Considering the involvement of miR-663 in replicative and stress-induced senescence and its relation with various physiological stressors, we hypothesize that miR-663 influences cell cycle arrest after encountering cellular stress, however this hypothesis remains speculative in nature. Indeed, miR-663 was observed to act as a tumor suppressor by decreasing the proliferation of human gastric cancer cells both *in vitro* as *in vivo* [31]. Also, the antioxidant resveratrol with possible antitumorigenic properties was found to impair the oncogenic miR-155 through upregulation of miR-663 [23]. However, in contrast to our hypothesis oncogenic properties of miR-663 in nasopharyngeal cancer cell lines have been described as well [22]. In this study, miR-663 was shown to target p21 and herewith induce cell cycle progression.

One of the strengths of this study is the large number of human donors that were included. These donors are part of an extensively phenotyped cohort, fibroblasts from their skin biopsies were grown under highly standardized conditions. A limitation of the study is the cross-sectional design, which does not allow for the observation of a causal relation. Furthermore we only measured miR-663 and none of its potential targets. Therefore, we cannot elucidate whether higher stress-induced levels of miR-663 are a mere stress response, a by-product of stress-induced senescence, or plays a part in one of the senescence pathways. Also, while treatment of fibroblasts with rotenone increases ROS levels, SAβgal and decreases growth rate [32], it was shown that the stress-induced senescence by rotenone is not conditionally dependent on the generation of ROS [33]. Therefore, the observed differences could be particular to rotenone as a stressor, and not necessarily dependent on increased ROS (in contrast to other stressors such as hydrogen peroxide). We tested our hypothesis in a model of human dermal fibroblasts, it could be that miR-663 induction upon stress and its relation with aging is specific for human dermal fibroblasts and is not universally present in other cell types. While we observe that chronological age of donors and in vitro miR-663 induction upon stress are associated, it of course remains an interesting but unresolved questions whether this phenomenon has in vivo consequences.

In conclusion, we have shown the association of miR-663 levels upon stress with chronological age categories in human dermal fibroblasts. Future investigations should focus on the targets of miR-663 and the causality of this association to strengthen these findings.

Acknowledgements

We would like to thank Corine de Koning-Treurniet, Joke Blom and Pim Dekker for their work in the laboratory.
This work was supported by the Austrian Science Fund [P 24498-B20]; Genome Research Austria GEN-AU [Project 820982 „Non-coding RNAs"], grants by the Herzfelder'sche Familienstiftung to RGV and CE.R.I.E.S to JG, SenterNovem, IGE01014 and IGE5007, NGI/NWO; 05040202 and 050-060-810.

References

(1) Schoenmaker M, de Craen AJ, de Meijer PH et al. Evidence of genetic enrichment for exceptional survival using a family approach: the Leiden Longevity Study. *Eur J Hum Genet* 2006;14:79-84.

(2) Westendorp RG, van HD, Rozing MP et al. Nonagenarian siblings and their offspring display lower risk of mortality and morbidity than sporadic nonagenarians: The Leiden Longevity Study. *J Am Geriatr Soc* 2009;57:1634-1637.

(3) Wijsman CA, Rozing MP, Streefland TC et al. Familial longevity is marked by enhanced insulin sensitivity. *Aging Cell* 2011;10:114-121.

(4) Dekker P, Maier AB, van HD et al. Stress-induced responses of human skin fibroblasts in vitro reflect human longevity. *Aging Cell* 2009;8:595-603.

(5) Waaijer ME, Parish WE, Strongitharm BH et al. The number of p16INK4a positive cells in human skin reflects biological age. *Aging Cell* 2012;11:722-725.

(6) Baker DJ, Wijshake T, Tchkonia T et al. Clearance of p16Ink4a-positive senescent cells delays ageing-associated disorders. *Nature* 2011;479:232-236.

(7) Ghildiyal M, Zamore PD. Small silencing RNAs: an expanding universe. *Nat Rev Genet* 2009;10:94-108.

(8) Chen LH, Chiou GY, Chen YW, Li HY, Chiou SH. MicroRNA and aging: a novel modulator in regulating the aging network. *Ageing Res Rev* 2010;9 Suppl 1:S59-S66.

(9) Grillari J, Grillari-Voglauer R. Novel modulators of senescence, aging, and longevity: Small non-coding RNAs enter the stage. *Exp Gerontol* 2010;45:302-311.

(10) Marasa BS, Srikantan S, Martindale JL et al. MicroRNA profiling in human diploid fibroblasts uncovers miR-519 role in replicative senescence. *Aging (Albany NY)* 2010;2:333-343.

(11) Maes OC, Sarojini H, Wang E. Stepwise up-regulation of microRNA expression levels from replicating to reversible and irreversible growth arrest states in WI-38 human fibroblasts. *J Cell Physiol* 2009;221:109-119.

(12) Hackl M, Brunner S, Fortschegger K et al. miR-17, miR-19b, miR-20a, and miR-106a are down-regulated in human aging. *Aging Cell* 2010;9:291-296.

(13) Bootsma-van der Wiel A, Gussekloo J, de Craen AJ, Van EE, Bloem BR, Westendorp RG. Common chronic diseases and general impairments as determinants of walking disability in the oldest-old population. *J Am Geriatr Soc* 2002;50:1405-1410.

(14) Maier AB, le CS, de Koning-Treurniet C, Blom J, Westendorp RG, van HD. Persistence of high-replicative capacity in cultured fibroblasts from nonagenarians. *Aging Cell* 2007;6:27-33.

(15) Dekker P, de Lange MJ, Dirks RW et al. Relation between maximum replicative capacity and oxidative stress-induced responses in human skin fibroblasts in vitro. *J Gerontol A Biol Sci Med Sci* 2011;66:45-50.

(16) Li N, Ragheb K, Lawler G et al. Mitochondrial complex I inhibitor rotenone induces apoptosis through enhancing mitochondrial reactive oxygen species production. *J Biol Chem* 2003;278:8516-8525.

(17) Chomczynski P, Sacchi N. Single-step method of RNA isolation by acid guanidinium thiocyanate-phenol-chloroform extraction. *Anal Biochem* 1987;162:156-159.

(18) Lardizabal MN, Nocito AL, Daniele SM, Ornella LA, Palatnik JF, Veggi LM. Reference genes for real-time PCR quantification of microRNAs and messenger RNAs in rat models of hepatotoxicity. *PLoS One* 2012;7:e36323.

(19) Sharbati-Tehrani S, Kutz-Lohroff B, Bergbauer R, Scholven J, Einspanier R. miR-Q: a novel quantitative RT-PCR approach for the expression profiling of small RNA molecules such as miRNAs in a complex sample. *BMC Mol Biol* 2008;9:34.

(20) Son DJ, Kumar S, Takabe W et al. The atypical mechanosensitive microRNA-712 derived from pre-ribosomal RNA induces endothelial inflammation and atherosclerosis. *Nat Commun* 2013;4:3000.

(21) Marques FZ, Campain AE, Tomaszewski M et al. Gene expression profiling reveals renin mRNA overexpression in human hypertensive kidneys and a role for microRNAs. *Hypertension* 2011;58:1093-1098.

(22) Yi C, Wang Q, Wang L et al. MiR-663, a microRNA targeting p21(WAF1/CIP1), promotes the proliferation and tumorigenesis of nasopharyngeal carcinoma. *Oncogene* 2012.

(23) Tili E, Michaille JJ, Adair B et al. Resveratrol decreases the levels of miR-155 by upregulating miR-663, a microRNA targeting JunB and JunD. *Carcinogenesis* 2010;31:1561-1566.

(24) Liu ZY, Zhang GL, Wang MM, Xiong YN, Cui HQ. MicroRNA-663 targets TGFB1 and regulates lung cancer proliferation. *Asian Pac J Cancer Prev* 2011;12:2819-2823.

(25) Ni CW, Qiu H, Jo H. MicroRNA-663 upregulated by oscillatory shear stress plays a role in inflammatory response of endothelial cells. *Am J Physiol Heart Circ Physiol* 2011;300:H1762-H1769.

(26) Afonyushkin T, Oskolkova OV, Bochkov VN. Permissive role of miR-663 in induction of VEGF and activation of the ATF4 branch of unfolded protein response in endothelial cells by oxidized phospholipids. *Atherosclerosis* 2012.

(27) Borgan E, Navon R, Vollan HK et al. Ischemia caused by time to freezing induces systematic microRNA and mRNA responses in cancer tissue. *Mol Oncol* 2011;5:564-576.

(28) Buratti E, De CL, Stuani C, Romano M, Baralle M, Baralle F. Nuclear factor TDP-43 can affect selected microRNA levels. *FEBS J* 2010;277:2268-2281.

(29) Liang P, Lv C, Jiang B et al. MicroRNA profiling in denatured dermis of deep burn patients. *Burns* 2012;38:534-540.

(30) Pizzimenti S, Ferracin M, Sabbioni S et al. MicroRNA expression changes during human leukemic HL-60 cell differentiation induced by 4-hydroxynonenal, a product of lipid peroxidation. *Free Radic Biol Med* 2009;46:282-288.

(31) Pan J, Hu H, Zhou Z et al. Tumor-suppressive mir-663 gene induces mitotic catastrophe growth arrest in human gastric cancer cells. *Oncol Rep* 2010;24:105-112.

(32) Dekker P, van Baalen LM, Dirks RW et al. Chronic inhibition of the respiratory chain in human fibroblast cultures: differential responses related to subject chronological and biological age. *J Gerontol A Biol Sci Med Sci* 2012;67:456-464.

(33) Goncalves AP, Maximo V, Lima J, Singh KK, Soares P, Videira A. Involvement of p53 in cell death following cell cycle arrest and mitotic catastrophe induced by rotenone. *Biochim Biophys Acta* 2011;1813:492-499.

Chapter 2

DNA damage markers in dermal fibroblasts *in vitro* reflect chronological donor age

M.E.C. Waaijer, E. Croco, R.G.J. Westendorp, P.E. Slagboom, J.M. Sedivy,
A. Lorenzini*, A.B. Maier*
* *These authors contributed equally*

Aging (Albany NY). 2016 Jan;8(1):147-57

Abstract

The aging process is accompanied by an accumulation of cellular damage, which compromises the viability and function of cells and tissues. We aim to further explore the association between *in vitro* DNA damage markers and the chronological age of the donor, as well as long-lived family membership and presence of cardiovascular diseases. Therefore, numbers of 53BP1 foci, telomere-associated foci (TAF) and micronuclei were measured in cultured dermal fibroblasts obtained from three age groups of donors (mean age 22, 63 and 90 years). Fibroblasts were cultured without a stressor and with 0.6 µM rotenone for 3 days. We found that 53BP1 foci and TAF were more frequently present in fibroblasts of old donors compared to middle-aged and young donors. No association between micronuclei and donor age was found. Within the fibroblasts of the middle-aged donors we did not find associations between DNA damage markers and long-lived family membership or cardiovascular disease. Results were comparable when fibroblasts were stressed *in vitro* with rotenone. In conclusion, we found that DNA damage foci of cultured fibroblasts are significantly associated with the chronological age, but not biological age, of the donor.

Introduction

The DNA damage theory of aging is based on the efficacy of maintenance and repair mechanisms to ensure longevity [1;2]. DNA damage which is not repaired can compromise the function and viability of the cell and therefore the integrity of tissues, eventually contributing to aging and a decreased lifespan. Cells with DNA damage foci, marked by DNA damage response (DDR) factors such as DDR mediator protein 53BP1 or phosphorylated H2AX, have been found more frequently in old compared to young animals [3]. Some of these DNA damage foci are localized specifically on telomeric DNA, so-called telomere associated foci (TAF), which have a higher prevalence at higher age in several animal tissues as well [4-7]. Furthermore, a higher number of micronuclei *in vitro*, as a marker of unresolved DNA damage and chromosomal instability, associates with a lower maximum lifespan in various mammal species [8].

Research on DNA damage and human aging is scarce, especially including extreme ages. Lymphocytes derived from older donors showed more DNA damage foci compared to young donors [9]. A similar trend was observed in cultured primary fibroblasts strains derived from donors of different ages, albeit in a very low number of strains (5 donors) [9]. In a recent study, numbers of 53BP1 foci in dermal fibroblasts were also positively associated with the age of the donor [10]. Micronuclei numbers were shown to be higher at higher age in lymphocytes (reviewed in [11] and buccal cells [12]. However, an inverse relation between the number of 53BP1 foci and micronuclei has also been described between mouse and human cells [8].

In the present study we significantly extent the published literature on the relation of DNA damage foci and chronological age in human fibroblasts by a higher number of donors with a broad age range. Furthermore, we study if DNA damage is associated with biological age (membership of long-lived family and presence of cardiovascular and/or metabolic disease).

Methods

Study design

In the prospective population-based Leiden 85-plus Study all inhabitants of Leiden (The Netherlands) aged 85 years were invited to participate [13]. A biobank of fibroblasts from skin biopsies of 68 of the surviving 90 year old donors was established from December 2003 to May 2004, as well as fibroblasts from skin biopsies of 27 young donors (18-25 years) from August to November 2006 [14]. In the Leiden Longevity Study (LLS) factors contributing to familial longevity are studied [15]. Middle-aged offspring of nonagenarian siblings were included in the study, with their age and environmentally matched partners as controls. The offspring of these families were shown to have lower mortality rates and better clinical characteristics such as fewer cases of hypertension and diabetes mellitus [16] compared to their partners. From 150 offspring-partners pairs skin biopsies were obtained and a biobank with their fibroblasts was established from November 2006 to May 2008. Both studies were approved by the Medical Ethical Committee of the Leiden University Medical Center and written informed consent was obtained from all donors.

Characteristics of the donors

For each donor demographic characteristics were available, information on medical history was obtained from the participants' treating physicians and data on smoking habits was obtained through questionnaires. Cardiovascular and/or metabolic diseases were defined as disease history of myocardial infarction, cerebrovascular accident, hypertension and diabetes mellitus.

Culture conditions and experimental set-up

Skin biopsies were taken from the sun-unexposed upper inner arm and fibroblast strains were cultured under predefined, highly standardized conditions as published earlier [14]. Ten strains of young donors and ten strains of old donors were randomly selected out of the Leiden 85-plus Study. Forty strains of middle-aged offspring from long-lived families and 40 strains of their partners were randomly chosen (LLS). The methods of culture conditions and experimental set-up have been described previously [17]. In short, fibroblast strains were thawed at day 0 (fibroblasts from Leiden 85-plus Study at passage 11, fibroblasts from LLS at passage 7) and subsequently passaged 3 more times over 17 days to multiply the number of fibroblasts. At day 18 the fibroblasts were seeded at 4400 cells per chamber in Permanox slides, in batches of eight strains per condition. To stress the fibroblast strains the medium (Dulbecco's Modified Eagle Medium:F-12 (1:1) medium supplemented with 10% fetal calf serum (batch no. 40G4932F), 1 mM MEM sodium pyruvate, 10 mM HEPES, 2 mM glutamax I, antibiotics (100 U/mL penicillin, 100 μg/mL streptomycin, and 0.25–2.5 μg/mL amphotericin B, all obtained from Gibco, Breda, The Netherlands) was supplemented for 72 hours with 0.6 μM rotenone (Sigma, St Louis, MO). Each experiment was performed in duplicate. At day 21 fibroblasts were fixed with 4% paraformaldehyde in ice-cold PBS for 20 minutes and washed 3 times with ice-cold PBS. The samples were subsequently stored at 2-8°C before further analysis.

Detection of DNA damage markers: 53BP1 foci, TAF and micronuclei

Fibroblasts were permeabilized with 0.2% Triton X-100 (Sigma, St Louis, MO, USA) in PBS (PBST-0.2) during a 20 minute incubation. Fibroblasts were further washed for 5 minutes with PBS 3 times and then covered for 1 hour with blocking buffer (4% BSA in PBST-0.1). Next, fibroblasts were incubated with primary Rabbit anti 53BP1 antibodies (Novus Biologicals LLC, Littleton, CO, USA) diluted to a 1:1000 concentration in blocking buffer for 2 hours in humidified chambers at room temperature. Fibroblasts were washed 3 times for 15 minutes with PBST-0.1 before incubation for 1 hour with Alexa 488-conjugated Goat anti-rabbit antibodies (Invitrogen, Breda, The Netherlands) diluted to a 1:1000 concentration in blocking buffer. After 3 times 15 minute washing steps with PBST-0.1, the secondary antibodies were cross-linked to the sample with 20 minute incubation with 4% paraformaldehyde in PBS. Fibroblasts were washed 3 times for 5 minutes with PBS and then dehydrated by covering them with increasingly higher concentrations of ethanol (70%, 80% and 95%) at a 3 minute duration per step and then air-dried. Nuclear DNA was denatured in hybridization buffer containing 0.5 μg /ml (C3TA2)3-Cy3-labeled Peptide Nucleic Acid (PNA) telomeric probe (Panagene Inc, Daejeon, South Korea) at 85° C for 5 minutes. Afterwards fibroblasts were further incubated overnight in the same buffer at room temperature and in the dark. On the following day samples were washed twice with 70 % formamide/0.67 x SSC (0.3 M NaCl, 30 mM Na3citrate x 2H2O, pH=7), followed by a 10 minute wash with 2 x SSC and a 10 minute wash with PBS. The fibroblasts were then incubated for 1 hour with Donkey anti-goat alexa-488 antibodies (Invitrogen, Breda, the Netherlands) diluted to a 1:1000 concentration in blocking buffer. The samples were washed 3 times for 15 minutes with PBST-0.1, rinsed with distilled water. The samples were then mounted with DAPI containing Prolong Gold antifade mounting medium (Invitrogen, Breda, the Netherlands).

Photographs of the samples were taken with a Leica DM5500 B microscope (Leica Microsystems, Rijswijk, the Netherlands). 53BP1 foci and micronuclei per nucleus were counted manually and automatically, which yielded consistent results at low counts, but measurements diverged at higher counts. Overall, manual and automatic counts were significantly correlated, with coefficients >0.5, thus manual counts of 53BP1 foci and micronuclei were chosen for the subsequent analysis.

Per individual donor on average 114 nuclei (rotenone-stressed state) and 124 nuclei (non-stressed state) were scored for 53BP1 foci and micronuclei. Clearly identifiable glaring dots inside the nucleus were manually counted as 53BP1 foci. Micronuclei were scored in nuclei whose surrounding area was entirely visible. We excluded from the count all nuclei lying at the edge of the image, eliminating the risk of underestimating micronuclei. Micronuclei, morphologically identical but smaller than the main nucleus, were scored according to the following characteristics as described previously [18]: 1) the diameter of micronuclei should be 1/16th to 1/3rd of the mean diameter of the main nucleus; 2) micronuclei should not be linked or connected to the main nucleus; 3) micronuclei may touch but not overlap the main nucleus and the micronuclear boundary should be distinguishable from the nuclear boundary.

Table 1. Characteristics of the donors.

	Young	Middle-aged		Old
	(N=10)	Offspring (N=40)	Partners (N=40)	(N=10)
Demographic data				
Female, no.(%)	7 (70.0)	20 (50.0)	20 (50.0)	6 (60.0)
Age, years, mean (SD)	22.8 (1.5)	63.1 (7.1)	63.2 (7.6)	90.2 (0.5)
Anthropometric data, mean (SD)				
Body mass index, kg/m^2	22.2 (1.8)[a]	26.8 (4.7)[b]	25.6 (3.4)[c]	25.4 (3.8)
Co-morbidities, no./total known (%)				
Myocardial infarction	0/10 (0.0)	0/37 (0.0)	0/38 (0.0)	3/10 (30.0)
Cerebrovascular accident	0/10 (0.0)	1/38 (2.6)	2/38 (5.3)	2/10 (20.0)
Hypertension	0/10 (0.0)	9/38 (23.7)	8/38 (21.1)	5/10 (50.0)
Diabetes mellitus	0/10 (0.0)	2/37 (5.4)	5/37 (13.5)	2/10 (20.0)
Malignancies	0/10 (0.0)	1/36 (2.8)	2/36 (5.6)	1/10 (10.0)
Chronic obstructive pulmonary disease	0/10 (0.0)	1/38 (2.6)	2/37 (5.4)	1/10 (10.0)
Rheumatoid arthritis	0/10 (0.0)	0/38 (0.0)	0/38 (0.0)	3/10 (30.0)
Intoxications, no./total known (%)				
Smoking, current	0/10 (0.0)	6/38 (15.8)	4/38 (10.0)	1/10 (10.0)

SD: standard deviation. a: N=8, b: N=38, c: N=39. Offspring: offspring of nonagenarian siblings, i.e. member of a long-lived family. Partners: the partners of the offspring of nonagenarian siblings.

Micronuclei usually have the same staining intensity as the main nuclei, but occasionally staining may be more intense. For telomere-associated foci 100 randomly selected nuclei per donor were automatically scored for the number of 53BP1 foci together with the number of visible telomeres by using the program Stacks [19-21] which enabled to exclude the background from analysis. All counts were performed blind with respect to donor age and offspring or partner origin.

Statistics

All analyses were performed using IBM SPSS Statistics 20 software package. As most nuclei had few foci and micronuclei, the data distribution was skewed, thus foci and micronuclei counts are presented as the percentage of nuclei with ≥1 and ≥2 53BP1 foci/TAF per nucleus, and percentage of cells with ≥1 and ≥2 micronuclei per cell. Analogous to an earlier study [9] we also computed the percentage of nuclei with ≥3 53BP1 foci/TAF per nucleus and the percentage of cells with ≥3 micronuclei per cell, however these were very low hindering further comparison. We thus used 2 thresholds in this study: the minimum threshold of ≥1 and a threshold of ≥2. Analyses of Table 2 were performed by using linear mixed models, taking the repeated measurements of duplicate experiments into account with the covariance structure compound symmetry. Adjustments were made for random batch effects and for gender. For the supplementary analysis on whole-genome 53BP1 foci and telomere associated foci dependent on long-lived family member status a second model was used that additionally

Table 2. 53BP1 foci, TAF and micronuclei dependent on chronological age of the donor.

	Chronological age	
	Slope (SE)	P-value
Non-stressed state		
% nuclei with ≥1 53BP1 foci/nucleus	0.23 (0.06)	<0.001
% nuclei with ≥2 53BP1 foci/nucleus	0.15 (0.04)	<0.001
% nuclei with ≥1 TAF/nucleus	0.16 (0.05)	0.001
% nuclei with ≥2 TAF/nucleus	0.05 (0.04)	0.147
% cells with ≥1 micronuclei/cell	0.00 (0.01)	0.711
% cells with ≥2 micronuclei/cell	0.00 (0.00)	0.411
Rotenone stressed state		
% nuclei with ≥1 53BP1 foci/nucleus	0.29 (0.07)	<0.001
% nuclei with ≥2 53BP1 foci/nucleus	0.16 (0.06)	0.005
% nuclei with ≥1 TAF/nucleus	0.16 (0.04)	<0.001
% nuclei with ≥2 TAF/nucleus	0.06 (0.02)	0.003
% cells with ≥1 micronuclei/cell	0.01 (0.02)	0.787
% cells with ≥2 micronuclei/cell	0.01 (0.01)	0.330
Δ stressed and non-stressed state		
% nuclei with ≥1 53BP1 foci/nucleus	0.06 (0.05)	0.243
% nuclei with ≥2 53BP1 foci/nucleus	0.01 (0.04)	0.796
% nuclei with ≥1 TAF/nucleus	0.00 (0.04)	0.904
% nuclei with ≥2 TAF/nucleus	0.00 (0.04)	0.945
% cells with ≥1 micronuclei/cell	-0.01 (0.02)	0.725
% cells with ≥2 micronuclei/cell	0.01 (0.01)	0.416

The slope of the adjusted regression line is given (linear mixed model, with adjustment for gender, batch and repeated measurements; independent variable: age in years, continuously). SE: standard error. TAF: telomere-associated foci. Δ: difference.

adjusted for chronological age. In the supplementary analyses on whole-genome 53BP1 foci and telomere associated foci dependent on the presence of cardiovascular or metabolic diseases, this second model consisted of additional adjustments for chronological age and long-lived family member status. A chi-square for linearity (linear by linear test) was performed in the association between micronuclei counts and 53BP1 foci. Absolute micronuclei counts (of both duplicate experiments) were linked to the presence of 53BP1 foci within the same cell. Due to the low number of high micronuclei counts, all micronuclei counts equal to or higher than 3 were combined in one category.

Results

Donor characteristics are shown in Table 1.

Table 2 shows the association of the percentages of fibroblast nuclei with ≥1/≥2 53BP1 foci, TAF and fibroblasts with ≥1/≥2 micronuclei with chronological age. In the non-stressed state, the percentages of nuclei with both ≥1 and ≥2 53BP1 foci per nucleus were positively associated with chronological age (both $P<0.001$). The percentage of nuclei with ≥1 TAF per nucleus was also positively associated with age ($P=0.001$), but the percentage of nuclei with ≥2 TAF per nucleus was not significantly associated ($P=0.147$). The percentages of cells with ≥1/≥2 micronuclei per cell were not associated with the age of the donor ($P=0.711$ and $P=0.411$ respectively).

In the rotenone-stressed state, depicted in Table 2 as well, the percentages of nuclei with ≥1 and ≥2 53BP1 foci per nucleus were positively associated with age ($P<0.001$ and $P=0.005$ respectively). The percentages of nuclei with ≥1 and ≥2 TAF were also positively associated with age ($P<0.001$ and $P=0.003$, respectively). The percentage of cells with ≥1/≥2 micronuclei per cell were not significantly associated with age ($P=0.787$ and $P=0.330$). No associations of the differences between the stressed and non-stressed state of 53BP1 foci, TAF and micronuclei was found with age (all: $P>0.05$).

Figure 1 visualizes the associations between percentages of 53BP1 foci, TAF positive nuclei and percentages of micronuclei positive fibroblasts with chronological age. The data points and regression lines are shown separately for the non-stressed state, the rotenone-stressed state and the difference between rotenone-stressed and non-stressed state.

Figure 2 shows the association of the absolute counts of 53BP1 foci and micronuclei on a single cell level. Most of the fibroblasts had 0 and some 1 micronuclei per cell. Cells with 2

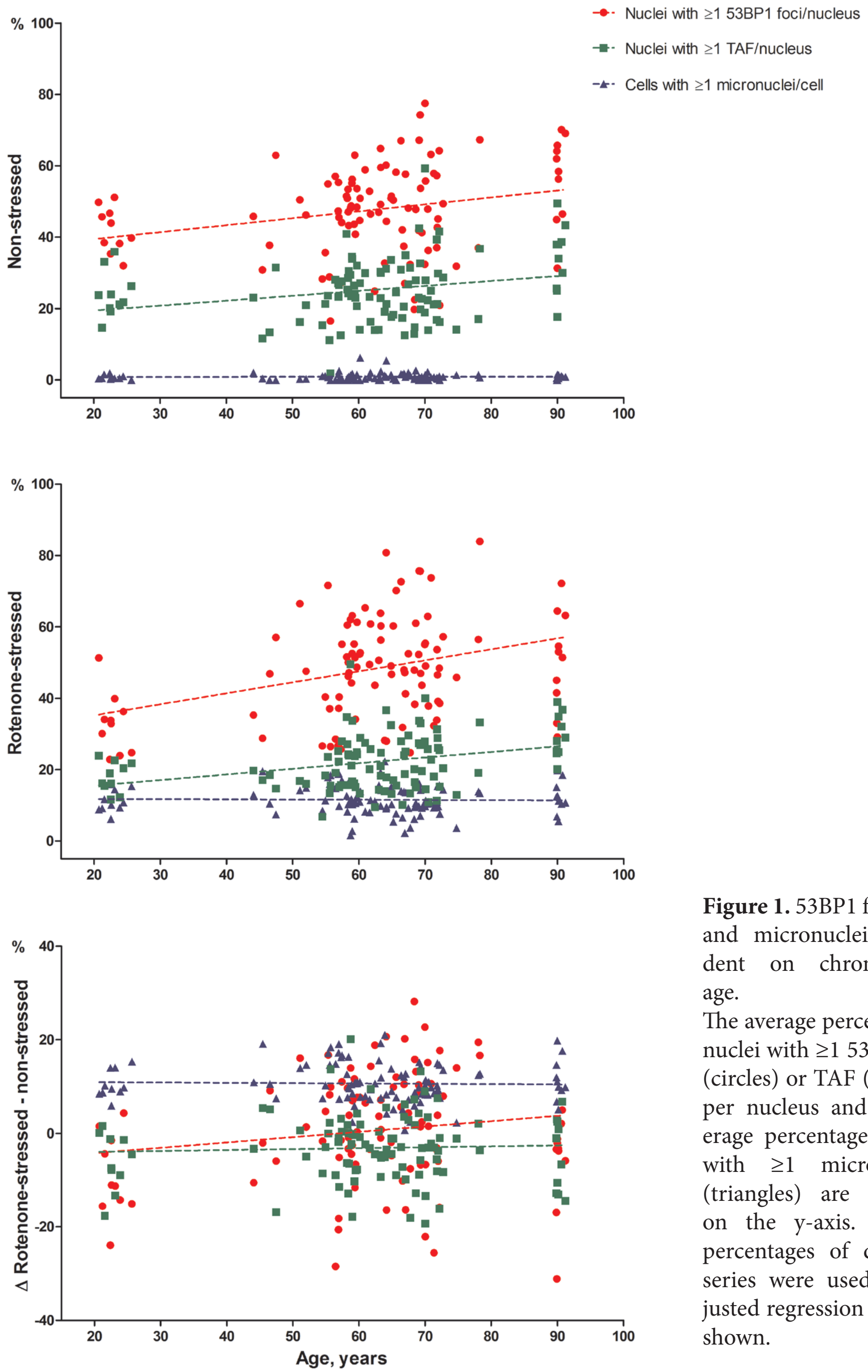

Figure 1. 53BP1 foci, TAF and micronuclei dependent on chronological age.
The average percentage of nuclei with ≥1 53BP1 foci (circles) or TAF (squares) per nucleus and the average percentage of cells with ≥1 micronucleus (triangles) are depicted on the y-axis. Average percentages of duplicate series were used. Unadjusted regression lines are shown.

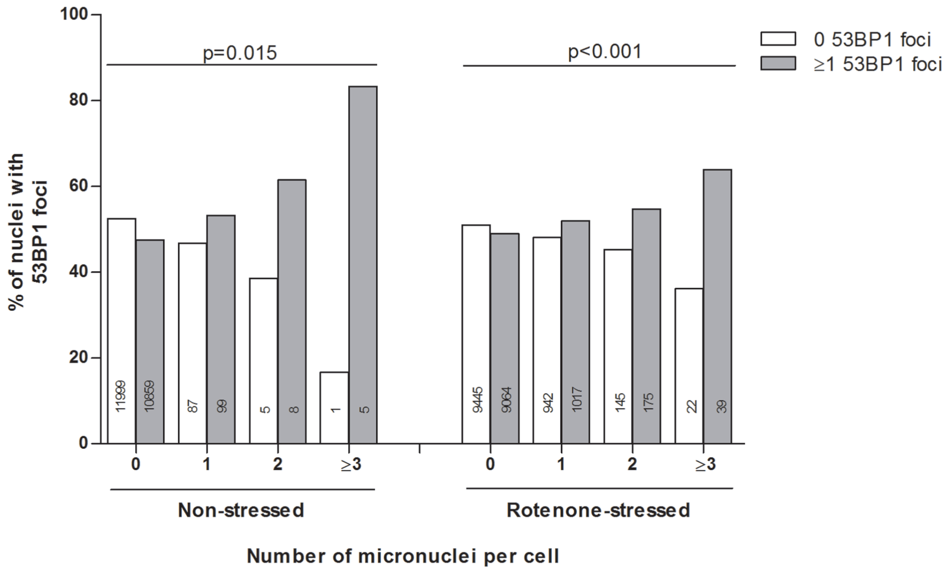

Figure 2. The association of the absolute number of micronuclei and 53BP1 foci.
Dependence of 0 or ≥1 53BP1 foci on individual micronuclei counts (both duplicate series). Micronuclei counts equal to or higher than 3 were combined in one category: ≥3. Linear by linear association tests were performed to test the linearity of differences in proportions.

or more micronuclei were rarely present. The linear by linear association of the distribution of 53BP1 foci and micronuclei count categories was significant in both non-stressed control state and rotenone-stressed state, with more frequent presence of ≥1 53BP1 foci in cells with more micronuclei (P=0.015 and P<0.001, respectively).

The association of DNA damage markers and biological age within the middle-aged group is shown in Supplementary table 1 and 2. No significant differences in average percentage of nuclei with ≥1/≥2 53BP1 foci, TAF or micronuclei were observed between offspring and partners and those middle-aged donors without and those with one or more cardiovascular and/or metabolic disease.

Discussion

In the present study, we showed that *in vitro* 53BP1 foci and TAF, but not micronuclei, are significantly positively associated with the chronological age of the donor that the fibroblasts were derived from. No association of 53BP1 foci and TAF was found within the middle-aged group dependent on the membership of a long-lived family or the presence of cardiovascular and/or metabolic disease. We found evidence for a positive association between micronuclei and 53BP1 foci.

Our results on chronological age and 53BP1 foci and TAF are in line with our previous studies that showed *in vitro* responses of fibroblasts dependent on the life histories of the donors [22;23]. Our results regarding 53BP1 foci and chronological age are in line with other studies that have observed a positive association of DNA damage foci (containing e.g. DDR mediator protein 53BP1 or phosphorylated H2AX) with chronological age in cells derived from mice [24] and in several animal tissues [3;6;25]. Unrepaired TAF also accumulate with aging in primates [4;7]. In humans, DNA damage foci are more prevalent in lymphocytes as well as primary fibroblasts of older donors compared to young [9;10]. We solidify these observations within a large group of donors and extent the available knowledge to extreme ages. Notable, the numbers of foci were higher in our study compared to the study by Waldera-Lupa et al. Since the number of foci increase towards replicative senescence [26] the higher number of foci is likely due to the higher passage number of our fibroblasts, although all strains were in early IIa stage [27]. The positive association between DNA damage foci with donor age in our study supports the role of DNA damage in human aging. Fibroblasts from donors with Werner syndrome exhibit more DNA foci compared to normal donors as well [9]. On the other hand, the donors aged 90 years have apparently reached this age despite the number of DNA damage foci, indicating that the higher numbers of DNA damage foci are a consequence of high age.

In contrast to the positive association of 53BP1 foci and TAF with chronological age, no association was found with biological donor age. This might be explained by the fact that many of the cardiovascular and/or metabolic diseases manifest around middle age, so only had little time to exert any ‘imprint’, while the differences in chronological age were much higher. Furthermore, in this relatively healthy group of middle-aged donors, the prevalence of cardiovascular and/or metabolic disease was low. Therefore, lack in contrast of the studied sample cannot be excluded. In a recent study higher numbers of micronuclei within lymphocytes of 52 patients with metabolic syndrome has been found compared to normal controls [28].

Although an inverse association of micronuclei *in vitro* has been found with maximum lifespan of different mammal species [8], we did not find a positive association between micronuclei and chronological age of the donor. In contrast, other studies have found such an association in human peripheral blood lymphocytes (age range of studies: 0-85 years) [29-32] or buccal cells (<40 compared to ≥40 years) [12]. Several explanations can be suggested: firstly, in dermal fibroblasts the baseline frequency of micronuclei is not dependent on age. Alternatively, during the cell expansion before starting the experiments, micronuclei positive fibroblasts could have been discarded or degraded their micronuclei [33]. Micronuclei can also disappear in daughter cells by being incorporated into the main nuclei [34].

We did not observe a substantial influence of rotenone on 53BP1 foci or TAF, which could be explained by its mostly aneugenic action [35;36]. As expected, stressing the fibroblasts with rotenone did results in higher numbers of micronuclei, but this higher prevalence of micronuclei in fibroblasts after rotenone incubation was also not associated with chronological donor age, similarly with previous results of human lymphocytes treated with irradiation [37;38] or mitomycin-C [39].

The strength of the study is the number of donors of a wide chronological age range. We have used several DNA damage markers in non-stressed and stressed conditions and all experiments were conducted under highly standardized conditions. One limitation of this study is the use of rotenone as stressor; other stressors could yield different results. The acquisition of biopsies and subsequent culturing of fibroblasts was done in a highly standardized manner, minimizing variation due to differences in handling. To further minimize potential random batch effects we additionally adjusted for this in our statistical analyses.

In conclusion, we showed a significant association between the prevalence of *in vitro* 53BP1 foci and TAF positive fibroblasts and the chronological age of the donor, emphasizing the link between DNA damage and human aging. However the fact that 53BP1 foci and TAF were not associated with biological age, and that micronuclei were not linked to chronological age in the present study indicates the need of further study into the influence of genome stability on *in vivo* aging. Specifically, the results of this study within primary human cells should be expanded to human aged tissues.

Acknowledgements

We would like to thank the following persons for their invaluable efforts in the experimental work and data processing: Martijn van Baalen, Mark van der Bij, Joke Blom, Pim Dekker, Sarah Gesualdi and Corine de Koning-Treurniet.
This work was supported by RFO 2013 of University of Bologna [to AL], the Innovation Oriented research Program on Genomics (SenterNovem; IGE01014 and IGE5007), the Netherlands Genomics Initiative/Netherlands Organization for scientific research (NGI/NWO; 05040202 and 050-060-810), the EU funded Network of Excellence Lifespan (FP6 036894), and NIH grant R37 AG016694 [to JMS].

Supplementary table 1 - 53BP1 foci, TAF and micronuclei dependent on membership of a long-lived family.

	Familial longevity		
	Offspring N=40	Partners N=40	P-value
Non-stressed state			
% nuclei with ≥1 53BP1 foci/nucleus	47.3 (2.90)	48.1 (2.90)	0.730
% nuclei with ≥2 53BP1 foci/nucleus	13.9 (1.83)	14.7 (1.83)	0.565
% nuclei with ≥1 TAF/nucleus	23.0 (1.62)	26.3 (1.62)	0.070
% nuclei with ≥2 TAF/nucleus	5.18 (1.12)	5.43 (1.13)	0.862
% cells with ≥1 micronuclei/cell	1.05 (0.17)	0.92 (0.14)	0.606
% cells with ≥2 micronuclei/cell	0.09 (0.04)	0.10 (0.04)	0.897
Rotenone-stressed state			
% nuclei with ≥1 53BP1 foci/nucleus	47.8 (3.04)	49.4 (3.05)	0.487
% nuclei with ≥2 53BP1 foci/nucleus	19.3 (2.67)	20.5 (2.68)	0.543
% nuclei with ≥1 TAF/nucleus	21.4 (1.49)	21.9 (1.51)	0.748
% nuclei with ≥2 TAF/nucleus	3.97 (0.54)	4.76 (0.55)	0.232
% cells with ≥1 micronuclei/cell	12.1 (0.61)	10.9 (0.63)	0.198
% cells with ≥2 micronuclei/cell	2.06 (0.18)	1.81 (0.19)	0.343
Δ stressed and non-stressed state			
% nuclei with ≥1 53BP1 foci/nucleus	0.24 (2.96)	1.27 (2.97)	0.586
% nuclei with ≥2 53BP1 foci/nucleus	5.44 (1.94)	5.96 (1.95)	0.737
% nuclei with ≥1 TAF/nucleus	-1.50 (1.15)	-4.01 (1.18)	0.088
% nuclei with ≥2 TAF/nucleus	-1.09 (0.94)	-0.62 (0.97)	0.728
% cells with ≥1 micronuclei/cell	11.0 (0.63)	10.1 (0.66)	0.295
% cells with ≥2 micronuclei/cell	1.96 (0.18)	1.71 (0.19)	0.332

The adjusted estimated means within offspring and partners are given (linear mixed model, adjustment for gender, age, batch and repeated measurements). SE: standard error, Δ: difference.

Supplementary table 2 - 53BP1 foci, TAF and micronuclei dependent on presence of cardiovascular and/or metabolic diseases.

	Cardiovascular and/or metabolic diseases			
	Absent N=52	Present N=21	P for trend[a]	P for trend[b]
Non-stressed state				
% nuclei with ≥1 53BP1 foci/nucleus	47.0 (2.60)	46.5 (3.11)	0.847	0.487
% nuclei with ≥2 53BP1 foci/nucleus	13.8 (1.38)	13.1 (1.69)	0.621	0.493
% nuclei with ≥1 TAF/nucleus	24.6 (1.48)	23.3 (2.07)	0.589	0.216
% nuclei with ≥2 TAF/nucleus	4.80 (1.00)	6.06 (1.46)	0.453	0.337
% cells with ≥1 micronuclei/cell	1.07 (0.16)	0.95 (0.24)	0.689	0.562
% cells with ≥2 micronuclei/cell	0.11 (0.03)	0.08 (0.05)	0.632	0.764
Rotenone-stressed state				
% nuclei with ≥1 53BP1 foci/nucleus	47.1 (2.78)	48.2 (3.40)	0.729	0.775
% nuclei with ≥2 53BP1 foci/nucleus	18.7 (2.35)	19.6 (2.87)	0.726	0.849
% nuclei with ≥1 TAF/nucleus	21.7 (1.52)	20.2 (1.89)	0.399	0.174
% nuclei with ≥2 TAF/nucleus	4.48 (0.53)	3.49 (0.71)	0.193	0.077
% cells with ≥1 micronuclei/cell	11.6 (0.58)	11.6 (0.86)	0.977	0.358
% cells with ≥2 micronuclei/cell	1.97 (0.17)	1.91 (0.25)	0.857	0.992
Δ stressed and non-stressed state				
% nuclei with ≥1 53BP1 foci/nucleus	-0.01 (2.86)	1.49 (3.25)	0.537	0.675
% nuclei with ≥2 53BP1 foci/nucleus	5.00 (1.88)	6.55 (2.28)	0.439	0.805
% nuclei with ≥1 TAF/nucleus	-2.37 (1.09)	-3.08 (1.55)	0.690	0.851
% nuclei with ≥2 TAF/nucleus	-0.22 (0.88)	-2.45 (1.31)	0.161	0.067
% cells with ≥1 micronuclei/cell	10.6 (0.60)	10.6 (0.90)	0.961	0.339
% cells with ≥2 micronuclei/cell	1.85 (0.17)	1.83 (0.25)	0.940	0.864

Only donors from LLS were included in this analysis. The adjusted estimated means within both groups (disease absent or present) are given. Linear mixed model: model 1 ([a]) adjustment for gender, batch and repeated measurements. Model 2 ([b]): as model 1 plus adjustment for age and long-lived family member status. SE: standard error, Δ: difference.

References

(1) Hoeijmakers JH. DNA damage, aging, and cancer. *N Engl J Med* 2009;361:1475-1485.
(2) Lopez-Otin C, Blasco MA, Partridge L, Serrano M, Kroemer G. The hallmarks of aging. *Cell* 2013;153:1194-1217.
(3) Wang C, Jurk D, Maddick M, Nelson G, Martin-Ruiz C, von ZT. DNA damage response and cellular senescence in tissues of aging mice. *Aging Cell* 2009;8:311-323.
(4) Hewitt G, Jurk D, Marques FD et al. Telomeres are favoured targets of a persistent DNA damage response in ageing and stress-induced senescence. *Nat Commun* 2012;3:708.
(5) Herbig U, Ferreira M, Condel L, Carey D, Sedivy JM. Cellular senescence in aging primates. *Science* 2006;311:1257.
(6) Jeyapalan JC, Ferreira M, Sedivy JM, Herbig U. Accumulation of senescent cells in mitotic tissue of aging primates. *Mech Ageing Dev* 2007;128:36-44.
(7) Fumagalli M, Rossiello F, Clerici M et al. Telomeric DNA damage is irreparable and causes persistent DNA-damage-response activation. *Nat Cell Biol* 2012;14:355-365.
(8) Fink LS, Roell M, Caiazza E et al. 53BP1 contributes to a robust genomic stability in human fibroblasts. *Aging (Albany NY)* 2011;3:836-845.
(9) Sedelnikova OA, Horikawa I, Redon C et al. Delayed kinetics of DNA double-strand break processing in normal and pathological aging. *Aging Cell* 2008;7:89-100.
(10) Waldera-Lupa DM, Kalfalah F, Safferling K et al. Characterization of Skin aging Associated Secreted Proteins (SAASP) Produced by Dermal Fibroblasts Isolated from Intrinsically Aged Human Skin. *J Invest Dermatol* 2015.
(11) Peace BE, Succop P. Spontaneous micronucleus frequency and age: what are normal values? *Mutat Res* 1999;425:225-230.
(12) Bonassi S, Coskun E, Ceppi M et al. The HUman MicroNucleus project on eXfoLiated buccal cells (HUMN(XL)): the role of life-style, host factors, occupational exposures, health status, and assay protocol. *Mutat Res* 2011;728:88-97.
(13) Bootsma-van der Wiel A, Gussekloo J, de Craen AJ, Van EE, Bloem BR, Westendorp RG. Common chronic diseases and general impairments as determinants of walking disability in the oldest-old population. *J Am Geriatr Soc* 2002;50:1405-1410.
(14) Maier AB, le CS, de Koning-Treurniet C, Blom J, Westendorp RG, van HD. Persistence of high-replicative capacity in cultured fibroblasts from nonagenarians. *Aging Cell* 2007;6:27-33.
(15) Schoenmaker M, de Craen AJ, de Meijer PH et al. Evidence of genetic enrichment for exceptional survival using a family approach: the Leiden Longevity Study. *Eur J Hum Genet* 2006;14:79-84.
(16) Westendorp RG, van HD, Rozing MP et al. Nonagenarian siblings and their offspring display lower risk of mortality and morbidity than sporadic nonagenarians: The Leiden Longevity Study. *J Am Geriatr Soc* 2009;57:1634-1637.
(17) Dekker P, de Lange MJ, Dirks RW et al. Relation between maximum replicative capacity and oxidative stress-induced responses in human skin fibroblasts in vitro. *J Gerontol A Biol Sci Med Sci* 2011;66:45-50.
(18) Thomas P, Fenech M. Cytokinesis-block micronucleus cytome assay in lymphocytes. *Methods Mol Biol* 2011;682:217-234.
(19) Smeenk G, Wiegant WW, Vrolijk H, Solari AP, Pastink A, van AH. The NuRD chromatin-remodeling complex regulates signaling and repair of DNA damage. *J Cell Biol* 2010;190:741-749.
(20) Weeke-Klimp A, Bax NA, Bellu AR et al. Epicardium-derived cells enhance proliferation, cellular maturation and alignment of cardiomyocytes. *J Mol Cell Cardiol* 2010;49:606-616.
(21) Jonsdottir AB, Dirks RW, Vrolijk J et al. Centriole movements in mammalian epithelial cells during cytokinesis. *BMC Cell Biol* 2010;11:34.
(22) Dekker P, Maier AB, van HD et al. Stress-induced responses of human skin fibroblasts in vitro reflect human longevity. *Aging Cell* 2009;8:595-603.
(23) Waaijer ME, Wieser M, Grillari-Voglauer R, van HD, Grillari J, Maier AB. MicroRNA-663 induction upon oxidative stress in cultured human fibroblasts depends on the chronological age of the donor. *Biogerontology* 2014;15:269-278.

(24) Sedelnikova OA, Horikawa I, Zimonjic DB, Popescu NC, Bonner WM, Barrett JC. Senescing human cells and ageing mice accumulate DNA lesions with unrepairable double-strand breaks. *Nat Cell Biol* 2004;6:168-170.
(25) Schuler N, Rube CE. Accumulation of DNA damage-induced chromatin alterations in tissue-specific stem cells: the driving force of aging? *PLoS One* 2013;8:e63932.
(26) d'Adda di FF, Reaper PM, Clay-Farrace L et al. A DNA damage checkpoint response in telomere-initiated senescence. *Nature* 2003;426:194-198.
(27) Maier AB, Westendorp RG. Relation between replicative senescence of human fibroblasts and life history characteristics. *Ageing Res Rev* 2009;8:237-243.
(28) Karaman A, Aydin H, Geckinli B, Cetinkaya A, Karaman S. DNA damage is increased in lymphocytes of patients with metabolic syndrome. *Mutat Res Genet Toxicol Environ Mutagen* 2015;782:30-35.
(29) Fenech M, Morley AA. The effect of donor age on spontaneous and induced micronuclei. *Mutat Res* 1985;148:99-105.
(30) Bukvic N, Gentile M, Susca F et al. Sex chromosome loss, micronuclei, sister chromatid exchange and aging: a study including 16 centenarians. *Mutat Res* 2001;498:159-167.
(31) Bolognesi C, Abbondandolo A, Barale R et al. Age-related increase of baseline frequencies of sister chromatid exchanges, chromosome aberrations, and micronuclei in human lymphocytes. *Cancer Epidemiol Biomarkers Prev* 1997;6:249-256.
(32) Bonassi S, Fenech M, Lando C et al. HUman MicroNucleus project: international database comparison for results with the cytokinesis-block micronucleus assay in human lymphocytes: I. Effect of laboratory protocol, scoring criteria, and host factors on the frequency of micronuclei. *Environ Mol Mutagen* 2001;37:31-45.
(33) Terradas M, Martin M, Tusell L, Genesca A. Genetic activities in micronuclei: is the DNA entrapped in micronuclei lost for the cell? *Mutat Res* 2010;705:60-67.
(34) Crasta K, Ganem NJ, Dagher R et al. DNA breaks and chromosome pulverization from errors in mitosis. *Nature* 2012;482:53-58.
(35) Matsumoto K, Ohta T. Rotenone induces aneuploidy, polyploidy and endoreduplication in cultured Chinese hamster cells. *Mutat Res* 1991;263:173-177.
(36) Melo KM, Grisolia CK, Pieczarka JC, de Souza LR, Filho JS, Nagamachi CY. FISH in micronucleus test demonstrates aneugenic action of rotenone in a common freshwater fish species, Nile tilapia (Oreochromis niloticus). *Mutagenesis* 2014;29:215-219.
(37) Fenech M, Morley AA. Ageing in vivo does not influence micronucleus induction in human lymphocytes by X-irradiation. *Mech Ageing Dev* 1987;39:113-119.
(38) Muller WU, Bauch T, Stuben G, Sack H, Streffer C. Radiation sensitivity of lymphocytes from healthy individuals and cancer patients as measured by the comet assay. *Radiat Environ Biophys* 2001;40:83-89.
(39) Franceschi C, Monti D, Scarfi MR et al. Genomic instability and aging. Studies in centenarians (successful aging) and in patients with Down's syndrome (accelerated aging). *Ann N Y Acad Sci* 1992;663:4-16.

Chapter 3

Do senescence markers correlate in vitro and in situ within individual human donors?

M.E.C. Waaijer, D.A. Gunn, D. van Heemst, P.E. Slagboom, J.M. Sedivy, R.W. Dirks, H.J. Tanke, R.G.J. Westendorp, A.B. Maier

In preparation

Abstract

Cellular senescence can be detected by several markers both *in vitro* and *in situ*, but little is known on how well senescence markers correlate within individual donors. By using data from highly standardized experiments, correlations between the same *in vitro* senescence markers were studied in duplicate short-term experiments, and between short-term and long-term experiments. In addition, different *in vitro* senescence markers measured within the short-term and long-term experiments were tested amongst each other for correlation. The different *in vitro* senescence markers were also tested for correlations with *in situ* p16INK4a cell positivity. From a total of 100 donors (aged 20-91 years), cultured dermal fibroblasts were assessed for reactive oxygen species (ROS), telomere-associated foci (TAF), p16INK4a and senescence-associated β-gal (SAβ-gal), both in non-stressed conditions and after supplementing the medium with 0.6 μM rotenone for 3 days (short-term experiment). In cultured fibroblast from 40 of the donors, telomere shortening, levels of ROS and SAβ-gal were additionally assessed, with or without 20 nM rotenone for 7 weeks (long-term experiment). In skin tissue from 52 of the donors, the number of p16INK4a positive dermal cells was assessed *in situ*. More than half of the correlations of the same senescence markers *in vitro* between duplicate experiments and between short-term versus long-term experiments were significant (with an average coefficient of 0.498). Half of the different senescence marker correlations were significant (average coefficient of 0.349) within the short-term experiments and within the long-term experiments. Within middle-aged donors, the different senescence markers *in vitro* were not significantly correlated intra-individually with *in situ* p16INK4a positivity. In conclusion, caution is warranted in comparing results obtained using different senescence markers and in extrapolating *in vitro* to *in vivo* findings.

Introduction

Five decades ago, Hayflick and Moorhead first described the phenomenon of limited replicative capacity of cultured primary cells, termed cellular replicative senescence [1;2]. It was postulated that this *in vitro* phenomenon of stable cell cycle arrest might be related to aging of the whole organisms *in vivo*. Since then many studies have focussed on cellular senescence *in vitro*, and have identified several triggers inducing senescence as well as pathways leading to senescence (reviewed in [3]). Considerable interest has also been given to the possible *in vivo* implications of senescence; by studying relevant functions, including embryonic development and attenuating liver fibrosis as well as consequences of senescence in animal models, notably age-related diseases, and tumorigenesis in neighboring cells [4-8]. In the last few decades [9] human tissues have been studied to detect cellular senescence *in situ*, providing knowledge on the prevalence of senescent cells in humans at older ages or with disease.

Apart from growth arrest, several other markers of cellular senescence have been studied (reviewed in [10]). A frequently used marker is senescence-associated β- galactosidase (SAβ-gal) activity, which is upregulated in, but not essential for senescence[9;11]. Other markers are based on triggers of senescence such as DNA damage foci or reactive oxygen species (ROS), expression of genes involved in cell cycle arrest or factors that are secreted by senescent cells[3;10;12]. Most of these markers have been established by detecting senescence *in vitro*, but some can also be used *in situ* [13]. However the number of studies in fibroblasts reporting on senescence *in situ* compared to *in vitro* is disproportionally small [14], and there is a lack of knowledge concerning the correlation of senescence markers between these conditions. In addition, only few attempts have been made to study the correlation between different senescence markers.

Our aim is therefore to study the correlations between (A) the same senescence markers and (B) different senescence markers within individual donors, using an unique dataset of highly standardized experiments including (1) *in vitro* short-term experiments; (2) *in vitro* long-term experiments, and (3) *in situ* within skin biopsies. Correlations were tested between the same senescence markers: (1A) *in vitro* between duplicate experiments and (2A) *in vitro* between short-term and long-term experiments. In addition, correlations between different senescence markers were tested: (1B) between *in vitro* markers within the same short-term experiments; (2B) between *in vitro* markers within the same long-term experiments; and (3B) intra-individually between *in vitro* markers and *in situ* p16INK4a positivity.

Methods

Study design

The Leiden 85-plus Study is a prospective population-based study[15] of inhabitants of Leiden (the Netherlands). Participants aged 90 years and young controls aged 18-25 years donated skin biopsies of the upper inner arm to establish fibroblast cultures[16]. As previously described [17], in the Leiden Longevity Study factors contributing to familial longevity are studied. Skin biopsies for *in situ* staining and fibroblast cultures were obtained from middle-aged to old (mean 63 years) offspring of nonagenarian sibling and their partners [16]. All participants in these studies have given written informed consent, and both studies were approved by the Medical Ethical Committee of the Leiden University Medical Center.

In vitro senescence markers

Detailed methods have been described previously [18-20]. In short, fibroblast strains from 10 young donors (passage 14), from 80 middle-aged donors (40 offspring of long-lived families and 40 partners – passage 10), and from 10 old donors (passage 14) were randomly selected for subsequent experiments. Fibroblasts were cultured for 3 days with or without 0.6 μM rotenone added to the medium (short-term experiments). The following senescence markers

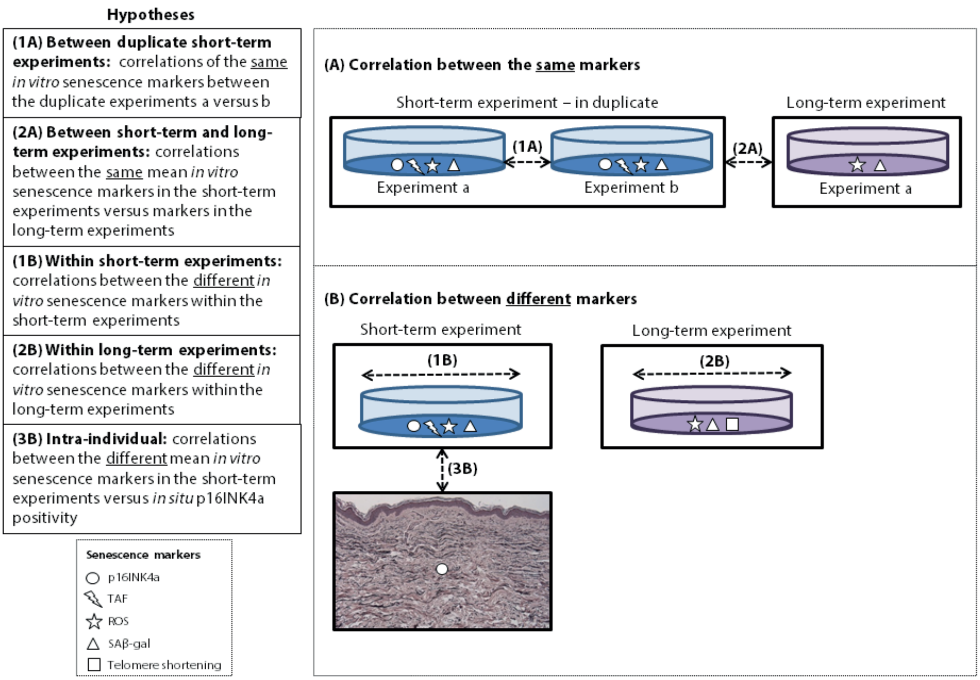

Figure 1. Explanation of hypotheses tested.

were assessed in fibroblast cultures in non-stressed and in rotenone-stressed conditions: median fluorescence intensity value of β galactosidase (SAβ-gal) and mean fluorescence intensity value of reactive oxygen species (ROS) were measured using flow cytometry, and the percentage of immunocytochemically stained p16INK4a positive fibroblasts was counted. The number of telomere-associated foci (TAF) was determined using immunofluorescence and PNA telomeric probe (53BP1 positive foci located at telomeres). 100 randomly selected nuclei were automatically scored for TAF. TAF are presented as the percentage of nuclei with ≥1 TAF per nucleus. These experiments were conducted in duplicate (experiments a and b) [18;20] (i.e. in parallel conducted repeated experiments for each strain). Furthermore alongside the above mentioned experiments, 10 fibroblasts strains from young, 20 from middle-aged (10 offspring, 10 partners) and 10 from old donors were randomly selected and cultured for 7 weeks, with or without 20 nM rotenone to generate chronic stress (long-term experiments). The median fluorescence intensity values of β galactosidase (SAβ-gal) and reactive oxygen species (ROS) were measured using flow cytometry. Telomere length was assessed with a flow-FISH kit and was expressed as the percentage compared to the reference cell line. The telomere shortening rate was further determined by comparing these measurements to telomere length at baseline and dividing the difference by the number of cumulative population doublings [19].

In situ senescence marker

As detailed previously [21], in order to detect p16INK4a in the formalin fixed paraffin embedded skin tissue, immunohistochemistry staining was used. Dermal p16INK4a cell counts were restricted to morphologically determined fibroblasts and normalized for the area of the dermis the cells were counted in. Dermal p16INK4a positivity is given as the number of p16INK4a positive cells per 1 mm^2.

Statistics

All analyses were performed using IBM SPSS Statistics 20. Not all data was normally distributed, these variables were naturally log transformed before evaluating the correlations by calculating the Pearson partial correlation coefficient, adjusted for experiment batch. The studied correlations are explained in Figure 1. First, correlations of the same senescence markers were analyzed using data of (1A) the short-term experiments a and b (duplicate experiments); (2A) the mean results of duplicates in the short-term experiments and the single measurements of the long-term experiments (as this experiment was performed once). Secondly, correlations between different senescence markers were analyzed using (1B) the mean results of duplicates within the short-term experiments; (2B) the single measurements within the long-term experiment; and (3B) the mean of the *in vitro* markers in the short-term experiments (mean results of duplicates) and *in situ* p16INK4a positivity. All *in vitro* markers were measured in a non-stressed and (rotenone) stressed condition. For data visualization the percentage of fibroblasts staining positive for p16INK4a *in vitro* was plotted against the number of p16INK4a positive dermal cells *in situ*.

Results

Table 1 supplies the anthropometric and medical characteristics of the donors from whom the skin biopsies were obtained based on age (young, mean 23 years; middle-aged, mean 63 years; old, mean 90 years).
First, we studied correlations between the same markers, both in non-stressed and stressed conditions. The correlation of duplicates of each senescence marker (p16INK4a, TAF, ROS and SAβ-gal) were tested between experiment a and b of the short term experiments (Table 2). Most markers were significantly associated between experiments a and b (coefficients > 0.400), except for ROS which showed low, non-significant correlation coefficients.
Table 3 shows the correlations between ROS and SAβ-gal in the short-term versus the long-term experiments. ROS measures in the short-term experiment were significantly correlated to ROS in the long-term experiment. SAβ-gal was not significantly correlated between the short-term and long-term experiments.

Table 1. Characteristics of donors.

	Young (N=10)	Middle-aged (N=80)	Old (N=10)
Female, no.(%)	7 (70.0)	40 (50.0)	6 (60.0)
Age, years	22.8 (1.5)	63.2 (7.3)	90.2 (0.5)
Member of long-lived family	n/a	40 (50.0)	n/a
Body mass index, kg/m^2	22.2 (1.8)[a]	26.2 (4.1)[b]	25.4 (3.8)
Co-morbidities			
Cerebrovascular accident	0/10 (0.0)	3/76 (3.9)	2/10 (20.0)
Chronic obstructive pulmonary disease	0/10 (0.0)	3/75 (4.0)	1/10 (10.0)
Diabetes mellitus	0/10 (0.0)	7/74 (9.5)	2/10 (20.0)
Hypertension	0/10 (0.0)	17/76 (22.4)	5/10 (50.0)
Malignancies	0/10 (0.0)	3/72 (4.2)	1/10 (10.0)
Myocardial infarction	0/10 (0.0)	0/75 (0.0)	3/10 (30.0)
Rheumatoid arthritis	0/10 (0.0)	0/76 (0.0)	3/10 (30.0)
Smoking, current	0/10 (0.0)	10/76 (13.2)	1/10 (10.0)

SD: standard deviation. a: N=8, b: N=77. N/a: not applicable. Data are depicted as either mean (SD) or number (%). Diseases and intoxications are given as no./total known (%).

Secondly, we studied correlations between different senescence markers. In the Supplementary Material, correlations between different senescence markers within the short-term

Table 2. Senescence markers and their correlations between duplicate short-term experiments (1A).

	Distribution of markers			
	Experiment a	Experiment b	Correlation coefficient	P-value
Non-stressed				
p16INK4a, %	0.90 (0.45; 1.65)	1.61 (0.76; 2.71)	0.702	<0.001
TAF, %/nucleus	24.2 (16.9; 31.0)	24.4 (18.5; 32.1)	0.418	<0.001
ROS, FI	1477 (1280; 1706)	1455 (1295; 1762)	-0.111	0.354
SAβ-gal, FI	2959 (2389; 3813)	2987 (2187; 3951)	0.527	<0.001
Stressed				
p16INK4a, %	2.17 (1.10; 4.17)	4.70 (2.33; 6.48)	0.623	<0.001
TAF, %/nucleus	20.6 (14.8; 27.9)	21.9 (16.0; 26.7)	0.414	<0.001
ROS, FI	2003 (1734; 2376)	1972 (1653; 2366)	0.139	0.244
SAβ-gal, FI	4251 (3405; 5345)	4044 (3180; 5233)	0.452	<0.001

N=100. Marker distribution is given as median (IQR). Correlations are Pearson's partial correlation coefficient, adjusted for batch. All markers in experiment a were correlated with the same markers in experiment b. FI: fluorescence intensity. PD: population doublings. P16INK4a: percentage of p16INK4a positive cells; TAF (telomere associated foci): percentage of nuclei with ≥1 TAF/nucleus; ROS: mean fluorescence intensity peak reactive oxygen species; SAβ-gal: median fluorescence intensity peak senescence-associated β galactosidase.

Table 3. Senescence markers and their correlations between short-term versus long-term experiments (2A).

	Distribution of markers			
	Short-term experiment	Long-term experiment	Correlation coefficient	P-value
Non-stressed				
ROS, FI	1559 (1356; 1734)	1500 (1366; 2205)	0.419	0.010
SAβ-gal, FI	2973 (2445; 3732)	3452 (2905; 4660)	-0.009	0.959
Stressed				
ROS, FI	2095 (1753; 2324)	1835 (1553; 2205)	0.426	0.009
SAβ-gal, FI	4171 (3530; 5231)	4090 (3417; 5205)	-0.006	0.972

N=40. Correlations are Pearson's partial correlation coefficient, adjusted for batch. All mean markers of short-term experiments A and B were correlated with the same markers in the long-term experiment. FI: fluorescence intensity. ROS: mean fluorescence intensity peak reactive oxygen species; SAβ-gal: median fluorescence intensity peak senescence-associated β galactosidase.

(Supplementary Table 1) and long-term experiments (Supplementary Table 2) are given. In the short-term experiment each marker was tested against the 3 other markers, both in non-stressed (6 combinations) and stressed condition (6 combinations). Of these 12 senescence marker combinations, 6 were significantly correlated (in non-stressed and stressed conditions 3 each). P16INK4a showed the highest correlations with other markers. In the long-term experiment a total of 6 marker combinations were tested in both non-stressed and stressed conditions of which 3 senescence marker combinations were significantly correlated, mainly with ROS (2 in the non-stressed condition, 1 in the stressed condition).

In vitro senescence markers (both in non-stressed and stressed conditions) were tested for correlation with *in situ* p16INK4a positivity of dermal fibroblasts (Table 4). No significant correlations were observed between *in situ* p16INK4a positivity and any of the *in vitro* senescence markers (ROS, TAF, SAβ-gal or p16INK4a). In Figure 2, *in vitro* p16INK4a positivity in non-stressed and stressed conditions are plotted against *in situ* p16INK4a positivity of dermal fibroblasts, further showing this lack of intra-individual correlation.

Table 4. Intra-individual correlations: in vitro senescence markers versus in situ p16INK4a positive human fibroblasts (3B).

	Coefficient	P-value
Non-stressed		
p16INK4a	0.064	0.655
TAF	-0.030	0.835
ROS	-0.097	0.498
SAβ-gal	-0.042	0.772
Stressed		
p16INK4a	0.091	0.527
TAF	0.014	0.922
ROS	-0.095	0.506
SAβ-gal	0.023	0.871

Values are depicted as Pearson's partial correlation coefficient, adjusted for batch. Data for *in situ* and *in vitro* senescence markers were available for N=52 donors. P16INK4a positive dermal fibroblasts: number of positive cells per 1mm2 dermis. All *in vitro* variables are the mean of short-term experiments. P16INK4a: % of p16 positive cells; ROS: mean fluorescence intensity peak; SAβ-gal: median fluorescence intensity peak; telomere-associated foci (TAF): % of nuclei with ≥1 53BP1 foci per nucleus, coinciding with telomeric DNA.

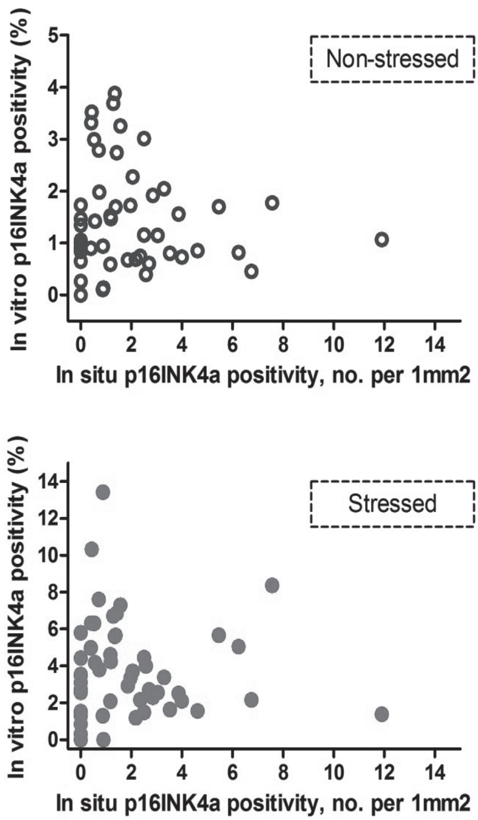

Figure 2. Intra-individual correlations: in vitro versus in situ p16INK4a positivity
Each dot represents an individual donor, N=52. *In vitro* p16INK4a positivity: percentage of p16INK4a positive cells - mean of experiments A and B. *In situ* p16INK4a positivity: number of p16INK4a positive cells per $1mm^2$ dermis.

Discussion

In individual donors the same senescence markers more than half correlations were significantly correlated *in vitro* (1A) between duplicate experiments and (2A) between short-term versus long-term experiments, with high correlation coefficients. Within the experiments the different senescence markers were significantly correlated to each other, within both the short-term (1B) and long-term experiments (2B), in half of the correlations tested. On average correlation coefficients were lower than for the same markers correlations. Assessment of (3B) correlations between *in situ* p16INK4a positivity with different *in vitro* senescence markers showed a lack of correlation, both with *in vitro* markers in non-stressed and stressed conditions.

The significant correlations of the same markers between duplicate experiments (in the short-term experiments) and between the short-term and long-term experiments indicate senescence markers are reasonably stable *in vitro* under standardized conditions. Most correlations between duplicate experiments show that the experiments were adequately reproducible, and the influence of technical issues is limited. However, ROS showed poor reproducibility between duplicates which hampers interpretation of other tested associations with ROS. Although the same markers were also correlated between the short-term and long-term experiments, this was less often the case than for the between duplicate experiment correlations. This finding is not surprising, as cell strains of an individual could respond to short-term and long-term stress differently. Indeed, in a previous study the relation between results of short-term and long-term experiments of senescence markers was also not always consistent: SAβ-gal in the stressed condition in the short-term experiment was negatively associated with the maximum replicative capacity of the strain (a long-term outcome), whereas a positive but nonsignificant trend was seen in the non-stressed condition [22].

Because senescence can be triggered in response to multiple factors and be induced through different pathways, it has been advised to use a marker of cell cycle arrest plus at minimum two senescence markers [23]. On individual cell level there is no hundred percent concordance of multiple different markers, as is the case for e.g. p16 and SAβ-gal [24], p16 and p21 [25], and γH2AX foci and p21 [26]. One of these studies also showed that SAβ-gal, senescence associated heterochromatin foci and the combination of Ki67 with γH2A.X foci were superior to other marker combinations in predicting growth curves of MRC5 fibroblast cultures [26]. A recent review [27] discussed the shortcomings of frequently used markers to assess *in vitro* senescence and particularly the difficulties of using these markers to detect *in vivo* senescence. We confirm the importance of this stance based on our results on correlations between different senescence markers. Only a half of the tested senescence marker combinations were significantly correlated within the experiment. The *in vitro* senescence marker that was most correlated to other *in vitro* senescence markers was p16INK4a. This was also the marker with the highest correlation coefficient between experiment a and b (between duplicate experiments). This stableness of duplicates could thus explain the observation that p16INK4a correlated most frequently to the other markers.

A recent review has shown that while some *in vitro* observations on fibroblast ageing have also been observed *in situ* in skin tissue, many observations have not been tested *in situ* yet [14]. To our knowledge, this is the first study in humans to directly correlate senescence markers *in* *vitro* and *in situ* in cultured fibroblasts and biopsies from the same individual to assess whether both are reflective of a common (epi)genetic propensity to induce cellular senescence. In mice microRNA expression profiles were compared in cultured cells and aged mouse brains, which showed only very little similarities in expression [28]. The lack of correlation between *in vitro* and *in situ* senescence markers we have observed, was not altogether surprising. While experimental set-ups allow controlling of many variables, this also decreases the natural context of human cells. It has been observed that the process of establishing fibroblasts strains from skin biopsies itself can result in a selection of a subgroup of fibroblasts. Fibroblasts from subsequent outgrowths of single skin biopsies were shown to differ in their proliferation capacities [29]. Outgrowth from different dermal layers results in higher culture survival time in fibroblasts from the papillary dermis compared to reticular dermis [30;31]. Also, different culturing conditions were shown to have effects on replicative lifespan [32], and the process of cell culture itself has been suggested to drive some of the senescence findings *in vitro* [33;34]. We used atmospheric oxygen culture conditions which in itself is thought to be a stressor [35]. This can be seen in our scatterplot showing some individuals with high p16INK4a positivity *in situ* and low p16INK4a positivity *in vitro*, which might have resulted from selection of senescence resistant fibroblasts during expansion. Therefore, *in vitro* experimental data from cells derived from one individual might not be representative for the cell populations in their tissues under *in vivo* conditions. Due to this lack of intra-individual correlation we demonstrated here, problems might arise in extrapolating observations from *in vitro* experiments to *in vivo* implications. On the other hand, perhaps the *in vitro* characteristics of the selected subpopulation of primary cells could still reflect *in vivo* cellular capacities in specific situations, such as disease or in the presence of environmental stressors.

This study uses unique data on multiple senescence markers *in vitro* established from 100 individual fibroblast strains. We regard the high number of fibroblast strains as a strong point of this study. All culturing procedures and experiments were conducted under highly standardized conditions. A limitation of the study is that we did not include a marker for proliferation such as Ki-67. The association between *in vitro* and *in situ* p16INK4a positivity could only be evaluated in 52 subjects that had both measurements, and in a middle-aged age range. While this limited the power to detect significant associations, we could also not discern any trend for correlation. Another limitation of the present study is at the same time a limitation of many human studies in general: we have detected p16INK4a *in situ*, but cannot (yet) study cellular senescence *in vivo* in humans. Studies aiming to detect cellular senescence *in vivo* in animal models have shown that inter-individual variability is high, especially at older ages [36;37]. Inter-individual variation of senescence might also be influenced by genetic polymorphisms. In human peripheral blood T-cells, one atherosclerotic disease-related SNP was shown to associate with decreased expression of INK4/ARF transcripts [38]. Further analysis of intra-individual correlation between *in vitro* and *in vivo* senescence associated markers within animal models could help to better explore this lack of correlation. Another limitation of our study is that for *in situ* measurements we only have data of one senescence marker, p16INK4a, whilst consensus is lacking on which (panel of) markers should be used to appropriately detect senescent cells *in situ*.

In conclusion this study shows unique data on senescence markers in human fibroblasts *in vitro* and *in situ* in human skin tissue, which can help in interpreting *in vitro* senescence results. On an individual donor level, *in vitro* markers of senescence correlated within and between experiments, but *in vitro* senescence markers and *in situ* fibroblast p16INK4a positivity were not correlated. Therefore, while *in vitro* studies on cellular senescence can provide us with valuable mechanistic insights, the validity of its use as a model to study the natural variation in human aging should be questioned and further tested. Caution is warranted when extrapolating results from *in vitro* studies towards *in vivo* implications.

Acknowledgements

We would like to thank Joke Blom, Pim Dekker and Corine de Koning-Treurniet for their work in the laboratory; and Barbara Strongitharm and William Parish for the p16INK4a counts.

This work was funded by the Innovation Oriented Research Program on Genomics (SenterNovem; IGE01014 and IGE5007), The Netherlands Genomics Initiative/Netherlands Organization for

Scientific Research (NGI/NWO; 05040202 and 050-060-810), Unilever PLC and the EU funded Network of Excellence Lifespan (FP6 036894).

Supplementary table 1. Correlations between the different in vitro markers within the short-term experiment (1B).

	p16INK4a	TAF	ROS	SAβ-gal
Non-stressed				
p16INK4a	n/a	-	-	-
TAF	**0.253 (0.011)**	n/a	-	-
ROS	**0.321 (0.001)**	-0.048 (0.636)	n/a	-
SAβ-gal	0.151 (0.134)	0.054 (0.598)	**0.232 (0.021)**	n/a
Stressed				
p16INK4a	n/a	-	-	-
TAF	**0.227 (0.024)**	n/a	-	-
ROS	**0.299 (0.003)**	0.038 (0.706)	n/a	-
SAβ-gal	0.162 (0.109)	**0.215 (0.032)**	0.115 (0.255)	n/a

N=100. Values are depicted as Pearson's correlation coefficient (P-value), partial correlation with adjustment for batch. n/a: not applicable. P16INK4a: % of p16 positive cells; Telomere-associated foci (TAF): % of nuclei with ≥1 53BP1 foci coinciding with telomeric DNA per nucleus; ROS: mean fluorescence intensity peak; SAβ-gal: median fluorescence intensity peak. All *in vitro* variables are the mean of duplicate experiments.

Supplementary table 2. Correlations between the different in vitro markers within the long-term experiment (2B).

	ROS	SAβ-gal	Telomere shortening
Non-stressed			
ROS	n/a	-	-
SAβ-gal	**0.341 (0.042)**	n/a	-
Telomere shortening	**-0.466 (0.004)**	-0.011 (0.949)	n/a
Stressed			
ROS	n/a	-	-
SAβ-gal	**0.436 (0.008)**	n/a	-
Telomere shortening	-0.220 (0.198)	-0.030 (0.862)	n/a

N=40. Values are depicted as Pearson's correlation coefficient (P-value), partial correlation with adjustment for batch. n/a: not applicable. ROS: mean fluorescence intensity peak; SAβ-gal: median fluorescence intensity peak; Telomere shortening: percentage of shortening per population doubling

References

(1) Hayflick L, Moorhead PS. The serial cultivation of human diploid cell strains. *Exp Cell Res* 1961;25:585-621.

(2) Hayflick L. The limited in vitro lifetime of human diploid cell strains. *Exp Cell Res* 1965;37:614-636.

(3) Burton DG, Krizhanovsky V. Physiological and pathological consequences of cellular senescence. *Cell Mol Life Sci* 2014;71:4373-4386.

(4) Baker DJ, Wijshake T, Tchkonia T et al. Clearance of p16Ink4a-positive senescent cells delays ageing-associated disorders. *Nature* 2011;479:232-236.

(5) Storer M, Mas A, Robert-Moreno A et al. Senescence is a developmental mechanism that contributes to embryonic growth and patterning. *Cell* 2013;155:1119-1130.

(6) Munoz-Espin D, Canamero M, Maraver A et al. Programmed cell senescence during mammalian embryonic development. *Cell* 2013;155:1104-1118.

(7) Coppe JP, Patil CK, Rodier F et al. Senescence-associated secretory phenotypes reveal cell-nonautonomous functions of oncogenic RAS and the p53 tumor suppressor. *PLoS Biol* 2008;6:2853-2868.

(8) Krizhanovsky V, Yon M, Dickins RA et al. Senescence of activated stellate cells limits liver fibrosis. *Cell* 2008;134:657-667.

(9) Dimri GP, Lee X, Basile G et al. A biomarker that identifies senescent human cells in culture and in aging skin in vivo. *Proc Natl Acad Sci U S A* 1995;92:9363-9367.

(10) Pazolli E, Stewart SA. Senescence: the good the bad and the dysfunctional. *Curr Opin Genet Dev* 2008;18:42-47.

(11) Lee BY, Han JA, Im JS et al. Senescence-associated beta-galactosidase is lysosomal beta-galactosidase. *Aging Cell* 2006;5:187-195.

(12) Moiseeva O, Bourdeau V, Roux A, Deschenes-Simard X, Ferbeyre G. Mitochondrial dysfunction contributes to oncogene-induced senescence. *Mol Cell Biol* 2009;29:4495-4507.

(13) Sharpless NE, Sherr CJ. Forging a signature of in vivo senescence. *Nat Rev Cancer* 2015;15:397-408.

(14) Tigges J, Krutmann J, Fritsche E et al. The hallmarks of fibroblast ageing. *Mech Ageing Dev* 2014;138:26-44.

(15) Bootsma-van der Wiel A, Gussekloo J, de Craen AJ, Van EE, Bloem BR, Westendorp RG. Common chronic diseases and general impairments as determinants of walking disability in the oldest-old population. *J Am Geriatr Soc* 2002;50:1405-1410.

(16) Maier AB, le CS, de Koning-Treurniet C, Blom J, Westendorp RG, van HD. Persistence of high-replicative capacity in cultured fibroblasts from nonagenarians. *Aging Cell* 2007;6:27-33.

(17) Schoenmaker M, de Craen AJ, de Meijer PH et al. Evidence of genetic enrichment for exceptional survival using a family approach: the Leiden Longevity Study. *Eur J Hum Genet* 2006;14:79-84.

(18) Dekker P, Gunn D, McBryan T et al. Microarray-based identification of age-dependent differences in gene expression of human dermal fibroblasts. *Mech Ageing Dev* 2012;133:498-507.

(19) Dekker P, van Baalen LM, Dirks RW et al. Chronic inhibition of the respiratory chain in human fibroblast cultures: differential responses related to subject chronological and biological age. *J Gerontol A Biol Sci Med Sci* 2012;67:456-464.

(20) Waaijer MEC, Croco E, Westendorp RGJ et al. DNA damage markers in dermal fibroblasts in vitro reflect chronological donor age. *Aging*. In press.

(21) Waaijer ME, Parish WE, Strongitharm BH et al. The number of p16INK4a positive cells in human skin reflects biological age. *Aging Cell* 2012;11:722-725.

(22) Dekker P, de Lange MJ, Dirks RW et al. Relation between maximum replicative capacity and oxidative stress-induced responses in human skin fibroblasts in vitro. *J Gerontol A Biol Sci Med Sci* 2011;66:45-50.

(23) Kuilman T, Michaloglou C, Mooi WJ, Peeper DS. The essence of senescence. *Genes Dev* 2010;24:2463-2479.

(24) Noppe G, Dekker P, de Koning-Treurniet C et al. Rapid flow cytometric method for measuring senescence associated beta-galactosidase activity in human fibroblasts. *Cytometry A* 2009;75:910-916.

(25) Herbig U, Jobling WA, Chen BP, Chen DJ, Sedivy JM. Telomere shortening triggers senescence of human cells through a pathway

involving ATM, p53, and p21(CIP1), but not p16(INK4a). *Mol Cell* 2004;14:501-513.
(26) Lawless C, Wang C, Jurk D, Merz A, Zglinicki T, Passos JF. Quantitative assessment of markers for cell senescence. *Exp Gerontol* 2010;45:772-778.
(27) Sharpless NE, Sherr CJ. Forging a signature of in vivo senescence. *Nat Rev Cancer* 2015;15:397-408.
(28) Bigagli E, Luceri C, Scartabelli T et al. Long-term Neuroglial Cocultures as a Brain Aging Model: Hallmarks of Senescence, MicroRNA Expression Profiles, and Comparison With In Vivo Models. *J Gerontol A Biol Sci Med Sci* 2016;71:50-60.
(29) Balin AK, Fisher AJ, Anzelone M, Leong I, Allen RG. Effects of establishing cell cultures and cell culture conditions on the proliferative life span of human fibroblasts isolated from different tissues and donors of different ages. *Exp Cell Res* 2002;274:275-287.
(30) Azzarone B, Macieira-Coelho A. Heterogeneity of the kinetics of proliferation within human skin fibroblastic cell populations. *J Cell Sci* 1982;57:177-187.
(31) Harper RA, Grove G. Human skin fibroblasts derived from papillary and reticular dermis: differences in growth potential in vitro. *Science* 1979;204:526-527.
(32) Unterluggauer H, Hutter E, Voglauer R et al. Identification of cultivation-independent markers of human endothelial cell senescence in vitro. *Biogerontology* 2007;8:383-397.
(33) Rubin H. Cell aging in vivo and in vitro. *Mech Ageing Dev* 1997;98:1-35.
(34) Berkenkamp B, Susnik N, Baisantry A et al. In vivo and in vitro analysis of age-associated changes and somatic cellular senescence in renal epithelial cells. *PLoS One* 2014;9:e88071.
(35) Betts DH, Perrault SD, King WA. Low oxygen delays fibroblast senescence despite shorter telomeres. *Biogerontology* 2008;9:19-31.
(36) Burd CE, Sorrentino JA, Clark KS et al. Monitoring tumorigenesis and senescence in vivo with a p16(INK4a)-luciferase model. *Cell* 2013;152:340-351.
(37) Sorrentino JA, Krishnamurthy J, Tilley S, Alb JG, Jr., Burd CE, Sharpless NE. p16INK4a reporter mice reveal age-promoting effects of environmental toxicants. *J Clin Invest* 2014;124:169-173.
(38) Liu Y, Sanoff HK, Cho H et al. INK4/ARF transcript expression is associated with chromosome 9p21 variants linked to atherosclerosis. *PLoS One* 2009;4:e5027.

Part II

Part II

Does skin tissue mirror the aging process?

Chapter 4

Chapter 4

Morphometric skin characteristics dependent on chronological and biological age: the Leiden Longevity Study

M.E.C. Waaijer, D.A. Gunn, S.D. Catt, M. van Ginkel, A.J.M. de Craen, N.M. Hudson, D. van Heemst, P.E. Slagboom, R.G.J. Westendorp, A.B. Maier

Age (Dordr). 2012 Dec;34(6):1543-52

Abstract

The effect of chronological age on skin characteristics is readily visible and its underlying histological changes have been a field of study for several years. However, the effect of biological age (i.e. a person's rate of ageing compared to their chronological age) on the skin has so far only been studied in facial photographs. Skin biopsies obtained from middle aged offspring of nonagenarian siblings that are genetically enriched for longevity were compared to their partners who represent the general Dutch population. Though of the same chronological age, the offspring were previously observed to be of a younger biological age than their partners. The biopsies were analysed on several aspects epidermal and elastic fibre morphology. We investigated whether these skin characteristics were dependent on chronological age, familial longevity (the difference between the offspring and partners) and Framingham heart risk scores, adjusted for external stressors. A decreased thickness and flattening of the epidermis as well as an increased amount of elastic fibres in the reticular dermis were observed with chronological age ($P<0.001$, $P<0.001$ and $P=0.03$ respectively), but no effect of familial longevity was found. The Framingham heart risk score was associated with some skin characteristics. A slower rate of skin ageing does not mark offspring from nonagenarian siblings. Epidermal and elastic fibre morphometric characteristics are not a potential marker for familial longevity in middle aged subjects enriched for familial longevity.

Introduction

As the largest organ of the human body, the skin constitutes an important functional and cosmetic interface with the exterior world. The disintegration of this protective barrier with age is partly visible as wrinkling and loss of elasticity. Although ageing is associated with a general progressive loss of skin integrity, significant inter-individual differences exist. Apart from the cosmetic aspect, these inter-individual differences provide a potential biomarker for biological age as a lower perceived age based on facial photographs is associated with survival, even after correction for gender and chronological age [1]. The inter-individual differences in skin features can be partly explained by external factors such as smoking, alcohol and sun damage [2]. However, there is increasing evidence that many of these differences in perceived age are genetically determined [1;3].

Wrinkling and the loss of elasticity are the result of several age related changes in the underlying histological structure. The epidermis shows a flattening at the epidermal-dermal junction and a decreasing thickness with increasing age [4-7]. Within the dermis, the amount and length of mature elastic fibres in the papillary dermis have been found to increase with chronological age [8]. In the reticular dermis the length of elastic fibres and the percentage of elastin at the upper inner arm have all been found to increase with age [8;9]. In addition, smoking has been positively correlated with an increased number and amount of elastic fibres in the reticular dermis of the upper inner arm [10], high-lighting the importance of controlling for confounding factors in studies of skin morphometric characteristics.

Within the present study we have investigated the effect of chronological and biological age on epidermal histologic characteristics and morphology of elastic fibres in the upper inner arm. To compare with biological age, we used two established markers for biological age, the Framingham cardiovascular disease (CVD) risk score [11] and familial longevity. Familial longevity was defined as differences between middle aged offspring from long lived nonagenarian siblings and, as controls, their partners. Though of the same chronological age, these offspring have been previously observed to be of a younger biological age than their partners as reflected by their lower mortality rate [12], beneficial glucose and lipid metabolism, preservation of insulin sensitivity and resistance to cellular stress [13-15]. We questioned whether a slower rate of skin ageing marks middle aged offspring of nonagenarian siblings compared to their partners.

Methods

Study cohort

In the Leiden Longevity Study genetically enriched subjects for familial longevity are compared with their partners to determine the genetic factors contributing to longevity.

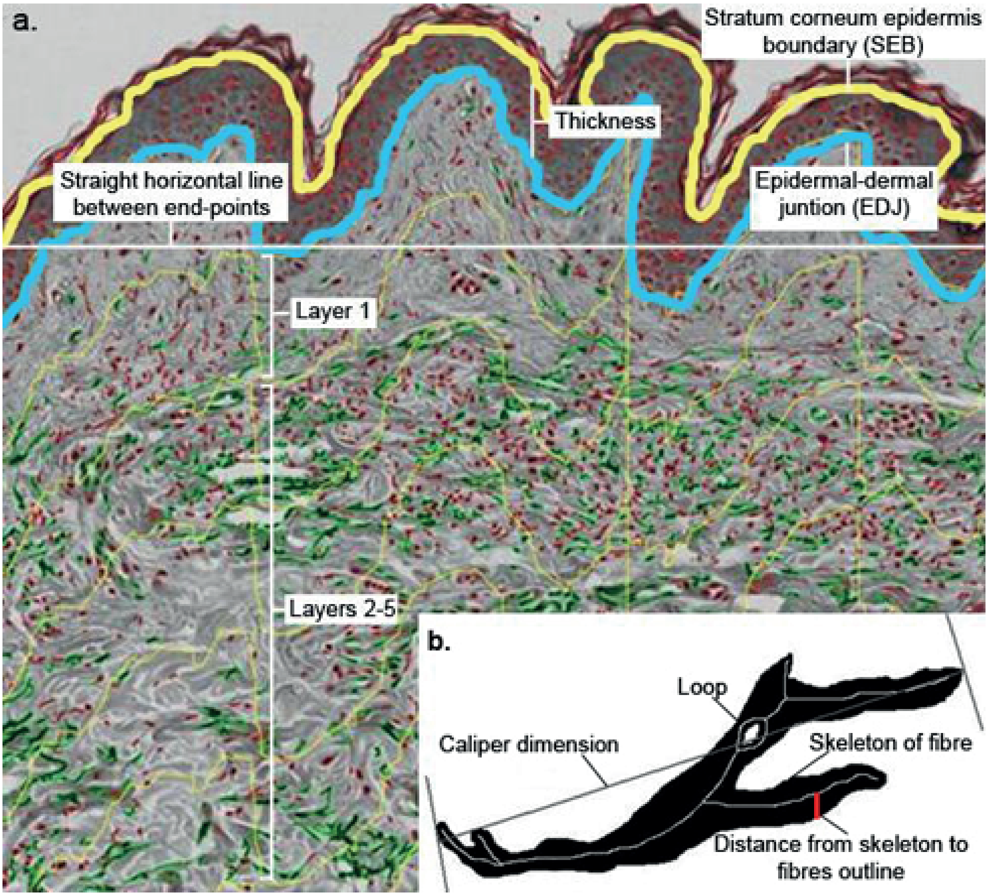

Figure 1. Measurements on the epidermis and dermis

a. Thickness based on the epidermal-dermal junction (EDJ): area covered by epidermis (area between the yellow and light blue lines) divided by the EDJ (light blue) length given in μm. Curvature based on the stratum corneum epidermis boundary (SEB): the ratio of the length of the straight horizontal line between the margins (white) and the length of the SEB (yellow). Area covered by elastic fibres (green: in-plane, red: end-on) given in μm^2. Layer 1: papillary dermis, layers 2 to 5: reticular dermis.

b. Area of a single elastic fibre: amount of area the fibre covers (μm^2). Length of an elastic fibre: length of the skeleton of the fibre (white) without half of the loop size if present plus for each end-point of the line the distance to the nearest point on the fibre's outline (μm). Thickness of an elastic fibre: ratio between size and length (nm). Curl of an elastic fibre: the ratio between the fibre's length and the maximum caliper dimension.

Four hundred and twenty one families consisting of 943 long-lived Caucasian siblings with 1671 of their offspring and 745 of the partners thereof were included in this cohort. The offspring carries on average 50% of the genetic propensity of their long lived parent [12]. Their partners, with whom most have shared the same environment for decades, were included as matched controls. There was no selection on demographic or health characteristics [12;13]. The current study includes 150 offspring and 150 partners thereof, from whom skin biopsies were taken in the period from November 2006 to May 2008. Of these 300 subjects, one subject eventually refused to have a biopsy taken and the biopsies of 13 subjects were excluded after quality check. Therefore, for the epidermis and layer 1 of the dermis data was available on 286 subjects. Nine subjects lacked data on layers 2 to 5 of the dermis and were therefore excluded from that analysis. The Medical Ethical Committee of the Leiden University Medical Center approved the study. Declaration of Helsinki protocols were followed and written informed consent was obtained from all participants.

Morphometric analysis of the skin

Skin biopsies (4mm) were taken from the sun-protected site of the inner upper arm, and fixed in formalin (Sigma) overnight (18-24 hours). After fixation, the biopsies were washed in fresh phosphate buffered saline twice and then dehydrated in 70% alcohol and stored at room temperature. The samples were embedded in paraffin wax and cut into sections of 4μm. Two sections of each biopsy were stained with Orcein dye. Hematoxylin and eosin staining (Sigma) was performed for quality checking purposes. A Leica DM 1000 microscope, with a Leica DFC420 Camera and Leica Application Suite Software was used to capture images of the slides with an objective magnification of x10. Image capture and analysis were performed blind to age, gender and the offspring/partner status of the subjects. To analyse the image data semi-automatically, image analysis software was constructed. The stratum corneum and epidermal-dermal boundary in the image were automatically delineated by the software. The epidermis was identified by its darker nature using an intensity threshold. The stratum corneum epidermis boundary was identified through absolute intensity and degree of striation (due to its layered nature) which was quantified using a variance filter. Thereafter, manual refinement was performed to ensure accurate delineation of the epidermal boundaries. In addition, manual exclusion of regions within the images were performed if they contained large structures (hair follicles, blood vessels, glands) or large areas of non-dermis i.e. blank areas, large gaps or tears in tissue and clusters of small non-dermis areas. Morphometric measurements of the epidermis and elastic fibres are depicted in Fig. 1. Epidermal measurements included the thickness of the epidermis derived from the area covered by epidermis divided by the length of the epidermal-dermal junction (EDJ). Furthermore the curvature in the epidermis was defined as the ratio of a straight line between the horizontal margins of the epidermis over the length of the stratum corneum-epidermis boundary (SEB). Within the dermis, the area covered by the elastic fibres, their number (both corrected for the size of image area they were measured in) and the morphometrical characteristics of individual elastic fibres were measured. These morphometrical characteristics included the area (μm^2), length (μm), thickness (μm) and the curl of an elastic fibre (defined by the ratio between its length and the caliper dimension). The elastic fibres were identified by applying an intensity threshold on the green channel of the red-green-blue color image. Resolving the measurements by depth was dealt with by using the epidermal-dermal junction as the zero-depth reference point. The dermis was divided into depth layers of 100µm. For each pixel on the epidermal-dermal junction the corresponding pixel 100µm lower on the y-axis was determined. Layer 1 represents the papillary dermis, layers 2 to 5 the reticular dermis. 9 biopsies had too little depth to supply data for layer 2 to 5.

Potential confounders

For each subject, demographic characteristics and facial photographs as well as factors known to influence skin characteristics were available (e.g. smoking and alcohol use). To control for potential sun-exposure effects on the arm, the photographs of the face were assessed by a dermatologist blind to age, gender and offspring or partner status to determine photo/sun-damage scores [3;16]. This nine-point (no photodamage to severe photodamage) photonumeric scale assesses the severity of cutaneous photodamage. Information on medical history was obtained from the participants' treating physicians, including history of myocardial infarction, stroke, hypertension, diabetes, malignancy, rheumatoid arthritis and chronic obstructive pulmonary disease (COPD). Information on medication use was obtained from the participants' pharmacists and divided in categories composed of anti-thrombotic, anti-COPD, anti-diabetic, other endocrine and nervous system and cardiovascular drugs including lipid lowering medication. Total cholesterol and HDL-cholesterol used for the Framingham CVD risk score were measured in non-fasted serum samples using the Hitachi Modular P 800 from Roche, Almere, Netherlands.

Statistics

All analyses were performed using SPSS 16.0 data editor software. The association of skin morphometric characteristics with chronological age and with offspring and partners status was analysed by linear regression using three different models. Chronological age: model 1 was adjusted for gender, model 2 was adjusted for the same covariates as for model 1 with further adjustment for external factors (smoking, alcohol and sun damage), model 3 additionally for the number of co-morbidities plus the number of medication categories. Familial longevity, comparing offspring (0) and partners (1): model 1 was adjusted for age and gender, models 2 and 3 were similar to those of chronological age.

Table 1. Characteristics of subjects.

	Offspring N=143	Partners N=143
Demographic data		
Female, %	43.4	58
Age, years	63.3 (6.0)	63.2 (7.1)
Body composition		
Height, cm	172.2 (9.1)	170.7 (8.6)
BMI, kg/m^2	26.6 (3.8)	26.8 (4.1)
Fat, %	28.4 (8.0)	31.4 (8.2)
Lean mass, %	67.5 (7.6)	64.6 (7.7)
Co-morbidities, no. (%)[a]		
MI	1 (0.8)	4 (3.1)
CVA	2 (1.6)	6 (4.7)
Hypertension	28 (22.0)	38 (29.7)
Diabetes mellitus	4 (3.2)	13 (10.2)
Malignancy	4 (3.1)	7 (5.6)
COPD	7 (5.5)	4 (3.1)
Rheumatoid arthritis	0 (0.0)	0 (0.0)
Number of co-morbidities (0-7)	0.3 (0.6)	0.6 (0.8)
Framingham Heart Risk[b]	16.8 (8.2)	16.5 (9.1)
Medication		
Medication categories[a]	0.6 (0.8)	0.8 (1.0)
Hormonal replacement therapy (former and current), no. (%)[e]	8 (14.0)	9 (11.4)
Intoxications[c]		
Users of alcohol, no. (%)	109 (78.4)	110 (79.1)
Former and/or current smoking, no. (%)	85 (61.6)	100 (71.9)
Photodamage score[d]	4.8 (1.2)	4.8 (1.2)
Menopausal status, no. (%)[e]		
Premenopausal	0 (0.0)	7 (8.8)
Perimenopausal	0 (0.0)	5 (6.3)
Postmenopausal	58 (100.0)	68 (85.0)

[a]N=129, [b]N=182, [c]N=268, [d]N=263, [e]N=58 and 80 (offspring, partners). Values are given as mean (SD) if not otherwise stated. BMI: body mass index, MI: myocardial infarction, CVA: cerebrovascular accident, COPD: chronic obstructive pulmonary disease. SD: standard deviation. Medication categories composed of anti-thrombotic, anti-COPD, anti-diabetic, other endocrine and nervous system and cardiovascular drugs (including lipid lowering medication). Photodamage was determined by scoring photographs of subjects with a nine-point photonumeric standard scale (no photodamage to severe photodamage).

To study the association between cardiovascular disease risk and morphometric characteristics of the skin, the Framingham CVD risk score was calculated as previously described [11]. Model 1 of the linear regression consisted of the 10-year risk prediction of cardiovascular disease, model 2 adjusted for the offspring/partner status, model 3 was additionally adjusted for sun damage. P-values of less than 0.05 were considered to be significant.

Results

In total, 286 subjects were included in the analysis after a quality check of the biopsies, consisting of 141 males and 145 females aged between 44 and 81 years. The characteristics of the subjects are summarized in Table 1. The offspring had experienced less age related diseases such as myocardial infarction, hypertension and type 2 diabetes mellitus. Use of hormonal replacement therapy was not different between the offspring and partners, however menopausal state differed significantly. Female partners were more frequently premenopausal compared to female offspring, most likely due to their younger age.

Table 2 shows the association between chronological age and morphometric characteristics of the epidermis and elastic fibres in the dermis with and without adjustment for potential confounders (estimates are given in the supplementary Table 1). With chronological age, the epidermal thickness significantly decreased whereas the curvature parameter increased significantly, indicating a flattening of the epidermis (both $P<0.001$). The decreasing thickness and the overall flattening of the epidermis with chronological age remained significant after adjustment for gender, external factors (smoking, alcohol and sun damage) and health status ($P=0.01$ and $P=0.001$ respectively). In the papillary dermis (layer 1), a trend towards a larger area covered by elastic fibres ($P=0.06$), a higher number of elastic fibres ($P=0.07$), a larger area covered by a single elastic fibre ($P=0.05$), an increased length of an elastic fibre ($P=0.08$) and more curliness of an elastic fibre ($P=0.02$) with chronological age was observed. However, these findings were diminished after adjustment for external factors and health status. The area covered by the elastic fibres and the number of elastic fibres in the reticular dermis (layers 2 to 5) were positively correlated with chronological age ($P=0.001$ and $P<0.001$ respectively). The increase in number of elastic fibres remained significant after adjustment for potential confounders ($P=0.03$). None of the other elastic fibre morphometric characteristics were significantly associated with chronological age.

Table 3 shows the effect of familial longevity status, i.e. offspring and partner comparison, on the epidermal and elastic fibre morphometric characteristics adjusted for potential confounders (estimates are given in the supplementary Table 2). No differences between

Table 2. Chronological age and morphometric skin characteristics.

	Chronological age (years)						
	1st quartile M:45.5-59.9 F:44.1-58.5	2nd quartile M:59.9-64.6 F:58.5-62.4	3rd quartile M:64.6-68.8 F:62.4- 66.8	4th quartile M:68.8-81.3 F:66.8-78.3	P-value Model 1	P-value Model 2	P-value Model 3
Epidermis[a]							
Thickness based on EDJ, μm	42.4 (0.69)	42.6 (0.88)	40.2 (0.76)	38.2 (0.78)	<0.001	<0.01	0.01
Curvature based on SEB[c]	803.2 (8.50)	824.5 (6.70)	849.9 (7.52)	839.0 (9.41)	<0.001	0.001	0.001
Dermis							
Elastic fibres, layer 1[a]							
Area covered by fibres[c]	23.7 (1.80)	28.0 (2.33)	27.9 (2.99)	29.1 (2.70)	0.06	0.26	0.67
Number of fibres	43.4 (3.92)	53.6 (5.21)	50.9 (5.01)	52.8 (5.06)	0.07	0.18	0.59
Area of a single fibre, μm^2	27.5 (0.79)	28.7 (0.96)	29.1 (1.04)	29.9 (1.42)	0.05	0.35	0.68
Length of a fibre, μm	15.3 (0.41)	15.8 (0.43)	16.2 (0.44)	16.0 (0.50)	0.08	0.30	0.66
Thickness of a fibre, nm	1928 (32.6)	1886 (21.4)	1893 (15.6)	1910 (23.0)	0.43	0.31	0.42
Curl of a fibre[c]	926.1 (4.97)	906.1 (8.10)	907.1 (5.73)	907.3 (7.06)	0.02	0.10	0.24
Elastic fibres, layer 2-5[c]							
Area covered by fibres[c]	57.3 (2.76)	67.1 (3.38)	71.5 (3.92)	72.5 (4.84)	0.001	0.02	0.14
Number of fibres	85.3 (3.47)	95.6 (3.38)	103.2 (4.16)	104.4 (4.84)	<0.001	0.01	0.03
Area of a single fibre, μm^2	47.8 (1.50)	51.4 (2.77)	51.3 (1.73)	49.2 (2.61)	0.29	0.31	0.82
Length of a fibre, μm	20.9 (0.47)	21.5 (0.68)	21.8 (0.49)	20.6 (0.76)	0.68	0.70	0.74
Thickness of a fibre, nm	2153 (18.2)	2177 (22.3)	2175 (18.3)	2155 (25.8)	0.35	0.26	0.74
Curl of a fibre[c]	909.4 (4.02)	903.5 (4.73)	902.5 (5.45)	898.3 (8.40)	0.49	0.97	0.98

[a]1[st] quartile: N=71, 2[nd] quartile: N= 72, 3[rd] quartile N=72, 4[th] quartile: N=71. [b]1[st] quartile: N=69, 2[nd] quartile: N= 72, 3[rd] quartile N=68, 4[th] quartile: N=68. M=male, F=female, [c]=x10^3. Values are given as mean (SE). EDJ=epidermal-dermal junction, SEB=stratum corneum epidermis boundary. P values are derived from linear regression analysis. Model 1: gender adjusted, model 2: as model 1 plus external factors (smoking, alcohol and sun damage), model 3: as model 2 plus health status (no. of co-morbidities, no. of medication categories). Estimates of the different models are given in supplementary table 1.

offspring and partners were observed in any of the epidermal and elastic fibre characteristics before and after adjusting for chronological age, gender, external factors and health status. Stratification by chronological age did not change the results (data not shown).

To determine whether skin morphometric characteristics were associated with cardiovascular disease risk, epidermal and elastic fibre characteristics were related to the Framingham CVD risk scores (10-year risk predictions for cardiovascular disease, FHR). The results are shown in supplementary Tables 3 and 4 for the epidermis and elastic fibres respectively. Epidermal and reticular elastic fibre (layer 2 to 5) morphometric characteristics were not significantly associated with the cardiovascular risk profile. The area covered by elastic fibres and the

Table 3. Comparison of offspring and partners for morphometric skin characteristics.

	Offspring	Partners	P-value Model 1	P-value Model 2	P-value Model 3
Epidermis[a]					
Thickness based on EDJ, µm	40.9 (0.56)	40.9 (0.58)	0.94	0.46	0.87
Curvature based on SEB[c]	832.2 (5.44)	826.2 (6.28)	0.62	0.22	0.86
Dermis					
Elastic fibres, layer 1[a]					
Area covered by fibres[c]	27.1 (1.89)	27.2 (1.64)	0.70	0.35	0.56
Number of fibres	49.9 (3.55)	50.5 (3.29)	0.91	0.91	0.91
Area of a single fibre, μm^2	29.1 (0.83)	28.5 (0.69)	0.31	0.18	0.35
Length of a fibre, µm	16.0 (0.32)	15.6 (0.31)	0.18	0.15	0.32
Thickness of a fibre, nm	1892 (12.1)	1916 (20.5)	0.42	0.64	0.40
Curl of a fibre[c]	909.7 (3.48)	913.5 (5.64)	0.53	0.15	0.16
Elastic fibres, layers 2-5[b]					
Area covered by fibres[c]	66.3 (2.55)	67.7 (2.64)	0.95	0.65	0.86
Number of fibres	97.1 (2.76)	97.1 (2.99)	0.89	0.32	0.52
Area of a single fibre, μm^2	50.7 (1.42)	49.2 (1.72)	0.42	0.41	0.35
Length of a fibre, µm	21.5 (0.42)	21.0 (0.45)	0.27	0.31	0.16
Thickness of a fibre, nm	2186 (13.4)	2145 (16.4)	0.15	0.12	0.21
Curl of a fibre[c]	909.1 (3.00)	897.9 (4.94)	0.15	0.14	0.15

[a]N=286, [b]N=277, [c]= x10^3. Values are given as mean (SE). P values are derived from linear regression analysis. EDJ=epidermal-dermal junction, SEB=stratum corneum epidermis boundary. Model 1: partner (1) and offspring (0), age and gender, model 2: as model 1 plus external factors (smoking, alcohol and sun damage), model 3: as model 2 plus health status (no. of co-morbidities, no. of medication categories). Estimates of the different models are given in supplementary table 2.

number of elastic fibres of the papillary dermis (layer 1) were negatively associated with the Framingham CVD risk scores (both P=0.10). Furthermore, the length of an elastic fibre and the area covered by an elastic fibre were significantly negatively related to the Framingham CVD risk scores in the papillary dermis after adjustment for potential confounders (layer 1, both P=0.01).

Discussion

In the present study we showed changes in morphometric characteristics of the epidermis: a decreased thickness and flattening with chronological age. In the reticular dermis the number of elastic fibres was increased with chronological age. None of the other morphometric characteristics were related to chronological age in our study population. Furthermore, none of the morphometric epidermal and elastic fibre characteristics differed in offspring from nonagenarian siblings, genetically enriched for familial longevity and their partners as environmentally matched controls. The Framingham CVD risk scores did associate with some characteristics of the papillary dermis, however other epidermal and elastic fibre morphometric characteristics did not clearly associate with the Framingham CVD risk scores.

The Leiden Longevity Study was designed as a case-control study. We have previously demonstrated that the middle aged offspring from long-lived nonagenarian siblings have a healthier metabolic profile, a lower prevalence of cardiovascular disease and a lower mortality rate compared to their partners [12;13]. Thus, this unique study design enables the study of longevity-related factors that are present at middle-age.

We first examined whether skin morphometric parameters of the upper inner arm were dependent on the chronological age of the donor. Consistent with the literature, we were able to show a deterioration of the epidermal structure with chronological age consisting of a reduced thickness and a flatter appearance [4-7]. In addition, we have further demonstrated that this relationship remains after adjustment for potential confounders. For elastin morphology, a distinction was made between papillary and reticular dermis, as fibroblasts from upper (papillary), mid and lower (reticular) dermal fibroblasts were observed to differentially express elastin *in vitro* [17]. An increase in the number, curl, area and length of the fibres were found in the papillary dermis, the latter two findings supporting a previous report on elastin morphology in the upper inner arm [8]. These associations disappeared after adjustment for potential confounders. In the reticular dermis (layers 2 to 5), a significant increase in the area covered by the elastic fibres with chronological age was found, supporting previous findings [7-9;18]. While we found that the number of fibres significantly increased with chronological age, even after adjustment for potential confounders, we did not find a significant difference in fibre length, contradicting previous reports [8;9]. These discrepancies might be due to different methodologies used, another cause might be the limited age range of our subjects.

A higher perceived age has been shown to be partly genetically determined and to be related with mortality [1;3]. In addition, skin wrinkling at the upper inner arm has been linked to health status [19]. Therefore, we next examined whether the histological changes of the skin serve as a marker of biological age, as defined by familial longevity and Framingham CVD risk. The Framingham CVD risk score is one the most established measures of disease outcome [11]. In addition, elastin accumulates in atherosclerotic carotid plaques [20] and it can bind to LDL particles in the arterial wall [21]. Furthermore, increased arterial stiffening has been linked to properties of elastin [22] and elastin morphology at the upper inner arm has been shown to correlate with that in temporal arteries [23]. Thus, we examined whether epidermal or elastic fibre morphometric characteristics were related to CVD risk. The Framingham CVD risk scores associated with the average area and length of elastin fibres in the papillary dermis, even after adjustment for potential confounders. This is the first time that elastin morphology in the skin has been linked to CVD disease risk. However, the decrease in area and length of elastin fibres with increased CVD risk was opposite to their tendency to increase with chronological age. Thus, although significant associations between elastin morphology in the skin and CVD risk has been found, replication of these results is warranted.

Previously we have described that skin fibroblasts derived from the offspring of nonagenarian siblings resembled the responses to cellular stress of fibroblast strains from young subjects, i.e. were biologically younger compared to their partners representing the general population [15]. Based on these findings we expected that the biological differences would have been visible in morphometric skin characteristics comparing the skin of offspring from nonagenarian siblings to their partners. However, none of the morphometric epidermal and elastic fibre characteristics differed dependent on familial longevity status.

To the best of our knowledge our study is the first to address skin morphometric characteristics in relation to familial longevity including 286 middle aged subjects. The large number of very well characterized subjects is a major strength of this study. However, the chronological age range was rather limited, ranging from 44 to 81 years, with most subjects in their 50th or 60th decade of life. This possibly explains the relatively small effects of chronological age on morphometric skin characteristics and could explain why the more subtle effects of familiar longevity were not found. Another strength of the study is the method used to analyse the slides quantitatively to reduce observer variation. However, it cannot be excluded, even after optimal adjustment of the software settings that measurements such as the morphology of elastic fibres were determined without some technical variability. It is therefore possible that the subtle effects dependent on biological age could not be detected. To minimize any technical influences all measurements were performed in batches including equal numbers of offspring and partner as well as young and old subjects. The sampling of biopsies was performed under highly standardized conditions. However, we cannot fully exclude that skin tissue may have been slightly altered due to the excision procedure. Indeed, during the quality checking procedure it was noted that some biopsies contained tears, which was suggestive of thin weak skin typically associated with elderly individuals [24]. Ethnic differences in skin morphometric characteristics have mainly been linked to photo ageing due to differences in pigmentation [25]. In a morphological study of facial skin comparing black and white women differences in several histological aspects of the skin such as epidermal focal atrophy and more dermal elastic fibres in skin obtained from white women compared to black women have been described [26]. Another study has reported a more curled epidermal-dermal junction and a slightly thicker epidermis in black skin but no apparent differences in collagen and elastic fibre architectural organization in the dermis [27]. In order to rule out these possible influences of ethnicity on our results only Caucasian subjects were included in our study. All biopsies were taken from the inner site of the upper arm in a highly standardized procedure to ensure maximal comparability of the data. Although seasonal effects on thickness of the epidermis have been previously described [28] these effects did not apply on the analysis of biological age (familial longevity), as skin biopsies of the offspring – partner couples were taken on the same day.

Unlike many previous reports examining skin epidermal and elastic fibre morphology, a number of potential confounders were taken into consideration in our analysis. Skin biopsies were taken from the upper inner arm to ensure minimal UV damage. Since the skin might still have been exposed to some UV light during its lifetime, we additionally adjusted for sun-damage scores obtained from facial photographs of the subjects. The effect of sun damage are also termed extrinsic ageing and are superimposed on the effects of intrinsic (chronological) ageing. Photo-exposed skin shows a broad band of elastic fibres in the papillary dermis including the upper part of the reticular dermis late in life. In the mid and deep reticular dermis the effect of sun damage is neglible [29]. Smoking is also a known possible confounder of skin morphometric characteristics, as the relative area, thickness and number of elastic fibres was observed to be increased in non sun-exposed skin of smokers compared to non-smokers [10;30]. We indeed observed changes in the association of chronological or biological age and skin morphometric characteristics when adjusting for external factors, indicating that external factors are closely linked to these morphometric characteristics. Moreover, several diseases have previously been linked to altered skin integrity such as the systemic disease diabetes mellitus type 2 due to increased cross-linking of proteins such as collagen [31]. Facial wrinkling has also been associated with COPD and smoking [32] and skin wrinkling at the upper inner arm to health status [19]. Since the association between morphometric characteristics and chronological age weakened after adjustment for disease status, chronological age might not be the most important driver for deterioration of measured epidermal and elastic fibre characteristics; these may largely been driven by external factors and health status. In support of this, in healthy middle aged subjects an association between cardiovascular disease risk and several histological skin characteristics was found.

In conclusion, typical changes of skin morphometric parameters were seen with chronological age. A slower rate of skin ageing was not found in offspring from nonagenarian siblings compared to their partners. Epidermal and elastic fibre morphometric characteristics, as measured from skin biopsies, are therefore not a potential biomarker for familial longevity in middle aged subjects. However, a link between elastic fibre morphology in the papillary dermis and CVD risk indicates that some aspects of skin morphometric characteristics are markers of health status. Further studies should concentrate on which particular aspects of health and CVD risk relate to skin morphometric characteristics to identify the mechanisms responsible for these links.

Acknowledgments

We thank C. de Koning-Treurniet and J. Blom for their help in the laboratory, T. Griffiths, S. Ogden and C.E.M. Griffiths for generating the photo/sun-damage scores and W. Parish for valuable advice and for quality checking the biopsies.
This work was funded by the Innovation Oriented research Program on Genomics (SenterNovem; IGE01014 and IGE5007), Unilever PLC, the Netherlands Genomics Initiative/ Netherlands Organization for scientific research (NGI/NWO; 05040202 and 050-060-810) and the EU funded Network of Excellence Lifespan (FP6 036894).

Supplementary table 1. Chronological age and morphometric skin characteristics.

	Chronological age (years)					
	Model 1		Model 2		Model 3	
	β (SE)	P-value	β (SE)	P-value	β (SE)	P-value
Epidermis[a]						
Thickness based on EDJ, μm	-0.26 (0.06)	<0.001	-0.21 (0.08)	<0.01	-0.22 (0.09)	0.01
Curvature based on SEB[c]	2.56 (0.62)	<0.001	2.62 (0.78)	0.001	2.96 (0.91)	0.001
Dermis						
Elastic fibres, layer 1[a]						
Area covered by fibres[c]	0.35 (0.17)	0.06	0.27 (0.24)	0.26	0.12 (0.27)	0.67
Number of fibres	0.66 (0.37)	0.07	0.62 (0.46)	0.18	0.28 (0.51)	0.59
Area of a single fibre, μm²	0.16 (0.08)	0.05	0.10 (0.10)	0.35	0.05 (0.12)	0.68
Length of a fibre, μm	0.06 (0.03)	0.08	0.04 (0.04)	0.30	0.02 (0.05)	0.66
Thickness of a fibre, nm	-1.46 (1.83)	0.43	-2.26 (2.22)	0.31	-2.16 (2.67)	0.42
Curl of an elastic fibre[c]	-1.21 (0.51)	0.02	-0.88 (0.53)	0.10	-0.71 (0.61)	0.24
Elastic fibres, layers 2-5[b]						
Area covered by fibres[c]	0.93 (0.28)	0.001	0.78 (0.34)	0.02	0.58 (0.40)	0.14
Number of fibres	1.17 (0.31)	<0.001	1.03 (0.38)	0.01	0.95 (0.44)	0.03
Area of a single fibre, μm²	0.18 (0.17)	0.29	0.22 (0.22)	0.31	0.06 (0.26)	0.82
Length of a fibre, μm	0.02 (0.05)	0.68	0.02 (0.06)	0.70	-0.02 (0.07)	0.74
Thickness of a fibre, nm	1.51 (1.60)	0.35	2.26 (2.02)	0.26	0.80 (2.37)	0.74
Curl of a fibre[c]	-0.30 (0.44)	0.49	-0.02 (0.56)	0.97	-0.02 (0.65)	0.98

[a]N=286, [b]N=277, [c]= x10^3. EDJ=epidermal-dermal junction, SEB=stratum corneum epidermis boundary. Linear regression analysis: β=Estimate; SE=Standard error. Model 1: gender adjusted, model 2: as model 1 plus external factors (smoking, alcohol and sun damage), model 3: as model 2 plus health status (no. of co-morbidities, no. of medication categories).

Supplementray table 2. Comparison of offspring and partner status and morphometric skin characteristics

	Familial longevity					
	Model 1		Model 2		Model 3	
	β (SE)	P-value	β (SE)	P-value	β (SE)	P-value
Epidermis, mean (SD)[a]						
Thickness based on EDJ, μm	-0.06 (0.79)	0.94	0.63 (0.85)	0.46	-0.16 (0.95)	0.87
Curvature based on SEB[c]	-4.00 (8.13)	0.62	-10.7 (8.76)	0.22	-1.80 (10.1)	0.86
Dermis, mean (SD)						
Elastic fibres, layer 1[a]						
Area covered by fibres[c]	-0.95 (2.49)	0.70	-2.54 (2.71)	0.35	-1.75 (3.03)	0.56
Number of fibres	-1.24 (4.83)	0.91	-5.24 (5.20)	0.91	-3.49 (5.67)	0.91
Area of a single fibre, μm²	-1.10 (1.07)	0.31	-1.54 (1.15)	0.18	-1.22 (1.30)	0.35
Length of a fibre, μm	-0.60 (0.44)	0.18	-0.67 (0.47)	0.15	-0.52 (0.52)	0.32
Thickness of a fibre, nm	19.4 (24.1)	0.42	11.9 (25.1)	0.64	25.1 (23.4)	0.40
Curl of a fibre[c]	4.17 (6.66)	0.53	8.69 (5.96)	0.15	9.48 (6.66)	0.16
Elastic fibres, layers 2-5[b]						
Area covered by fibres[c]	0.21 (3.64)	0.95	-1.79 (3.90)	0.65	-0.76 (4.37)	0.86
Number of fibres	-0.57 (4.03)	0.89	-4.25 (4.27)	0.32	-3.12 (4.81)	0.52
Area of a single fibre, μm²	-1.81 (2.26)	0.42	-2.02 (2.45)	0.41	-2.64 (2.83)	0.35
Length of a fibre, μm	-0.69 (0.62)	0.27	-0.68 (0.67)	0.31	-1.09 (0.76)	0.16
Thickness of a fibre, nm	-30.6 (21.0)	0.15	-36.0 (22.9)	0.12	-32.7 (26.1)	0.21
Curl of a fibre[c]	-8.44 (5.80)	0.15	-9.36 (6.38)	0.14	-10.3 (7.15)	0.15

[a]N=286, [b]N=277, [c]= x10^3. EDJ=epidermal-dermal junction, SEB=stratum corneum epidermis boundary. Linear regression analysis: β=Estimate; SE=Standard error. Model 1: partner (1) and offspring (0), age and gender, model 2: as model 1 plus external factors (smoking, alcohol and sun damage), model 3: as model 2 plus health status (no. of co- morbidities, no. of medication categories).

Supplementary table 3 Framingham heart risk prediction and epidermal morphometric characteristics.

	FHR score	
	β (SE)	P-value
Thickness based on EDJ, μm		
Model 1: logFHR	-0.95 (0.64)	0.14
Model 2: as model 1 offspring/partner	-0.95 (0.64)	0.14
Model 3: as model 2 plus sun damage	-0.56 (0.65)	0.39
Curvature based on SEB[a]		
Model 1: logFHR	9.88 (7.36)	0.18
Model 2: as model 1 offspring/partner	9.92 (7.37)	0.18
Model 3: as model 2 plus sun damage	8.83 (7.65)	0.25

Models 1 and 2: N=182, Model 3: N=173. EDJ=epidermal-dermal junction, SEB=stratum corneum epidermis boundary. [a]=x10^3. Linear regression analysis: β=Estimate; SE=Standard error. Model 1: the log of Framingham Heart Risk, FHR (%), 10-year risk prediction of cardiovascular disease, model 2: as model 1 plus offspring/partner, model 3: as model 2 plus sun damage.

Supplementary table 4 Framingham heart risk prediction and elastic fibre morphometric characteristics.

	FHR score			
	Layer 1[a]		Layers 2-5[b]	
	β (SE)	P-value	β (SE)	P-value
Area of dermis covered by elastic fibres[c]				
Model 1: logFHR	-2.97 (2.36)	0.21	-1.70 (3.33)	0.61
Model 2: as model 1 offspring/partner	-2.99 (2.36)	0.21	-1.78 (3.33)	0.59
Model 3: as model 2 and sun damage	-4.06 (2.43)	0.10	-3.80 (3.37)	0.26
Number of elastic fibres				
Model 1: logFHR	-5.68 (4.33)	0.19	0.73 (3.59)	0.84
Model 2: as model 1 offspring/partner	-5.70 (4.34)	0.19	0.68 (3.60)	0.85
Model 3: as model 2 and sun damage	-7.51 (4.47)	0.10	-1.73 (3.60)	0.63
Area of a single elastic fibre, μm²				
Model 1: logFHR	-2.00 (0.91)	0.03	-1.43 (2.02)	0.48
Model 2: as model 1 offspring/partner	-2.01 (0.91)	0.03	-1.41 (2.03)	0.49
Model 3: as model 2 and sun damage	-2.37 (0.93)	0.01	-1.79 (2.13)	0.40
Length of an elastic fibre, μm				
Model 1: logFHR	-0.97 (0.38)	0.01	-0.68 (0.54)	0.21
Model 2: as model 1 offspring/partner	-0.97 (0.38)	0.01	-0.67 (0.54)	0.22
Model 3: as model 2 and sun damage	-1.01 (0.40)	0.01	-0.77 (0.57)	0.18
Thickness of an elastic fibre, nm				
Model 1: logFHR	-15.6 (22.6)	0.49	20.1 (17.3)	0.25
Model 2: as model 1 offspring/partner	-16.0 (22.5)	0.48	20.5 (17.3)	0.24
Model 3: as model 2 and sun damage	-21.4 (23.1)	0.36	20.1 (18.0)	0.27
Curl of an elastic fibre[c]				
Model 1: logFHR	-1.78 (5.30)	0.74	3.61 (4.98)	0.47
Model 2: as model 1 offspring/partner	-1.83 (5.30)	0.73	3.79 (4.96)	0.45
Model 3: as model 2 and sun damage	1.61 (5.11)	0.75	6.11 (5.12)	0.23

[a] Models 1 and 2: N=182, Model 3: N=173, [b] Models 1, 2 and 3: N=178, Model 4: N=169.
[c]=x10^3. Linear regression analysis: β=Estimate; SE=Standard error. Model 1: the log of Framingham Heart Risk, FHR (%), 10-year risk prediction of cardiovascular disease, model 2: as model 1 plus offspring/partner, model 3: as model 2 plus sun damage.

References

(1) Christensen K, Thinggaard M, McGue M et al. Perceived age as clinically useful biomarker of ageing: cohort study. *BMJ* 2009;339:b5262.

(2) Warren R, Gartstein V, Kligman AM, Montagna W, Allendorf RA, Ridder GM. Age, sunlight, and facial skin: a histologic and quantitative study. *J Am Acad Dermatol* 1991;25:751-760.

(3) Gunn DA, Rexbye H, Griffiths CE et al. Why some women look young for their age. *PLoS One* 2009;4:e8021.

(4) Fenske NA, Lober CW. Structural and functional changes of normal aging skin. *J Am Acad Dermatol* 1986;15:571-585.

(5) Lavker RM, Zheng PS, Dong G. Morphology of aged skin. *Dermatol Clin* 1986;4:379-389.

(6) Fenske NA, Conard CB. Aging skin. *Am Fam Physician* 1988;37:219-230.

(7) Kurban RS, Bhawan J. Histologic changes in skin associated with aging. *J Dermatol Surg Oncol* 1990;16:908-914.

(8) Robert C, Lesty C, Robert AM. Ageing of the skin: study of elastic fiber network modifications by computerized image analysis. *Gerontology* 1988;34:291-296.

(9) Frances C, Branchet MC, Boisnic S, Lesty CL, Robert L. Elastic fibers in normal human skin. Variations with age: a morphometric analysis. *Arch Gerontol Geriatr* 1990;10:57-67.

(10) Just M, Ribera M, Monso E, Lorenzo JC, Ferrandiz C. Effect of smoking on skin elastic fibres: morphometric and immunohistochemical analysis. *Br J Dermatol* 2007;156:85-91.

(11) D'Agostino RB, Sr., Vasan RS, Pencina MJ et al. General cardiovascular risk profile for use in primary care: the Framingham Heart Study. *Circulation* 2008;117:743-753.

(12) Schoenmaker M, de Craen AJ, de Meijer PH et al. Evidence of genetic enrichment for exceptional survival using a family approach: the Leiden Longevity Study. *Eur J Hum Genet* 2006;14:79-84.

(13) Westendorp RG, van HD, Rozing MP et al. Nonagenarian siblings and their offspring display lower risk of mortality and morbidity than sporadic nonagenarians: The Leiden Longevity Study. *J Am Geriatr Soc* 2009;57:1634-1637.

(14) Wijsman CA, Rozing MP, Streefland TC et al. Familial longevity is marked by enhanced insulin sensitivity. *Aging Cell* 2010.

(15) Dekker P, Maier AB, van HD et al. Stress-induced responses of human skin fibroblasts in vitro reflect human longevity. *Aging Cell* 2009;8:595-603.

(16) Griffiths CE, Wang TS, Hamilton TA, Voorhees JJ, Ellis CN. A photonumeric scale for the assessment of cutaneous photodamage. *Arch Dermatol* 1992;128:347-351.

(17) Tajima S, Izumi T. Differential in vitro responses of elastin expression to basic fibroblast growth factor and transforming growth factor beta 1 in upper, middle and lower dermal fibroblasts. *Arch Dermatol Res* 1996;288:753-756.

(18) Gogly B, Godeau G, Gilbert S et al. Morphometric analysis of collagen and elastic fibers in normal skin and gingiva in relation to age. *Clin Oral Investig* 1997;1:147-152.

(19) Purba MB, Kouris-Blazos A, Wattanapenpaiboon N et al. Can skin wrinkling in a site that has received limited sun exposure be used as a marker of health status and biological age? *Age Ageing* 2001;30:227-234.

(20) Goncalves I, Moses J, Dias N et al. Changes related to age and cerebrovascular symptoms in the extracellular matrix of human carotid plaques. *Stroke* 2003;34:616-622.

(21) Noma A, Takahashi T, Wada T. Elastin-lipid interaction in the arterial wall. Part 2. In vitro binding of lipoprotein-lipids to arterial elastin and the inhibitory effect of high density lipoproteins on the process. *Atherosclerosis* 1981;38:373-382.

(22) Astrand H, Stalhand J, Karlsson J, Karlsson M, Sonesson B, Lanne T. In vivo estimation of the contribution of elastin and collagen to the mechanical properties in the human abdominal aorta: effect of age and sex. *J Appl Physiol* 2011;110:176-187.

(23) Gogly B, Godeau G, Septier D, Hornebeck W, Pellat B, Jeandel C. Measurement of the amounts of elastic fibers in the skin and temporal arteries of healthy aged individuals by automated image analysis. *Gerontology* 1998;44:318-323.

(24) Branchet MC, Boisnic S, Frances C, Robert AM. Skin thickness changes in normal aging skin. *Gerontology* 1990;36:28-35.

(25) Rawlings AV. Ethnic skin types: are there differences in skin structure and function? *Int J Cosmet Sci* 2006;28:79-93.

(26) Montagna W, Carlisle K. The architecture of black and white facial skin. *J Am Acad Dermatol* 1991;24:929-937.

(27) Girardeau S, Mine S, Pageon H, Asselineau D. The Caucasian and African skin types differ morphologically and functionally in their dermal component. *Exp Dermatol* 2009;18:704-711.

(28) Akasaka T, Yoshida A, Fukuda S, Takeuchi T, Katsuzaki N. Yearly changes in the physiological function of the skin. *Environmental Dermatology* 2002;9:1-10.

(29) El-Domyati M, Attia S, Saleh F et al. Intrinsic aging vs. photoaging: a comparative histopathological, immunohistochemical, and ultrastructural study of skin. *Exp Dermatol* 2002;11:398-405.

(30) Frances C, Boisnic S, Hartmann DJ et al. Changes in the elastic tissue of the non-sun-exposed skin of cigarette smokers. *Br J Dermatol* 1991;125:43-47.

(31) Wulf HC, Sandby-Moller J, Kobayasi T, Gniadecki R. Skin aging and natural photoprotection. *Micron* 2004;35:185-191.

(32) Patel BD, Loo WJ, Tasker AD et al. Smoking related COPD and facial wrinkling: is there a common susceptibility? *Thorax* 2006;61:568-571.

Chapter 5

Chapter 5

The number of p16INK4a positive cells in human skin reflects biological age.

M.E.C. Waaijer, W.E. Parish, B.H. Strongitharm, D. van Heemst, P.E. Slagboom, A.J.M. de Craen, J.M. Sedivy, R.G.J. Westendorp, D.A. Gunn, A.B. Maier

Aging Cell. 2012 Aug;11(4):722-5

Abstract

Cellular senescence is a defense mechanism in response to molecular damage which accumulates with ageing. Correspondingly, the number of senescent cells has been reported to be greater in older than in younger subjects, and furthermore associates with age-related pathologies. Inter-individual differences exist in the rate at which a person ages (biological age). Here, we studied whether younger biological age is related to fewer senescent cells in middle-aged individuals with the propensity for longevity, using p16INK4a as a marker for cellular senescence. We observed that a younger biological age associates with lower levels of p16INK4a positive cells in human skin.

Increasing experimental evidence indicates that the accumulation of molecular damage underlies the ageing process and age-related pathologies [1-3]. Cellular defense mechanisms that occur in response to molecular damage include macromolecule repair, apoptosis and cellular senescence. In tissues, the prevalence of senescent cells, i.e. cells with a permanently arrested cell cycle, has been shown to increase with chronological age, both in animal models [4-7] and in humans [8;9]. Furthermore, increased numbers of senescent cells were found to associate with age-related pathologies such as atherosclerotic lesions [10], diabetes [11] and renal disease [12;13]. Higher levels of p16INK4a were associated as well with higher serum creatinine after renal transplantation [14;15].

Within the Leiden Longevity Study (LLS), we have previously shown that middle aged offspring from long lived nonagenarian siblings are biological younger than their partners, who are age and environmentally matched controls (see [16] for study design details). This is reflected in a lower mortality rate [16], a lower prevalence of cardiometabolic diseases [17], beneficial glucose and lipid metabolism, preservation of insulin sensitivity [18] and resistance to cellular stress *in vitro* [19]. The cyclin dependent kinase inhibitor CDKN2A, commonly referred to as p16INK4a or p16, has been established as a general marker of cellular senescence as p16INK4a was observed to be expressed in most senescent cells in other studies [20-23]. Here, we compared the frequency of p16INK4a positive cells in human skin biopsies from the upper inner arm of 89 middle aged offspring with familial longevity ("better agers") with those of their 89 partners. We hypothesized that the younger biological age of the offspring would be reflected in lower numbers of p16INK4a positive cells when compared to their partners.

The age of the subjects varied from 46 to 81 years, with an average of 63 years. Further characteristics of the subjects are given in Table S1. Figure 1 shows representative figures of p16INK4a staining in both epidermis and dermis. The distribution of tertiles of p16INK4a positive cells differed considerably between offspring and partners in both epidermal cells and dermal fibroblasts. In the lowest tertile of p16INK4a positive cells the offspring significantly outnumbered the partners whereas in the highest tertile the partners significantly outnumbered the offspring (Figure 2). After adjustment for possible confounders such as age, gender and smoking these correlations remained essentially unaltered. Although these correlations were present in both epidermis and dermis, the correlation between the number of p16INK4a positive cells in the epidermis and those in the dermis was low (Pearson's correlation coefficient 0.119, P=0.115).

Next, to confirm that the number of p16INK4a positive cells in human skin is a marker of biological age, we studied the relationship between the number of p16INK4a positive cells and age-related pathologies. The number of cardiovascular diseases (CVD) and medication use was significantly associated with tertiles of p16INK4a positive cells in epidermal cells (Figure 2), also after adjustment for gender and smoking. There was no relationship between the tertiles of p16INK4a positive dermal fibroblasts and the number of CVD. However, a trend towards higher p16INK4a positivity in dermal fibroblasts and medication use was found.

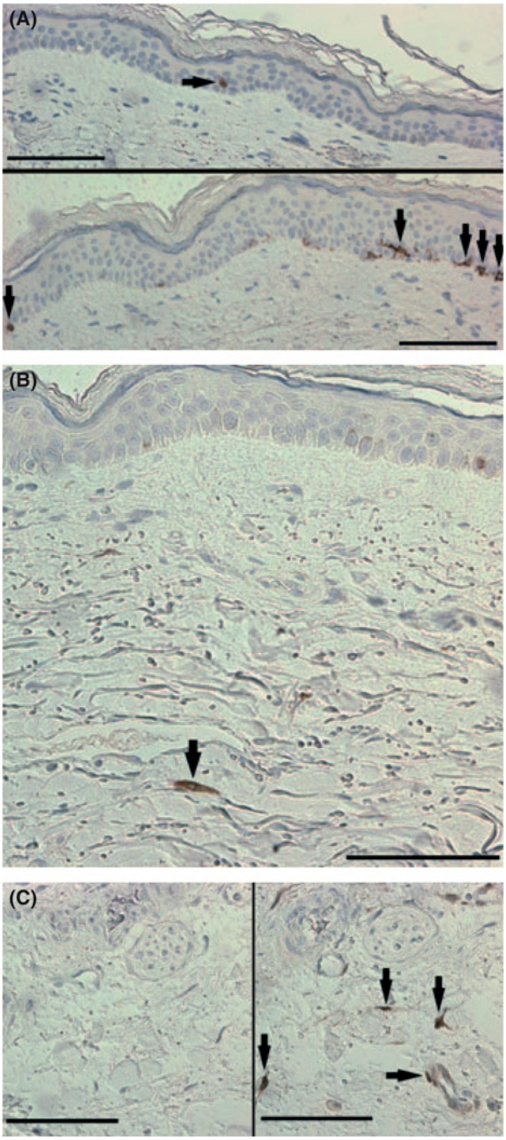

Figure 1. p16INK4a staining in human skin.
Figure 1a: representative p16INK4a staining of the epidermis from a subject in the middle tertile with 1 positive cell visible and an image of a section from a subject in the highest tertile (lower image with 5 positive cells visible). Epidermal staining was located along the basal membrane and mainly nuclear/perinuclear in nature although some cells displayed extensive cytoplasmic staining; note the dendritic nature of the fourth from right positive cell in the lower image characteristic of a melanocyte.
Figure 1b: representative p16INK4a staining of the dermis.
Figure 1c: negative control (no primary antibody, left image) and positive control (right image) of a skin sample used during all staining due to the consistent positive staining seen throughout the tissue. Line-bars represent 100µm (1 dermal counting field was 315µm by 315µm) and black arrows the locations of positively stained cells.

For the first time we have shown here that a marker of cellular senescence, p16INK4a, associates with familial longevity. In addition, we were able to reproduce earlier findings that cellular senescence *in situ* is associated with age-related pathologies. Although further evidence for the link between familial longevity and cellular senescence using other markers of senescence in skin or other tissues would strengthen these findings, the found association between p16INK4a and age-related disease is supported by a recent study. Clearance of p16INK4a positive cells in a mouse model was observed to delay the onset of age-related diseases [21]. Smoking, a well known risk factor for most age-related diseases was previously also found to associate with expression of p16INK4a in peripheral blood T-cells [24]. However, adjustment for smoking did not alter the results.
We have previously shown that skin fibroblasts from the middle-aged offspring respond to chemical stress *in vitro* with lower cellular senescence and higher apoptosis when compared to age-matched controls; this was comparable to the fibroblast response of young relative to old donors [19]. Thus, human familial longevity is not only associated with fewer p16INK4a positive skin cells *in situ*, it is also associated with fewer senescent cells after a cellular stressor *in vitro*.

It is tempting to speculate based on the evidence presented here that the accumulation of senescent cells contributes to tissue failure and ill health. A reduced rate of cellular senescence appears to be a characteristic of offspring from long-lived families both *in vitro* and *in situ*, indicating a role for cellular senescence in the healthy phenotype of familial longevity. We hypothesize that offspring, enriched for genetic effects on longevity, carry also other molecular defense mechanisms (such as repair of damage and apoptosis) of better quality than their partners, resulting in less cellular senescence. Thus, the healthy phenotype of humans enriched for familiar longevity could be related to cellular senescence. However, further work is required to determine if these findings are causative rather than associative in nature to better understand the role senescent cells have *in vivo*.

Methods

Study cohort
In the Leiden Longevity Study genetic factors contributing to longevity are studied by comparing subjects enriched for familial longevity with their partners [16]. On average 50% of the genetic propensity of their long lived parent is carried on to their offspring. Their partners, with whom most have shared the same environment for decades, were included as age and environmentally matched controls. The Medical Ethical Committee of the Leiden University Medical Center approved the study.

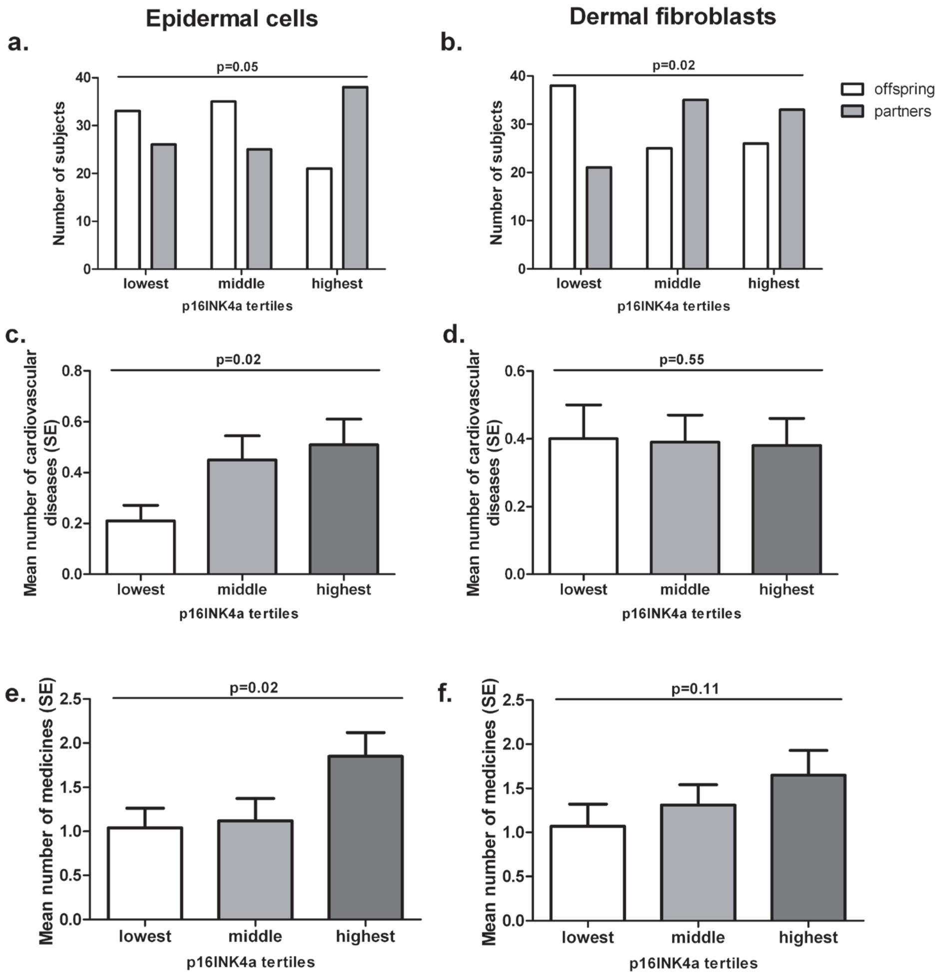

Figure 2. Tertiles of p16INK4a positivity in human skin.
Left column (a, c, e) presents epidermal cells, the right column (b, d, f) presents dermal fibroblasts. (a, b) A comparison of distribution of tertiles of p16INK4a positive cells between offspring from long-lived families and their partners, N=178. (c, d) Average number ± standard error (SE) of cardiovascular diseases over tertiles of p16INK4a positive cells, N=155. (e, f) Average number ± SE of medicines over tertiles of p16INK4a positive cells, N=136.
Tertiles of p16INK4a positive epidermal cells: lowest ≤0.30 (median=0.00), middle 0.30-1.30 (median=0.55), highest ≥1.30 (median=3.09) cells per mm length of the epidermal-dermal junction. Tertiles of p16INK4a positive dermal fibroblasts: lowest ≤0.72 (median=0.00), middle 0.72-2.05 (median=1.29), highest ≥2.05 (median 3.20) cells per 1mm2 dermis. P-values are adjusted for age, gender and smoking in a and b; for gender and smoking in c, d, e and f.

Skin biopsies

Skin biopsies (4mm) were taken from the sun-protected site of the inner upper arm, and fixed in formalin (Sigma) overnight (18-24 hours). After fixation, the biopsies were washed in fresh phosphate buffered saline twice and then dehydrated in 70% alcohol and stored at room temperature. The samples were embedded in paraffin wax and cut into sections of 4µm.

Immunohistochemistry

Mouse monoclonal antibody clone E6H4 (CINtec Histology Kit, MTM Laboratories) raised against human p16INK4a protein was used, which has been previously validated as specific to the p16INK4a protein in human tissue samples [25]. CINtec clinical test reagents were used according to the manufacturers' instructions (CINtec Histology Kit, MTM Laboratories) to detect p16INK4a in the formalin fixed paraffin embedded skin tissue. Serial sections were treated for 30 minutes with one of the following, negative controls: no antibody solution (CINtec kit) or CINtec anti-p16INK4a antibody. Sections were counterstained with Mayer's hematoxylin, washed and mounted in glycergel (DAKO).

Cell counting

For dermal fibroblast counts, cell identification and counting was carried out in the papillary and upper to mid reticular areas using a x40 objective. Counts were restricted to nucleated linear or oval cells; thus, stained small circular bodies which may have been cross-sections of fibroblasts were omitted. The area of dermis available for counting varied greatly between sections due to variations in dermal depth and the presence of blood vessels, hair follicles and sebaceous glands. Thus, to control for the size of area examined for positive cells, we used a graticule (Zeis, Netzmikrometer 12) in the x10 eye piece which covered a 0.1 mm^2 area under the x40 objective. As the graticule was divided into 10x10 squares it enabled counting to be carried out in quarter graticule fields where appropriate (e.g. a hair follicle covered some of the graticule field). The total number of graticule areas (termed fields) screened per section was captured.

For positive p16INK4a cells in the epidermis, positive cells were counted along the full length of the 4 mm epidermis, this number was then corrected for the length of the epidermal-dermal junction as all cells were located in or immediately above the basal membrane.

Demographic and medical information

Demographic characteristics and medical information were available for each subject. Information on medical history was obtained from the participants' treating physicians, information on medication use from the participants' pharmacists. Cardiovascular diseases included cerebrovascular accident, myocardial infarction, hypertension and diabetes mellitus. For the number of medicines, the absolute number of different medicines was used.

Statistics

All analyses were performed using SPSS 16.0 data editor software. The data was divided into three in principle equal-sized data subsets. These tertiles of p16INK4a positivity were computed for the epidermis and dermis separately. The tertiles of p16INK4a positive epidermal cells were distributed as following: lowest ≤0.30, middle 0.30-1.30, highest ≥1.30 cells per mm length of the epidermal-dermal junction. For the tertiles of p16INK4a positive dermal fibroblasts: lowest ≤0.72, middle 0.72-2.05, highest ≥2.05 cells per 1mm^2 dermis. The association between p16INK4a positivity in both epidermal cells and dermal fibroblasts with offspring or partner status was analysed by using the Pearson chi-square test on a cross table based on p16INK4a positivity tertiles. Logistic regression was used to adjust the p-values for age and gender. Linear regression was used to calculate the association between p16INK4a positivity and number of cardiovascular diseases and number of medicines.

Acknowledgements

We thank N.M. Hudson for her help with skin tissue processing.
This work was funded by SenterNovem, IGE01014 and IGE5007, NGI/NWO; 05040202 and 050-060-810, Unilever PLC and FP6 036894.

Supplementary table 1. Characteristics of subjects.

	Offspring (N=89)	Partners (N=89)
Demographic data		
Female, %	50.6	50.6
Age, years	63.4 (6.17)	63.4 (7.07)
Body composition		
Height, cm	172 (8.34)	171 (8.98)
Body mass index, kg/m²	26.6 (4.23)	26.5 (3.45)
Fat, %	28.8 (8.53)	30.3 (7.7)
Lean mass, %	67.0 (8.10)	65.7 (7.32)
Co-morbidities, no. (%) [b]		
Myocardial infarction	1 (1.2)	2 (2.4)
Cerebrovascular accident	2 (2.4)	5 (6.1)
Hypertension	19 (23.5)	24 (29.3)
Diabetes mellitus	3 (3.7)	8 (9.9)
Malignancy	2 (2.5)	4 (5.0)
Chronic obstructive pulmonary disease	3 (3.7)	3 (3.7)
Rheumatoid arthritis	0 (0)	0 (0)
Number of cardiovascular diseases [b]	0.30 (0.56)	0.48 (0.72)
Number of medicines [c]	1.24 (1.68)	1.46 (1.74)
Intoxications [a]		
Users of alcohol (>1 unit/week), no. (%)	63 (75.0)	68 (80.0)
Former and/or current smoking, no. (%)	46 (54.8)	59 (69.4)

[a] N=169, [b] N=164, [c] N=136 Values are given as mean (SD) if not otherwise stated. SD: standard deviation.

References

(1) Stadtman ER. Protein oxidation in aging and age-related diseases. *Ann N Y Acad Sci* 2001;928:22-38.

(2) Pamplona R. Membrane phospholipids, lipoxidative damage and molecular integrity: a causal role in aging and longevity. *Biochim Biophys Acta* 2008;1777:1249-1262.

(3) Hamilton ML, Van RH, Drake JA et al. Does oxidative damage to DNA increase with age? *Proc Natl Acad Sci U S A* 2001;98:10469-10474.

(4) Janzen V, Forkert R, Fleming HE et al. Stem-cell ageing modified by the cyclin-dependent kinase inhibitor p16INK4a. *Nature* 2006;443:421-426.

(5) Krishnamurthy J, Ramsey MR, Ligon KL et al. p16INK4a induces an age-dependent decline in islet regenerative potential. *Nature* 2006;443:453-457.

(6) Molofsky AV, Slutsky SG, Joseph NM et al. Increasing p16INK4a expression decreases forebrain progenitors and neurogenesis during ageing. *Nature* 2006;443:448-452.

(7) Herbig U, Ferreira M, Condel L, Carey D, Sedivy JM. Cellular senescence in aging primates. *Science* 2006;311:1257.

(8) Ressler S, Bartkova J, Niederegger H et al. p16INK4A is a robust in vivo biomarker of cellular aging in human skin. *Aging Cell* 2006;5:379-389.

(9) Dimri GP, Lee X, Basile G et al. A biomarker that identifies senescent human cells in culture and in aging skin in vivo. *Proc Natl Acad Sci U S A* 1995;92:9363-9367.

(10) Minamino T, Miyauchi H, Yoshida T, Ishida Y, Yoshida H, Komuro I. Endothelial cell senescence in human atherosclerosis: role of telomere in endothelial dysfunction. *Circulation* 2002;105:1541-1544.

(11) Sone H, Kagawa Y. Pancreatic beta cell senescence contributes to the pathogenesis of type 2 diabetes in high-fat diet-induced diabetic mice. *Diabetologia* 2005;48:58-67.

(12) Melk A, Schmidt BM, Vongwiwatana A, Rayner DC, Halloran PF. Increased expression of senescence-associated cell cycle inhibitor p16INK4a in deteriorating renal transplants and diseased native kidney. *Am J Transplant* 2005;5:1375-1382.

(13) Sis B, Tasanarong A, Khoshjou F, Dadras F, Solez K, Halloran PF. Accelerated expression of senescence associated cell cycle inhibitor p16INK4A in kidneys with glomerular disease. *Kidney Int* 2007;71:218-226.

(14) Koppelstaetter C, Schratzberger G, Perco P et al. Markers of cellular senescence in zero hour biopsies predict outcome in renal transplantation. *Aging Cell* 2008;7:491-497.

(15) McGlynn LM, Stevenson K, Lamb K et al. Cellular senescence in pretransplant renal biopsies predicts postoperative organ function. *Aging Cell* 2009;8:45-51.

(16) Schoenmaker M, de Craen AJ, de Meijer PH et al. Evidence of genetic enrichment for exceptional survival using a family approach: the Leiden Longevity Study. *Eur J Hum Genet* 2006;14:79-84.

(17) Westendorp RG, van HD, Rozing MP et al. Nonagenarian siblings and their offspring display lower risk of mortality and morbidity than sporadic nonagenarians: The Leiden Longevity Study. *J Am Geriatr Soc* 2009;57:1634-1637.

(18) Wijsman CA, Rozing MP, Streefland TC et al. Familial longevity is marked by enhanced insulin sensitivity. *Aging Cell* 2011;10:114-121.

(19) Dekker P, Maier AB, van HD et al. Stress-induced responses of human skin fibroblasts in vitro reflect human longevity. *Aging Cell* 2009;8:595-603.

(20) Campisi J, d'Adda di FF. Cellular senescence: when bad things happen to good cells. *Nat Rev Mol Cell Biol* 2007;8:729-740.

(21) Baker DJ, Wijshake T, Tchkonia T et al. Clearance of p16Ink4a-positive senescent cells delays ageing-associated disorders. *Nature* 2011;479:232-236.

(22) Rodier F, Campisi J. Four faces of cellular senescence. *J Cell Biol* 2011;192:547-556.

(23) Krishnamurthy J, Torrice C, Ramsey MR et al. Ink4a/Arf expression is a biomarker of aging. *J Clin Invest* 2004;114:1299-1307.

(24) Liu Y, Sanoff HK, Cho H et al. Expression of p16(INK4a) in peripheral blood T-cells is a biomarker of human aging. *Aging Cell* 2009;8:439-448.

(25) Klaes R, Friedrich T, Spitkovsky D et al. Overexpression of p16(INK4A) as a specific marker for dysplastic and neoplastic epithelial cells of the cervix uteri. *Int J Cancer* 2001;92:276-284.

Chapter 6

P16INK4a positive cells in human skin are indicative of local elastic fibre morphology, facial wrinkling and perceived age

M.E.C. Waaijer*, D.A. Gunn*, P.D. Adams, J.S. Pawlikowski, C.E.M. Griffiths,
D. van Heemst, P.E. Slagboom, R.G.J. Westendorp, A.B. Maier
* Both authors contributed equally
Journal of Gerontology: Biological Sciences 2016 Aug;71(8):1022-8

Abstract

Senescent cells are more prevalent in aged human skin compared to young, but evidence that senescent cells are linked to other biomarkers of ageing is scarce. We counted cells positive for the tumour suppressor and senescence associated protein p16INK4a in sun-protected upper inner arm skin biopsies from 178 participants (45-81 years of age) of the Leiden Longevity Study. Local elastic fibre morphology, facial wrinkles and perceived facial age were compared to tertiles of p16INK4a counts, whilst adjusting for chronological age and other potential confounders.

The numbers of epidermal and dermal p16INK4a positive cells were significantly associated with age-associated elastic fibre morphologic characteristics, such as longer and a greater number of elastic fibres. The p16INK4a positive epidermal cells (identified as primarily melanocytes) were also significantly associated with more facial wrinkles and a higher perceived age. Participants in the lowest tertile of epidermal p16INK4a counts looked 3 years younger than those in the highest tertile, independently of chronological age and elastic fibre morphology.

In conclusion, p16INK4a positive cell numbers in sun-protected human arm skin are indicative of both local elastic fibre morphology and the extent of ageing visible in the face.

Introduction

Cellular senescence can be described as the inability of mammalian cells to undergo replication due to stable cell cycle arrest. Cells senesce in response to a variety of stresses such as DNA damage, oxidative stress and telomere shortening [1]. The relevance of cellular senescence to ageing has been shown in several animal models [2-4] and in humans [5-7] where the prevalence of senescent cells was higher in old compared to young tissues. Furthermore, links have been observed between senescent cells and biological age – an individual's physiological condition irrespective of their chronological age, for example due to beneficial familial characteristics or disease. We demonstrated that the offspring of nonagenarian siblings, who have a propensity for longevity, have less p16INK4a positive cells in the epidermis and dermis of upper-inner arm skin than aged-matched controls [8]. In addition, other studies have shown that higher p16INK4a expression levels in transplanted kidneys are predictive of worse transplant function [9], and p16INK4a positivity was associated with hypertensive histological changes in the kidney [10] and type 2 diabetic nephropathy [11]. A higher prevalence of senescent cells has also been linked to atherosclerosis [12] and lung emphysema [13]. Finally, removal of p16INK4a positive cells delayed the onset and progression of age-related disease in progeroid mice [14] supporting the notion that the presence of senescent cells can be detrimental to tissues.

The tissue with the most visible signs of deterioration with age is the skin which is accompanied by marked changes to its morphology. For example, the epidermis flattens and the number and size of elastic fibres increase with age [15]. How old an individual looks for their age (perceived facial age) is influenced not only by changes to skin morphology but also by subcutaneous changes that affect face shape such as the appearance of the nasolabial fold and facial sag [16-19]. About 50% of the variation in perceived age can be attributable to skin wrinkling [16] whereas the rest of the variation is likely predominately due to changes in face shape. Although skin wrinkling is strongly influenced by sun exposure [20-23], perceived age is also linked to ageing and disease. Higher perceived age associates with lower survival [24], higher glucose levels [25], higher cortisol levels [26], higher blood pressure in women [27] and increased carotid atherosclerosis [28]; and human familial longevity in men was associated with a lower perceived age [27].

Here, we studied whether the number of cells positive for the senescence associated protein p16INK4a in sun-protected upper inner arm skin, associated with local skin morphology and the extent of ageing visible in the face, i.e. facial wrinkles and perceived age. We hypothesised that higher numbers of p16INK4a positive cells in human skin would be associated with skin morphology typical in older individuals, more facial wrinkles and a higher perceived age independently of potential confounders such as age and smoking.

Methods

The study design of the Leiden Longevity Study (LLS) and all methodologies have been described previously [8;15;29;30]; we briefly describe the design below. Data from 178 LLS randomly selected participants were used in this study.

Study design

The LLS consists of men and women over 89 and 91 years of age respectively with at least one sibling who passes the same age criterion, the offspring of either long-lived sibling and the partners of the offspring (i.e. married to/civil partnership with the offspring) [30]. The offspring and their partners were the subjects in this study. The study protocol was approved by the Medical Ethics Committee of the Leiden University Medical Centre (following the declaration of Helsinki) and participants gave informed written consent.

Skin biopsies – p16INK4a staining and counting

Skin biopsies (4 mm) were taken from the sun-protected site of the upper-inner arm and fixed in formalin (Sigma) overnight (18–24 h). Biopsies were washed, dehydrated, embedded in paraffin wax and cut into 4 µm sections. As described previously [8], p16INK4a staining was carried out using the E6H4 antibody [31] as per the manufacturer's instructions (CINtec Histology Kit, MTM Laboratories). Counting of p16INK4 positive cells was carried out along

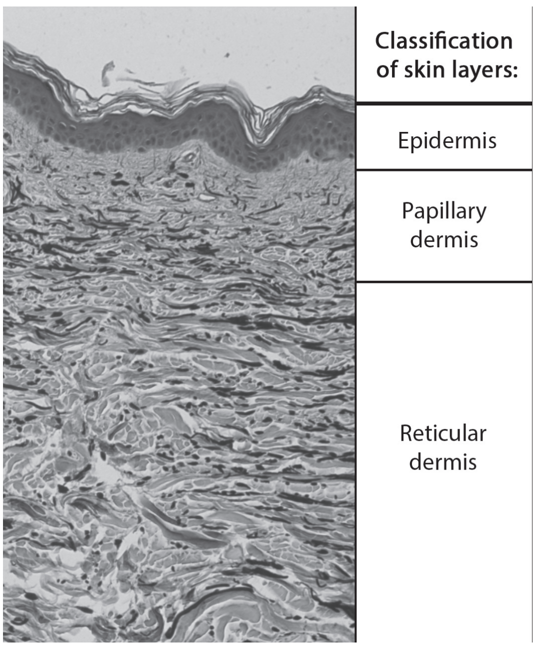

Figure 1. Example of a skin biopsy section with the classification of layers used in the study.
In this skin biopsy section stained with Orcein dye the epidermis and dermis were demarcated by defining the epidermal-dermal junction. The dermis was divided into depth layers of 100 micrometre, where layer 1 represented the papillary dermis and layers 2 to 5 the reticular dermis.

the full length of the epidermis and adjusted for the length of the epidermal-dermal junction. As all cells were located immediately above the basal membrane, no correction for epidermal depth was required. To identify the epidermal p16INK4a positive cell-type, dual staining for p16INK4a and S100 (X0311 Dako; a marker of melanocyte and Langerhans cells) was carried out on the same skin sections and positive cells along the basal membrane were counted. In addition, we stained skin sections for p16INK4a and MelA (clone A103, M7196 Dako, a more specific marker for melanocytes in the skin than S100) and examined adjacent sections for co-localisation of staining. Both methods have been detailed previously [32] and were carried out on 3 participants. For dermal cell counts, cell identification and counting was carried out in the papillary and upper to mid reticular areas using a 40 X objective. Counts were restricted to nucleated linear or oval cells morphologically determined as fibroblasts, and corrected for the measurement area.

Skin biopsies – morphology

The measurement of skin morphology characteristics has been described previously [15]. Two sections of each biopsy were stained with Orcein dye and the resulting skin sections imaged and assessed for epidermal and elastic fibre morphology. Epidermal measurements included the thickness of the epidermis (image area covered by epidermis divided by the length of the epidermal–dermal junction) and the curvature in the epidermis (the ratio of a straight line between the horizontal margins of the epidermis over the length of the stratum corneum–epidermis boundary). Within the dermis, the area covered by the elastic fibres and their number (both corrected for the size of image area they were measured in) as well as the area (micrometre squared), length (micrometre), thickness (micrometre) and the curl of an elastic fibre (the ratio between its length and the calliper dimension) were measured. The dermis was divided into depth layers of 100 micrometre, layer 1 represented the papillary dermis and layers 2 to 5 the reticular dermis (Figure 1). Due to the variability in skin biopsy thickness, the number of available subjects for skin morphology varied: N=177 for epidermis and papillary dermis, N=175 for reticular dermis.

Measurement of facial features

Wrinkle grading of the facial images was carried out as previously reported [16] utilising grading from two skin ageing experts; the mean value was used for further analyses. The methodology used for generating perceived facial age has been reported in detail elsewhere [16;29]. In brief, an en-face and a 45 degree photograph of the face were acquired for all participants (without the presence of any facial products), the images cropped around the neck and hair line before being presented, in a randomised order, to naive age assessors via a computer screen where they chose a 5-year age range dependent on how old they thought the participants looked. All participating assessors were unaware of presentation designs, subject ages and age ranges.

The mean perceived ages were generated from an average of 60 independent assessments of age (range: 59-61 assessments). Inter-rater reliability of the perceived age assessment was excellent (Cronbach's alpha 0.99).

Demographic characteristics

For each subject, demographic and lifestyle characteristics were obtained. Information on medical history (available for N=161-169 dependent on condition) was obtained from the participants' treating physicians, including history of myocardial infarction, stroke, hypertension, diabetes mellitus, malignancy, rheumatoid arthritis and chronic obstructive pulmonary disease. Information on skin-type (skin goes red, pink or tans upon sun exposure), sun exposure (how often one sunbathes and is outside) and sun bed use (number of occasions one uses a sun bed per year), body mass index (BMI, weight in kg/length in m^2) and smoking status (smokers include both former and current smokers, data available for N=169) was collected via questionnaires.

Statistics

All statistical analyses were performed with IBM SPSS Statistics 20 software. As the p16INK4a counts were not normally distributed, the data was divided into three equal-sized data subsets (low: N=59, middle: N=60, high: N=59) for the analyses. These tertiles of p16INK4a positivity were calculated for the epidermis and dermis separately. The tertiles of p16INK4a positive epidermal cells were distributed as following: lowest ≤ 0.30 (median = 0.00), middle 0.30–1.30 (median = 0.55), highest ≥ 1.30 (median = 3.09) cells per mm length of the epidermal–dermal junction. For the tertiles of p16INK4a positive dermal fibroblasts: lowest ≤ 0.72 (median = 0.00), middle 0.72–2.05 (median = 1.29), highest ≥ 2.05 (median 3.20) cells per 1 mm^2 dermis. For simplicity and as a reflection of overall morphology, composite scores were generated for morphology characteristics of the epidermis and elastic fibres in both the papillary and reticular dermis separately. For this, Z-scores of all skin morphology characteristics were calculated and added; the Z-scores of epidermal thickness and dermal curl of elastic fibres had inverse associations with age so were multiplied by -1 (see [15]. Hence, a higher elastin morphology composite score reflected a combination of elastic fibre characteristics associated with a greater chronological age.

To estimate skin morphology composite score means for each p16INK4a tertile and to calculate the P-value for trend, linear mixed models were used. In model 1, adjustments were made for age, sex and long-lived family member status. For model 2, model 1 was expanded with further adjustments for skin tanning type, sun bed use, sun exposure (although the skin was from a sun-protected site, these adjustments ensured sun exposure influences on the data was minimal), smoking, and BMI; we also adjusted for the number of cardiovascular and metabolic diseases (including cerebrovascular accident, myocardial infarction, hypertension and diabetes mellitus) as we previously found links between such parameters and number of p16INK4a cells in skin [8]. The wrinkle grading and perceived age adjustment models 1 and 2 were as described above. Model 3, however, included an additional adjustment for the elastic fibre morphology composite scores of both the papillary and reticular dermis. Also for perceived age only, model 4 consisted of model 3 plus adjustment for the wrinkle grading.

Table 1. Characteristics of the study participants

	N=178
Age[a], years	63.4 (6.6)
Male[b]	88 (49.4)
Long-lived family member[b]	89 (50.0)
Skin tanning type[b]	
Red	75 (42.1)
Pink	62 (34.8)
Tans	41 (23.0)
Sun bed use[b]	
Never	127 (71.3)
1-5 times per year	29 (16.3)
≥ 6 times per year	22 (12.4)
Sun exposure[b]	
Rarely outside	23 (12.9)
Often outside	113 (63.5)
Mostly outside	42 (23.6)
Former and/or current smokers[b]	105 (62.1)
Co-morbidities[b]	
Myocardial infarction	3 (1.8)
Cerebrovascular accident	7 (4.3)
Hypertension	43 (26.4)
Diabetes mellitus	11 (6.8)
Malignancy	6 (3.7)
Chronic obstructive pulmonary disease	6 (3.7)
Rheumatoid arthritis	0 (0.0)
Body mass index[a], kg/m2	26.5 (3.8)

Data are depicted as either [a]: mean (standard deviation) or [b]: number (%).

Results

Table 1 shows the characteristics of 178 study participants. The mean age of participants was 63 years with equal numbers of men and women, and half were members of a long-lived family (i.e. the offspring), while the other half consisted of their partners.

Since the association with the number of p16INK4a positive cells and chronological age has been described previously, we examined whether this could be confirmed in our cohort. In an univariate analysis, tertiles of epidermal p16INK4a positivity were positively associated with chronological age (P for trend=0.023), but tertiles of dermal p16INK4a positivity were not associated (P for trend =0.964).

We next investigated whether the number of p16INK4a positive cells associated with local skin morphology, facial wrinkles and perceived age. Epidermal p16INK4a positivity was not associated with epidermal morphology, but was positively associated with the dermal elastic fibre morphology in the papillary dermis even after adjustment for potential confounders (Table 2 and Figure 2: P for trend <0.001, model 2). A trend between epidermal p16INK4a positivity and dermal elastic fibre morphology in the reticular dermis was seen in model 1 (P for trend=0.064), and after adjustment for further confounders a positive association was observed (P for trend=0.016, model 2). Likewise, dermal p16INK4a positivity was not associated with epidermal morphology but was associated with the elastic fibre morphology in both the papillary and reticular dermis (Table 2 and Figure 2: P for trend =0.041 and P for trend =0.010 respectively, model 2). Analyses using each individual skin morphological characteristic rather than a composite score demonstrated similar associations (Supplementary tables 1 and 2).

Next, we assessed the association of p16INK4a positivity tertiles with wrinkle grading and perceived age. Higher tertiles of epidermal p16INK4a positivity were significantly associated with a higher mean wrinkle grade, even after adjustment for potential confounders including the papillary and reticular elastic fibre composite scores (Table 3 and Figure 2: P for trend =0.033, model 3). Furthermore, higher tertiles of epidermal p16INK4a positivity were associated with a higher perceived age (P for trend =0.005, model 3). The trend remained after adjustment for the wrinkle grading (one of the components of perceived age) (Table 3: P for trend =0.076, model 4). Dermal p16INK4a positivity was not significantly associated with the wrinkle grading or perceived age (Table 3 and Figure 2), although there was a tendency for it to associate with perceived age after adjusting for the wrinkle grading (Table 3: P for trend = 0.064, model 4).

Table 2. Skin morphology composite scores dependent on tertiles of P16INK4a positivity.

	Tertiles of epidermal p16INK4a positivity				Tertiles of dermal p16INK4a positivity			
	Low	Middle	High		Low	Middle	High	
	≤0.30	0.30-1.30	≥1.30	P for trend	≤0.72	0.72-2.05	≥2.05	P for trend
Composite score – Epidermis								
Model 1	-0.27 (0.21)	0.13 (0.20)	-0.10 (0.21)	0.803	-0.09 (0.20)	0.03 (0.20)	0.06 (0.20)	0.596
Model 2	-0.24 (0.25)	-0.10 (0.27)	-0.22 (0.27)	0.922	-0.42 (0.26)	-0.04 (0.26)	-0.11 (0.27)	0.337
Composite score - Papillary dermis, layer 1								
Model 1	-1.14 (0.55)	-0.81 (0.54)	1.94 (0.55)	<0.001	-1.05 (0.57)	0.74 (0.56)	0.30 (0.56)	0.103
Model 2	-1.45 (0.65)	-0.96 (0.70)	2.59 (0.59)	<0.001	-1.24 (0.73)	0.65 (0.72)	0.58 (0.77)	0.041
Composite score - Reticular dermis, layers 2 to 5								
Model 1	-0.50 (0.57)	-0.57 (0.57)	1.05 (0.57)	0.064	-1.36 (0.57)	0.87 (0.56)	0.48 (0.56)	0.027
Model 2	-0.82 (0.70)	-0.70 (0.77)	1.32 (0.76)	0.016	-1.67 (0.73)	0.84 (0.72)	0.66 (0.76)	0.010

All values are given as estimated mean with standard error (SE). Estimated means were calculated by using a linear mixed model: model 1: adjustment for age, sex and long-lived family member status; model 2: as model 1 plus skin tanning type, sunbed use, sun exposure, smoking, number of cardiovascular and metabolic diseases and body mass index. See supplementary material for the individual skin morphology characteristics dependent on p16INK4a positivity. Epidermal p16INK4a positivity: number of cells staining positive for p16INK4a per mm length of the epidermal–dermal junction, dermal p16INK4a positivity: number of cells staining positive for p16INK4a per 1 mm^2 dermis

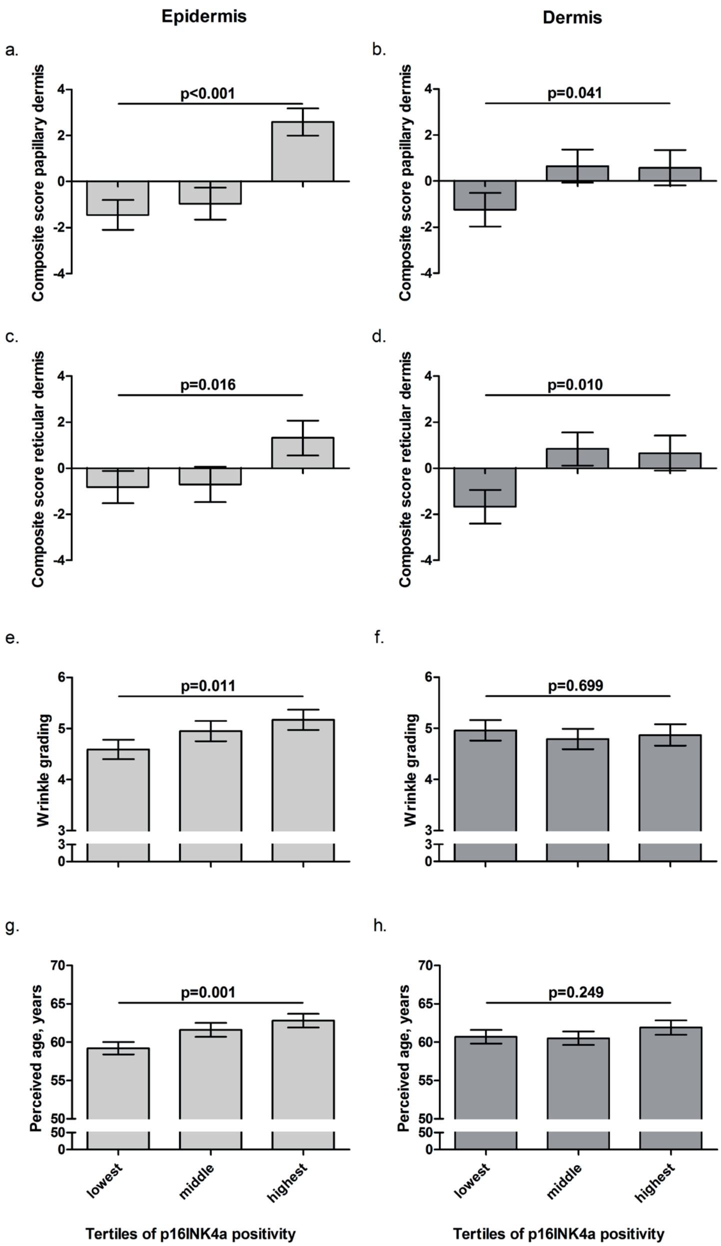

Figure 2. Elastic fibre composite scores, wrinkle grading and perceived age dependent on tertiles of p16INK4a positivity.
All values are given as estimated mean ± standard error. Estimated means were calculated with a linear mixed model. Adjustment was made for chronological age, sex, long-lived family member status, skin tanning type, sunbed use, sun exposure, smoking, number of cardiovascular diseases and body mass index.

Table 3. Wrinkle grading and perceived age dependent on tertiles of p16INK4a positivity.

	Tertiles of epidermal p16INK4a positivity				Tertiles of dermal p16INK4a positivity			
	Low ≤0.30	Middle 0.30-1.30	High ≥1.30	P for trend	Low ≤0.72	Middle 0.72-2.05	High ≥2.05	P for trend
Wrinkle grading								
Model 1	4.47 (0.15)	4.77 (0.15)	5.04 (0.15)	0.007	4.88 (0.15)	4.76 (0.15)	4.66 (0.14)	0.301
Model 2	4.59 (0.19)	4.95 (0.20)	5.17 (0.20)	0.011	4.96 (0.20)	4.79 (0.20)	4.87 (0.21)	0.699
Model 3	4.63 (0.19)	4.90 (0.20)	5.15 (0.21)	0.033	4.99 (0.20)	4.78 (0.20)	4.84 (0.20)	0.565
Perceived age (in years)								
Model 1	58.9 (0.68)	60.3 (0.67)	62.2 (0.68)	0.001	60.3 (0.70)	60.4 (0.69)	60.7 (0.69)	0.656
Model 2	59.2 (0.83)	61.6 (0.90)	62.8 (0.89)	0.001	60.7 (0.90)	60.5 (0.89)	61.9 (0.94)	0.249
Model 3	59.4 (0.83)	61.5 (0.90)	62.4 (0.93)	0.005	60.9 (0.90)	60.3 (0.87)	61.7 (0.93)	0.400
Model 4	59.7 (0.62)	60.9 (0.66)	61.1 (0.69)	0.076	60.0 (0.65)	60.1 (0.63)	61.4 (0.65)	0.064

All values are given as estimated mean with standard error (SE). Estimated means were calculated by using a linear mixed model: model 1: adjustment for age, sex and long-lived family member status; model 2: as model 1 plus skin tanning type, sunbed use, sun exposure, smoking, number of cardiovascular diseases and body mass index; model 3: as model 2 plus elastic fibre composite score of the papillary dermis and elastic fibre composite score of the reticular dermis; model 4: as model 3 plus wrinkle grade. Epidermal p16INK4a positivity: number of cells staining positive for p16INK4a per mm length of the epidermal–dermal junction, dermal p16INK4a positivity: number of cells staining positive for p16INK4a per 1 mm^2 dermis

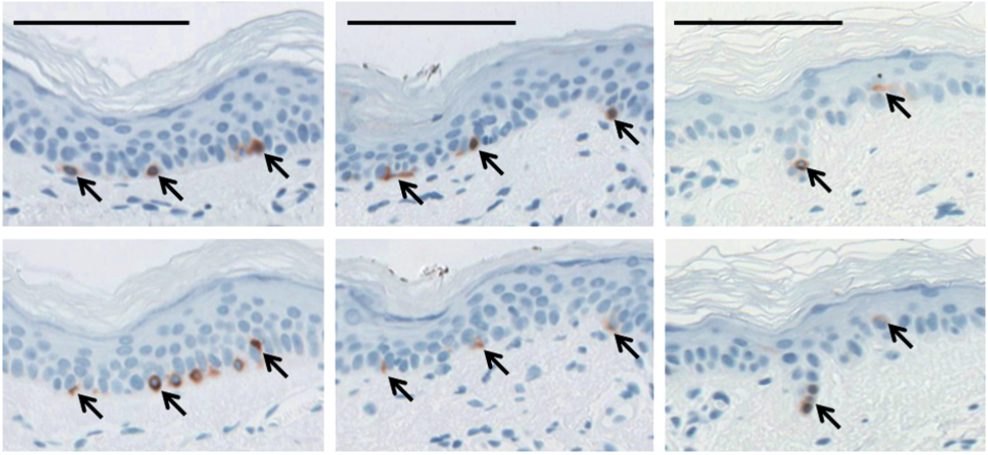

Figure 3. Staining for P16INK4a and MelA in adjacent skin sections from 3 participants.
Skin sections from each participant (columns) were stained for p16INK4a (top images) and MelA (bottom images). The p16INK4a positive cells (arrows in top images) co-localised with MelA positive staining (arrows in bottom images); black line represents 100μm.

We next examined whether the p16INK4a positive epidermal cells were melanocytes. All p16INK4a positive cells (n=23 for three participants selected at random from those with high numbers of p16INK4a epidermal positivity) were located adjacent to the basement membrane and were S100 positive (data not shown). Epidermal p16INK4a positive cells were also observed to co-localise to MelA positive cells in adjacent 4 μm skin biopsy sections (Figure 3).

Discussion

Firstly, we demonstrated an association between epidermal and dermal p16INK4a positivity in the upper-inner arm with local elastic fibre morphology in both layers of the dermis. Secondly, and independently of the associations described above, we found significant associations between p16INK4a positivity in the epidermis, but not dermis, with a higher wrinkle grading and higher perceived age.

With age, greater numbers of senescent cells are observed in mice and human tissues [2;6;7;33], due to an increase in senescent cells per se and/or failure to eliminate such cells by apoptosis or through clearance by the immune system. We found that epidermal p16INK4a positivity in the skin was associated with elastic fibre morphology analogous to changes with chronological age [15]. Of note, some of the associations were significant only after adjustment for potential confounders, highlighting the importance of external factors such as sun exposure and smoking. This association was particularly strong between elastic fibre characteristics in the papillary dermis nearest the p16INK4a positive epidermal cells and less strong in the reticular dermis, and vice versa for dermal p16INK4a positivity. This suggests an interaction between the localization of p16INK4a positive cells and elastic fibre structure. We speculate that this link could be explained by the effects of the senescence associated secretory phenotype (SASP) [34;35], since the factors secreted by senescent cells are likely to affect the surrounding tissue more than tissue located further away. In support of this, clearance of p16INK4a positive cells in progeroid mice delayed the onset of age-related diseases [14] and silencing p16INK4a in living skin equivalent models transformed the morphology of aged skin towards a younger phenotype [36], although the p16INK4a positive cells in the skin equivalent were keratinocytes rather than melanocytes. Due to the cross-sectional nature of the study however, we cannot rule out that the number of p16INK4a positive cells are purely reflecting the degree of ageing rather than a direct influence of the SASP on the dermis.

Perceived age has been previously linked to ageing: it predicts survival [24] and links to pathology such as carotid atherosclerosis. Here, epidermal p16INK4a positivity associated with wrinkle grading and perceived age, independently of the associations between elastic fibre morphology and p16INK4a positivity. Although the association between epidermal p16INK4a positivity and perceived age is attenuated after adjusting for the wrinkling grading (because of the correlation between wrinkling and perceived age), a trend still exists indicating that epidermal p16INK4a is also associated with non-wrinkling facial aging features. In the dermis, a trend between p16INK4a positivity and perceived age was found after adjustment for the wrinkle grading, indicating that fibroblast p16INK4a positivity in a sun-protected site reflects the non-wrinkle components of perceived age such as face shape changes with age [16;19]. The reason for the differing associations with perceived age of epidermal and dermal p16INK4a positivity is unclear. However, in sun-exposed sites large dermal changes are associated with skin wrinkling; hence, it could be that the number of p16INK4a positive fibroblasts in sun-exposed skin is more strongly associated with facial wrinkling, but this now needs testing.

Previously we have suggested that the p16INK4a positive epidermal cells were likely melanocytes [8]. In agreement with previous observations [32] all p16INK4a positive cells in the epidermis were S100 positive, coincided with MelA staining in adjacent skin sections, and were located predominately along the basal membrane indicating that the cells were primarily melanocytes. This supports the importance of p16INK4a in melanocyte senescence, as senescence is an important tumour suppression mechanism [37], p16INK4a expression loss associates with melanoma progression [38] and DNA mutations in the p16INK4a locus have been found in familial melanoma cases [39]. Here, the numbers of p16INK4a positive melanocytes were a good indicator of the extent of facial ageing. This result may reflect the efficiency of cellular mechanisms (e.g. DNA repair) required for protection of melanocytes to pro-ageing factors across the body. However, the link between p16INK4a expressing cells in sun-protected skin with facial ageing could also be due to variations within the LLS cohort of environmental exposures such as diet [40] and physical activity [33;41]. Thus, further work is required to determine what mechanisms are driving the link between p16INK4a positive melanocytes in human arm skin and facial ageing.

One of the limitations of our study is the cross-sectional design of the study, which does not allow for conclusions on causal rather than associative relationships. In addition, the subjects were members of long-lived families which we have previously shown to have lower numbers of p16INK4a positive cells in skin [8]. However, all results were adjusted for long-lived family member status. Another potential issue is that the biopsies were taken from the upper-inner arm, while perceived age and the wrinkle grading were derived from the face. However, we believe it a striking observation that despite this lack of direct spatial relationship, p16INK4a positivity within arm skin is significantly linked to a more global phenomenon such as perceived age. The observation that p16INK4a positive cells are primarily melanocytes within the skin samples in our study is supported by the fact the p16INK4a staining was seen exclusively in S100 positive cells. Also, melA staining of these p16INK4a positive cells in consecutive sections was observed. However, larger numbers of subjects would be required to conclusive rule out the presence of p16INK4a positive keratinocytes in sun-protected skin. Finally, due to the large number of participants we only used one, albeit widely used and validated [1;2;7;33], marker for cellular senescence which means we cannot definitively assign these results to cell senescence. Including other markers, such as SAβ-gal or DNA damage foci, would have provided more evidence to term the p16INK4a positive cells senescent. However, irrespective of whether cells expressing p16INK4a in situ are truly senescent or not, p16INK4a positive cells in human skin are indicative of local elastic fibre morphology and facial ageing, and thus be considered a marker of global skin ageing.

This is the largest study of cellular senescence in skin to-date (n=178 participants) and participants of the LLS were extensively phenotyped which allowed us to adjust the findings for potential confounders. Within these participants we previously reported that p16INK4a positivity in the skin was lower in long-lived family member than in their partners [8]. Now, to the best of our knowledge we are the first to show a significant link between p16INK4a positivity in one body site with signs of visible ageing (wrinkle grading and perceived age) in another, independently of long-lived family member status and of chronological age. P16INK4a positive cells in the skin were also linked to local elastic fibre morphology in a manner resembling the effects of chronological age. In addition, we show that the numbers of p16INK4a positive cells in the epidermis of sun-protected skin are restricted to the melanocyte cell population, highlighting the importance of the p16INK4a cell cycle checkpoint in melanocyte ageing. This study shows that p16INK4a positivity is, apart from a cellular senescence phenomenon and being linked to familial longevity, also strongly linked to human skin and facial ageing in vivo. Further work should focus on the causal factors driving the link between p16INK4a positive cells and skin ageing. Additionally, the importance of cellular senescence in human ageing should be explored in other tissues, to study whether it is a ubiquitous phenomenon of in vivo human ageing.

Acknowledgements

We would like to thank Nicole Hudson, Sharon Catt and Michael van Ginkel for the elastic fibre measures, Barbara Strongitharm and William Parish for the p16INK4a counts, Claire Brock for the MelA and p16INK4 co-staining, Peter Murray and Cyrena Tomlin for help creating the perceived ages, Tamara Griffiths and Stephanie Ogden for the wrinkle grading, Corine de Koning-Treurniet and Ton de Craen for the acquisition of photographs, and Joke Blom and Corine de Koning-Treurniet for their help in skin biopsy processing.

This study was supported by the Innovation Oriented research Program on Genomics (SenterNovem; IGE01014, IGE5007), the Centre for Medical Systems Biology (CMSB), the Netherlands Genomics Initiative/Netherlands Organization for scientific research (NGI/NWO 05040202, 050-060-810 (NCHA)), Unilever, the EU funded Network of Excellence Lifespan (FP6 036894) and the National Institute on Aging (NIA P01 AG031862). Individual co-authors were funded by: the Netherlands Genomics Initiative (NCHA 050-060-810) [PES] and T32HL007751 - NIH Training Grant in Mechanisms of Vascular Disease [JSP].

Supplementary table 1. Skin morphology dependent on tertiles of epidermal P16INK4a positivity.

	Tertiles of epidermal p16INK4a positivity			P for trend
	Low ≤0.30 (N=59)	Middle 0.30-1.30 (N=60)	High ≥1.30 (N=59)	
Epidermis				
Thickness, μm				
Model 1	39.0 (0.87)	39.8 (0.85)	41.2 (0.87)	0.084
Model 2	39.5 (1.06)	39.9 (1.15)	41.6 (1.14)	0.108
Curvaturea				
Model 1	827 (8.56)	844 (8.36)	843 (8.58)	0.182
Model 2	817 (11.1)	831 (12.0)	839 (11.9)	0.097
Papillary dermis (layer 1)				
Area covered by fibres, μm^2 [a]				
Model 1	23.3 (2.89)	24.5 (2.82)	37.2 (2.90)	0.001
Model 2	21.4 (3.54)	23.0 (3.85)	39.6 (3.80)	<0.001
Number of elastic fibres				
Model 1	43.1 (5.41)	45.1 (5.28)	68.8 (5.42)	0.001
Model 2	41.0 (6.41)	43.8 (6.96)	75.6 (6.89)	<0.001
Area covered by a single fibre, μm^2				
Model 1	27.3 (1.10)	27.7 (1.07)	32.6 (1.10)	0.001
Model 2	26.3 (1.32)	27.3 (1.43)	33.2 (1.42)	<0.001
Length of a fibre, μm				
Model 1	15.0 (0.47)	15.8 (0.46)	17.3 (0.47)	0.001
Model 2	14.7 (0.57)	15.7 (0.61)	17.7 (0.61)	<0.001
Thickness of a fibre, nm				
Model 1	1920 (28.1)	1866 (27.4)	1955 (28.1)	0.413
Model 2	1912 (37.6)	1849 (40.8)	1957 (40.4)	0.355
Curl of a fibrea				
Model 1	925 (6.26)	914 (6.11)	904 (6.27)	0.021
Model 2	922 (7.79)	910 (8.45)	894 (8.36)	0.004
Reticular dermis (layers 2-5)				
Area covered by fibres, μm^2 [a]				
Model 1	62.7 (3.65)	64.1 (3.62)	75.1 (3.66)	0.020
Model 2	61.0 (4.58)	62.4 (5.00)	76.4 (4.92)	0.008
Number of elastic fibres				
Model 1	95.7 (4.29)	103 (4.25)	112 (4.30)	0.010
Model 2	92.3 (5.30)	99.6 (5.79)	112 (5.70)	0.003
Area covered by a single fibre, μm^2				
Model 1	48.4 (1.85)	47.1 (1.83)	51.5 (1.85)	0.245
Model 2	47.6 (2.23)	47.3 (2.44)	52.5 (2.40)	0.080

Supplementary table 1. (continued)

	Tertiles of epidermal p16INK4a positivity			P for trend
	Low ≤0.30 (N=59)	Middle 0.30-1.30 (N=60)	High ≥1.30 (N=59)	
Length of a fibre, µm				
Model 1	20.7 (0.56)	20.7 (0.56)	21.8 (0.57)	0.148
Model 2	20.1 (0.69)	20.5 (0.75)	21.9 (0.74)	0.035
Thickness of a fibre, nm				
Model 1	2173 (20.6)	2159 (20.4)	2192 (20.6)	0.518
Model 2	2186 (26.6)	2184 (29.0)	2220 (28.6)	0.306
Curl of a fibrea				
Model 1	907 (5.47)	914 (5.43)	907 (5.49)	0.993
Model 2	909 (7.41)	918 (8.09)	908.9 (7.97)	0.980

All values are given as estimated mean (standard error). a= x10^3. Linear mixed model: model 1: adjustment for age, sex and long-lived family member status; model 2: as model 1 plus skin tanning type, sunbed use, sun exposure, smoking, number of cardiovascular and metabolic diseases and body-mass index. Independent variable: tertiles of p16INK4a positivity, dependent variables: skin morphology characteristics. Tertiles of p16INK4a positive epidermal cells: lowest ≤ 0.30 (median = 0.00), middle 0.30–1.30 (median = 0.55), highest ≥ 1.30 (median = 3.09) cells per mm length of the epidermal–dermal junction.

Supplementary table 2. Skin morphology dependent on tertiles of dermal P16INK4a positivity.

	Tertiles of dermal p16INK4a positivity			P for trend
	Low ≤0.72 (N=59)	Middle 0.72-2.05 (N=60)	High ≥2.05 (N=59)	
Epidermis				
Thickness, µm				
Model 1	40.3 (0.87)	40.5 (0.86)	39.2 (0.86)	0.383
Model 2	41.1 (1.11)	40.3 (1.10)	39.2 (1.16)	0.139
Curvature[a]				
Model 1	835 (8.56)	845 (8.50)	835 (8.45)	0.968
Model 2	821 (11.6)	838 (11.5)	822 (12.1)	0.971
Papillary dermis (layer 1)				
Area covered by fibres, µm^2 [a]				
Model 1	23.6 (2.95)	32.7 (2.93)	28.6 (2.91)	0.251
Model 2	21.9 (3.91)	32.0 (3.86)	29.1 (4.08)	0.132
Number of elastic fibres				
Model 1	43.6 (5.51)	61.0 (5.47)	52.5 (5.44)	0.277
Model 2	41.9 (7.12)	60.7 (7.03)	55.9 (7.42)	0.108
Area covered by a single fibre, µm^2				
Model 1	26.8 (1.11)	30.7 (1.11)	30.2 (1.10)	0.036

Supplementary table 2. Skin morphology dependent on tertiles of dermal P16INK4a positivity. (continued)

	Tertiles of dermal p16INK4a positivity			
	Low ≤0.72 (N=59)	Middle 0.72-2.05 (N=60)	High ≥2.05 (N=59)	P for trend
Model 2	26.2 (1.45)	30.1 (1.43)	30.3 (1.51)	0.022
Length of a fibre, μm				
Model 1	14.9 (0.47)	16.4 (0.47)	16.7 (0.47)	0.007
Model 2	14.8 (0.61)	16.3 (0.61)	16.9 (0.64)	0.005
Thickness of a fibre, nm				
Model 1	1928 (28.2)	1931 (28.0)	1882 (27.8)	0.245
Model 2	1913 (40.0)	1924 (39.5)	1882 (41.7)	0.502
Curl of a fibrea				
Model 1	920 (6.29)	916 (6.25)	908 (6.21)	0.207
Model 2	915 (8.33)	910 (8.23)	902 (8.69)	0.180
Reticular dermis (layers 2-5)				
Area covered by fibres, μm^2 [a]				
Model 1	59.4 (3.65)	73.0 (3.60)	69.5 (3.61)	0.062
Model 2	56.5 (4.79)	72.5 (4.72)	70.6 (5.01)	0.017
Number of elastic fibres				
Model 1	92.9 (4.23)	114 (4.17)	104 (4.19)	0.083
Model 2	87.6 (5.50)	110 (5.42)	105 (5.75)	0.011
Area covered by a single fibre, μm^2				
Model 1	44.9 (1.83)	51.3 (1.80)	50.8 (1.81)	0.025
Model 2	44.7 (2.31)	51.7 (2.28)	51.1 (2.42)	0.024
Length of a fibre, μm				
Model 1	19.9 (0.56)	21.5 (0.55)	21.8 (0.55)	0.013
Model 2	19.6 (0.71)	21.3 (0.70)	21.6 (0.75)	0.021
Thickness of a fibre, nm				
Model 1	2141 (20.4)	2205 (20.1)	2178 (20.2)	0.224
Model 2	2159 (27.6)	2225 (27.2)	2205 (28.8)	0.181
Curl of a fibrea				
Model 1	908 (5.49)	913 (5.41)	907 (5.43)	0.882
Model 2	912 (7.80)	914 (7.68)	908 (8.16)	0.678

All values are given as estimated mean (standard error). a= x10^3. Linear mixed model: model 1: adjustment for age, sex and long-lived family member status; model 2: as model 1 plus skin tanning type, sun bed use, sun exposure, smoking, number of cardiovascular and metabolic diseases and body-mass index. Independent variable: tertiles of p16INK4a positivity, dependent variables: skin morphology characteristics. Tertiles of p16INK4a positive dermal fibroblasts: lowest ≤0.72 (median=0.00), middle 0.72-2.05 (median=1.29), highest ≥2.05 (median 3.20) cells per 1mm2 dermis.

References

(1) Rodier F, Campisi J. Four faces of cellular senescence. *J Cell Biol* 2011;192:547-556.

(2) Krishnamurthy J, Torrice C, Ramsey MR et al. Ink4a/Arf expression is a biomarker of aging. *J Clin Invest* 2004;114:1299-1307.

(3) Herbig U, Ferreira M, Condel L, Carey D, Sedivy JM. Cellular senescence in aging primates. *Science* 2006;311:1257.

(4) Jeyapalan JC, Ferreira M, Sedivy JM, Herbig U. Accumulation of senescent cells in mitotic tissue of aging primates. *Mech Ageing Dev* 2007;128:36-44.

(5) Dimri GP, Lee X, Basile G et al. A biomarker that identifies senescent human cells in culture and in aging skin in vivo. *Proc Natl Acad Sci U S A* 1995;92:9363-9367.

(6) Melk A, Schmidt BM, Takeuchi O, Sawitzki B, Rayner DC, Halloran PF. Expression of p16INK4a and other cell cycle regulator and senescence associated genes in aging human kidney. *Kidney Int* 2004;65:510-520.

(7) Ressler S, Bartkova J, Niederegger H et al. p16INK4A is a robust in vivo biomarker of cellular aging in human skin. *Aging Cell* 2006;5:379-389.

(8) Waaijer ME, Parish WE, Strongitharm BH et al. The number of p16INK4a positive cells in human skin reflects biological age. *Aging Cell* 2012;11:722-725.

(9) Koppelstaetter C, Schratzberger G, Perco P et al. Markers of cellular senescence in zero hour biopsies predict outcome in renal transplantation. *Aging Cell* 2008;7:491-497.

(10) Westhoff JH, Hilgers KF, Steinbach MP et al. Hypertension induces somatic cellular senescence in rats and humans by induction of cell cycle inhibitor p16INK4a. *Hypertension* 2008;52:123-129.

(11) Verzola D, Gandolfo MT, Gaetani G et al. Accelerated senescence in the kidneys of patients with type 2 diabetic nephropathy. *Am J Physiol Renal Physiol* 2008;295:F1563-F1573.

(12) Minamino T, Miyauchi H, Yoshida T, Ishida Y, Yoshida H, Komuro I. Endothelial cell senescence in human atherosclerosis: role of telomere in endothelial dysfunction. *Circulation* 2002;105:1541-1544.

(13) Tsuji T, Aoshiba K, Nagai A. Alveolar cell senescence in patients with pulmonary emphysema. *Am J Respir Crit Care Med* 2006;174:886-893.

(14) Baker DJ, Wijshake T, Tchkonia T et al. Clearance of p16Ink4a-positive senescent cells delays ageing-associated disorders. *Nature* 2011;479:232-236.

(15) Waaijer ME, Gunn DA, Catt SD et al. Morphometric skin characteristics dependent on chronological and biological age: the Leiden Longevity Study. *Age (Dordr)* 2012;34:1543-1552.

(16) Gunn DA, Rexbye H, Griffiths CE et al. Why some women look young for their age. *PLoS One* 2009;4:e8021.

(17) Gosain AK, Klein MH, Sudhakar PV, Prost RW. A volumetric analysis of soft-tissue changes in the aging midface using high-resolution MRI: implications for facial rejuvenation. *Plast Reconstr Surg* 2005;115:1143-1152.

(18) Ozdemir R, Kilinc H, Unlu RE, Uysal AC, Sensoz O, Baran CN. Anatomicohistologic study of the retaining ligaments of the face and use in face lift: retaining ligament correction and SMAS plication. *Plast Reconstr Surg* 2002;110:1134-1147.

(19) Nkengne A, Bertin C, Stamatas GN et al. Influence of facial skin attributes on the perceived age of Caucasian women. *J Eur Acad Dermatol Venereol* 2008;22:982-991.

(20) Takema Y, Hattori M, Aizawa K. The relationship between quantitative changes in collagen and formation of wrinkles on hairless mouse skin after chronic UV irradiation. *J Dermatol Sci* 1996;12:56-63.

(21) Griffiths CE. The clinical identification and quantification of photodamage. *Br J Dermatol* 1992;127 Suppl 41:37-42.

(22) Warren R, Gartstein V, Kligman AM, Montagna W, Allendorf RA, Ridder GM. Age, sunlight, and facial skin: a histologic and quantitative study. *J Am Acad Dermatol* 1991;25:751-760.

(23) Gordon JR, Brieva JC. Images in clinical medicine. Unilateral dermatoheliosis. *N Engl J Med* 2012;366:e25.

(24) Christensen K, Thinggaard M, McGue M et al. Perceived age as clinically useful biomarker of ageing: cohort study. *BMJ* 2009;339:b5262.

(25) Noordam R, Gunn DA, Tomlin CC et al. High serum glucose levels are associated with a higher perceived age. *Age (Dordr)* 2013;35:189-195.

(26) Noordam R, Gunn DA, Tomlin CC et al. Cortisol serum levels in familial longevity and perceived age: the Leiden longevity study. *Psychoneuroendocrinology* 2012;37:1669-1675.

(27) Gunn DA, de Craen AJ, Dick JL et al. Facial appearance reflects human familial longevity and cardiovascular disease risk in healthy individuals. *J Gerontol A Biol Sci Med Sci* 2013;68:145-152.

(28) Kido M, Kohara K, Miyawaki S, Tabara Y, Igase M, Miki T. Perceived age of facial features is a significant diagnosis criterion for age-related carotid atherosclerosis in Japanese subjects: J-SHIPP study. *Geriatr Gerontol Int* 2012;12:733-740.

(29) Gunn DA, Murray PG, Tomlin CC, Rexbye H, Christensen K, Mayes AE. Perceived age as a biomarker of ageing: a clinical methodology. *Biogerontology* 2008;9:357-364.

(30) Schoenmaker M, de Craen AJ, de Meijer PH et al. Evidence of genetic enrichment for exceptional survival using a family approach: the Leiden Longevity Study. *Eur J Hum Genet* 2006;14:79-84.

(31) Klaes R, Friedrich T, Spitkovsky D et al. Overexpression of p16(INK4A) as a specific marker for dysplastic and neoplastic epithelial cells of the cervix uteri. *Int J Cancer* 2001;92:276-284.

(32) Pawlikowski JS, McBryan T, van TJ et al. Wnt signaling potentiates nevogenesis. *Proc Natl Acad Sci U S A* 2013;110:16009-16014.

(33) Liu Y, Sanoff HK, Cho H et al. Expression of p16(INK4a) in peripheral blood T-cells is a biomarker of human aging. *Aging Cell* 2009;8:439-448.

(34) Coppe JP, Patil CK, Rodier F et al. Senescence-associated secretory phenotypes reveal cell-nonautonomous functions of oncogenic RAS and the p53 tumor suppressor. *PLoS Biol* 2008;6:2853-2868.

(35) Kuilman T, Peeper DS. Senescence-messaging secretome: SMS-ing cellular stress. *Nat Rev Cancer* 2009;9:81-94.

(36) Adamus J, Aho S, Meldrum H, Bosko C, Lee JM. p16INK4A influences the aging phenotype in the living skin equivalent. *J Invest Dermatol* 2014;134:1131-1133.

(37) Campisi J. Senescent cells, tumor suppression, and organismal aging: good citizens, bad neighbors. *Cell* 2005;120:513-522.

(38) Keller-Melchior R, Schmidt R, Piepkorn M. Expression of the tumor suppressor gene product p16INK4 in benign and malignant melanocytic lesions. *J Invest Dermatol* 1998;110:932-938.

(39) Platz A, Hansson J, Mansson-Brahme E et al. Screening of germline mutations in the CDKN2A and CDKN2B genes in Swedish families with hereditary cutaneous melanoma. *J Natl Cancer Inst* 1997;89:697-702.

(40) Shi Q, Hubbard GB, Kushwaha RS et al. Endothelial senescence after high-cholesterol, high-fat diet challenge in baboons. *Am J Physiol Heart Circ Physiol* 2007;292:H2913-H2920.

(41) Melk A, Tegtbur U, Hilfiker-Kleiner D et al. Improvement of biological age by physical activity. *Int J Cardiol* 2014;176:1187-1189.

Part III

Part III

Does skin senescence mirror aging in vivo?

Chapter 7

Chapter 7

Markers of cellular senescence and chronological age in various human tissues: a systemic review of the literature

M.E.C. Waaijer, M.S. Slee-Valentijn, R.G.J. Westendorp, A.B. Maier

In preparation

Abstract

Background: Cellular senescence, a stable growth arrest of cells, is increasingly recognized as a driver of the aging process. Several studies report higher numbers of senescent cells in a variety of tissues of older humans when compared to the young.

Objective: To systemically describe the literature on the association between markers of cellular senescence and chronological age in different types of tissues.

Methods: We searched Pubmed, Web of Science and Embase for articles that reported on senescence markers dependent on age in any human tissue. Out of 3833 unique articles 43 articles reporting on this topic were identified, including 44 cohorts. Data was extracted on the origin of tissue, the type of markers being used, and the age and gender distribution of the donors. A total of 78 associations between senescence markers and age were reported.

Outcomes: Cohort sizes ranged from 3 to 176 donors, and varied widely in their age distribution. Out of the 78 associations, 34 were positive and statistically significant associations ($p<0.05$) between senescence markers and chronological age, six showed positive trends ($0.05<p<0.10$), 27 associations were inconclusive ($p>0.10$) and one association showed a negative statistically significant association ($p<0.05$). A large proportion of the positive associations were based on studies conducted in blood, whereas it was less often the case in kidney and skin.

Conclusion: Almost half of the associations between markers of cellular senescence and age show a positive significant association. This can be interpreted as proof of an evident biological phenomenon but it is unclear to what extent publication bias explains for these outcomes.

Introduction

Cellular senescence, a stable growth arrest of the cell, has been widely studied *in vitro*. This growth arrest of senescent cells functions as an effective anti-tumor mechanism at the cost of a diminished capacity to regeneration of tissues [1]. Furthermore, senescent cells have been shown to secrete proteins that disrupt functional integrity of tissues and have pro-inflammatory and tumorigenic properties that act on surrounding cells, termed the senescence-associated secretory phenotype (SASP) [2-7]. Senescent cells have been found to be more prevalent in several tissues of aged mammals *in vivo* [8-12] and the SASP has been implicated in the aging process [13]. Seminal experiments using progeroid and normally aged mice show that health span was markedly improved when senescent cells were cleared from tissues by inducing apoptosis [14-16]. These data indicate a causal link between the presence of senescent cells and the rate of aging.

Several attempts have been made to clarify the role of senescent cells in the aging process of humans. *In vitro,* cells derived from older humans more often show higher expression of markers indicative of senescence compared to cells derived from young humans [17-20]. Senescent cells have also been shown to be more frequently present in tissue sections from older compared to younger humans. Studies in various animal models show that these positive associations between senescence and chronological age markedly differ across various tissues [9;11;21] and may reflect different rates of tissue renewal and or different sensitivity to triggers of senescence.

Here we have conducted a systematic review of the literature reporting on the prevalence of senescent cells dependent on chronological age in various human tissues.

Methods

Selection of studies

A systematic search of the literature was performed on 13-05-2014 in PubMed, EMBASE and Web of Science using the terms "senescence", "tissue"/"biopsy"/"histology", different organ/tissue types and different markers for cellular senescence (see Supplementary methods for complete search strategies) with no limitations on publication dates. The search yielded 6709 articles, of which 2876 were duplicates. A total of 3833 articles were screened on title and abstract by one author (MW); exclusion criteria were (1) animal studies; (2) *in vitro* studies; (3) reviews; (4) conference abstracts; (5) method and theory papers; (6) editorials; and (7) articles in another language than English. Then 458 articles were further evaluated based on full text by two authors (MW and MS). The same set of exclusion criteria was applied but now included the following additional criteria: (8) the method how senescent cells were detected was not reported; (9) the sole use of telomere length as a marker of senescence; (10) the detection of senescent cells was not related to human tissue; (11) the presence of senescent cells was not linked to neither age or nor disease; (12) the presence of senescent cells was linked to malignant tumors.

The following senescence markers were included: markers of cell-cycle arrest (p16, p21, p53), lack of proliferation markers (Ki67, bmi1), senescence-associated β galactosidase (SAβ-gal), senescence-associated heterochromatic foci (SAHF), DNA damage markers, SASP factors (including cytokines, growth factors, proteases). The lack of or decline of the markers Ki67, bmi1, CD45RA+, CD27+ and CD28+ are considered 'negative' markers of senescence', as the absence of one of these markers is indicative of cellular senescence. Telomere length was excluded as a marker of senescence as determining telomere length in tissue samples is cumbersome [22], sensitivity and specificity of telomere length as a marker of cellular senescence is low [23], and the contribution of telomere attrition to cellular senescence *in vivo* is not established (reviewed in [24;25]).

In 12.2% of the evaluated full text articles evaluators had a different judgment regarding inclusion or exclusion and in 22.1% of the evaluated full text articles one evaluator was undecided regarding inclusion or exclusion. Discrepancies in the judgment between evaluators were solved by including a third author (AM). This resulted in a total of 134 included articles on the association between markers of senescence and chronological age or disease. For this systematic review we further excluded 91 articles because the relation of senescence with chronological age was not reported (only relation with disease reported). The flow diagram of the articles under study is illustrated in Figure 1.

Extraction of data

From each of the 43 included articles the following data were extracted: type and origin of tissue; the number age and gender of the subjects; the marker(s) of senescence and techniques used; the association between the senescence markers and age (primary result), variation of association senescence markers and age, statistical test. If no information on the trend and/or a statistical test was given, raw data points for individual subjects were extracted from figures if possible, in order to calculate the association between senescence markers and age. IBM Statistics SPSS 20 was used for analyses. The direction of association was defined as followed: a positive association is defined as higher senescence across higher age groups (i.e. a higher expression of a positive senescence marker, or a lower expression of a negative marker). A negative association is defined as lower senescence across higher age groups. Associations

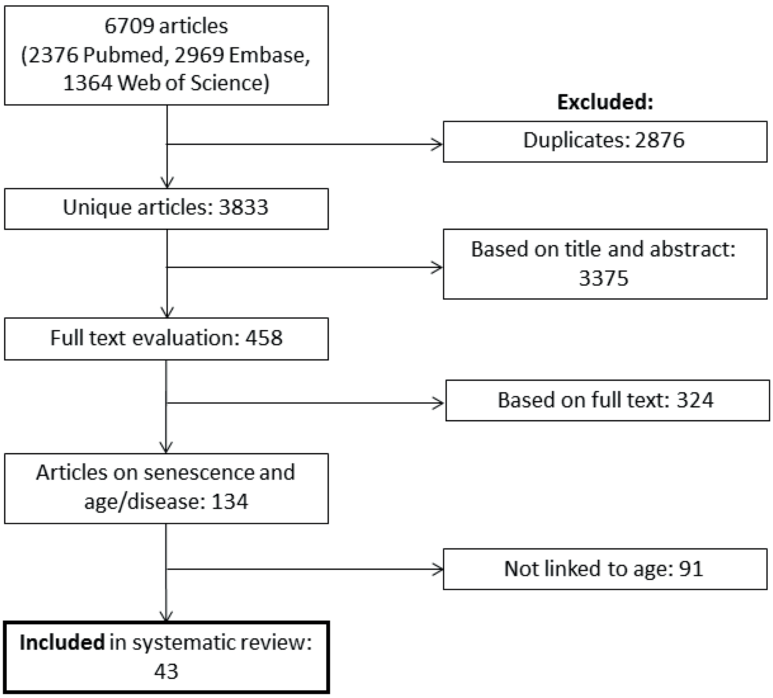

Figure 1. Flow chart of the in- and exclusion of articles.

were further classified by statistical significance. Associations were classified as a statistically significant association at $p<0.05$ and as a trend at $0.05<p<0.10$. All other outcomes were classified as inconclusive ($p>0.10$ or reported as 'ns – not significant' by the source article).

Results

Table 1 depicts the characteristics of the included cohorts (44 cohorts, from 43 articles) arranged by the tissue type that was sampled. Cohorts predominantly used blood (n=10), kidney (n=9) or skin (n=9) samples. Most tissues were acquired perioperatively or post-mortem, resulting in different medical conditions of subjects being studied. The size and the age distribution of the cohorts ranged widely, and only 22 out of 44 study cohorts provided information on gender. Several senescence markers were studied, and in some cohorts multiple markers were used. Among the most frequently used markers were p16 (n=20), SAβ-gal (n=7), p21 (n=5) and p53 (n=5). Most cohorts used either immunohistochemistry (IHC, n=21) or polymerase-chain reaction (PCR, n=10) techniques to detect senescence.

Table 1. Characteristics of included cohorts ordered by tissue type.

Tissue type	Origin of tissue	No. subjects	Age of subjects (yrs)	Gender M/F (%)	Marker	Technique	First author	Year of publication
Artery								
	Internal mammaries, coronary artery bypass surgery	24	M Mean 54.8, SE 5.5; O Mean 77.1, SE 2.2	100/0	p21; cyclin D	WB	Marchand	2011
	Sentinel lymph node biopsy (melanoma-associated profylactic procedure)	61	Y Mean 31.2, SE 1.3; O Mean 70.9, SE 1.4	59/41	p21; SASP (IL-6, IL-8, MCP-1)	PCR	Morgan	2013
Blood								
	Patients undergoing cardiac surgery	44	Y Median 32.8, IQR 28.1-42.1, O Median 69.1, IQR 61.0-74.6	59/41	CD45RA+CD27+/CD4+; CD45RA+CD27+/CD8+	FC	Ferrando-Martinez	2011
	Healthy controls accompanying liver transplant recipients	41	Mean 55.9; SD 13.2	39/61	CD8+CD28+; CD8+CD27+; CD4+CD28+; CD4+CD27+	FC	Gelson	2010
	Heterosexual participants	26	Mean 41; SD 13	81/19	CD45RA+CD31+CD4+; CD45RA+CD31-CD4+		Kilpatrick	2008
	Volunteers undergoing routine physical and medical examination and survivors of an epidemiological study of aging	178	Range 0-93	nr	CD28-CD8+; CD28-CD4+	FC	Lemster [a]	2008
	Healthy donors	36	Range 21-74	nr	CD28-CD57+	FC	Mondal	2013
	Healthy donors	51	Range 18-89	nr	CD28-CD8+	FC	Nociari	1999
	Cohort of breast cancer survivors, part received chemotherapy	176	Median 67; range 50-93	0/100	p16	PCR	Sanoff a	2014
	Prospective adjuvant cohort breast cancer patients, part received chemotherapy	33	Range 32-69	0/100	p16	PCR	Sanoff b	2014
	Healthy donors (no history of inflammatory or malignant disease)	74	Range 24.4-90.1	nr	Ki67	FC	Schonland	2003

Table 1. Characteristics of included cohorts ordered by tissue type. (continued)

Tissue type	Origin of tissue	No. subjects	Age of subjects (yrs)	Gender M/F (%)	Marker	Technique	First author	Year of publication
	Nonsmoking healthy volunteers, <1 hour exercise/week	47	Y Mean 21.8, SD 2.8; O Mean 50.9, SD 7.6	62/38	p53	WB	Werner	2011
Brain								
	Autopsied individuals, postmortem interval range 3 to 43.5 hours, uncertain for fetuses (died in utero)	21	Range fetal-90	40/60	p16	IF	Bhat [a]	2012
Eye								
	Post-mortem	9 (?)	Range <30-75	nr	BMI1; p16	WB; IF; IHC	Abdouh	2012
	Post-mortem, various causes of death	23	Y Median 48.0, IQR 45.5-55.0; O Median 72.5, IQR 72.0-74.0	61/39	SASP (IL1-RA)	IHC	Cao	2013
	Residual corneal tissues obtained after penetrating keratoplasty	27	Range 19-61	nr	p16; p21; p53	PCR	Song	2008
	Death to preservation interval <30 hours. Donor history and condition of tissue did not indicate damaged epithelium	33	Median 37; IQR 24-51	nr	p16	PCR	Wang	2012
Gastro-intestinal								
	Upper gastrointestinal endoscopy	46	Median 69.5; Range 29-90	nr	SAβ-gal	IHC	Going [b]	2002
Heart								
	Post-mortem, no cardiovascular cause of death, clinical/ anatomincal/ histological inclusion criteria provided	74	Range 19-104	57/43	p16	IF	Kajstura	2010
Kidney								

Table 1. Characteristics of included cohorts ordered by tissue type. (continued)

Tissue type	Origin of tissue	No. subjects	Age of subjects (yrs)	Gender M/F (%)	Marker	Technique	First author	Year of publication
	Nephrectomies and renal transplants	58	Range 17.8-93.3	nr	cyclin D	IHC	Berkenkamp	2014
	Nephrectomies and renal transplants	20	Mean 54.4; SD 18; Range 21-80	70/30	p16	IHC	Chkhotua	2003
	Renal transplants	33	Mean 48.0; SD 15.7	45/55	p16	PCR	Gingell-Littlejohn	2013
	Renal transplants	54	Mean 46.3; SD 16.0	69/31	p21	PCR	Koppelstaetter	2008
	Patients with IgA nephropathy	108	Mean 35; SD 11.9	54/46	SAβ-gal; p16; p21	IHC	Liu	2012
	Renal transplants.	73	Mean 46.9; SD 16.3	51/49	p16	PCR	McGlynn	2009
	Nephrectomies, renal transplants and post-mortem	42	Median 51.6; Range 8 weeks-88 years	55/45	p16; p53; p21; SASP (MMP-1, TGFβ1)	PCR	Melk [a]	2004
	Includes diseased kidneys	66	Y Mean 36.4, SD 9.6; M Mean 52.8, SD 20.5; O Mean 47.9, SD 19.5	50/50	p16	IHC	Sis	2007
	Biopsies and nephrectomies	17	Mean 61; SE 2	82/18	p16; SAβ-gal	IHC	Verzola	2008
Lung								
	Lung biopsy samples or surgical resection, judged normal by pathological examination	14	Range 43-82	nr	p16; mH2A	WB	Shivshankar	2011
Prostate								
	Benign tissue from hyperplastic transition zone, from radical prostatectomies	nr	Range 40- >70	100/0	SAβ-gal	IHC	Castro	2003

Table 1. Characteristics of included cohorts ordered by tissue type. (continued)

Tissue type	Origin of tissue	No. subjects	Age of subjects (yrs)	Gender M/F (%)	Marker	Technique	First author	Year of publication
	Specimens from transition zones of radical prostatectomies or transrectal ultrasound-guided biopsies	43	Median 62.0; IQR 57.5-66.0	100/0	SAβ-gal	IHC	Choi	2000
Skin								
	Patients undergoing Moh's micrographic surgery for skin cancer	20	Y Median 35.0, IQR 31.0-37.8; O Median 75.5, IQR 73.0-80.3	55/45	SAβ-gal	IHC	Dimri	1995
	Normal donors, sites of skin biopsies included scalp, eyelid, above the upper lip.	4	Y 1; O >60	nr	Lamin B	IHC	Dreesen [a]	2013
	Punch biopsies from patients undergoing cosmetic or dermatosurgical procedures (facial and abdominal skin)	36	Median 35.1; Range 6-77	50/50	p53	IHC	El-Domyati	2003
	Recruited from department of dermatology	4	Range 18-77	nr	Ki67	IF	Klement	2012
	Skin from circumcision and abdominal punch biopsy	2	Neonatal; 86	nr	p16	IHC	Lee	2010
	Post-chemotherapy	10	Median 18; Range 13-25	80/20	p16; p21	PCR	Marcoux [c]	2013
	Biopsies obtained for medical reasons, from all regions of the body, taken outside of disease-affected areas	33	Range 0-95	nr	p16	IHC	Ressler [a]	2006
	Patients undergoing Moh's micrographic surgery, noncancer tissue samples	53	Range 14-84	64/36	SAβ-gal	IHC	Severino	2000

Table 1. Characteristics of included cohorts ordered by tissue type. (continued)

Tissue type	Origin of tissue	No. subjects	Age of subjects (yrs)	Gender M/F (%)	Marker	Technique	First author	Year of publication
	Patients from department of dermatology, Fitzpatrick skin types I or II, exclusion criteria provided	25	Range 22-89	79/21	53BP1	IHC	Spandau	2012
Testis								
	Testicular tissue removed in surgeries unrelated to testicular germ cell tumours (e.g. prostate cancer, contralateral Leydig tumour), fetal tissue from spontaneous abortions	33	Range fetal-adult	100/0	γH2AX	IHC	Bartkova [a]	2011
Thymus								
	Surgery for reasons other than thymic pathology, no autoimmune disease	20	Range fetal-adult	nr	Ki67; p16	IHC	Kanavaros [a]	2001
Several tissues								
	Obtained from surgeries or autopsies	nr	nr	nr	p16	IHC	Nielsen [d]	1999
	Normal areas and tumor areas	nr	nr	nr	DDR (γH2AX, ATM, 53BP1, CHK2, p53)	IHC	Nuciforo [e]	2007

SD: standard deviation. SE: standard error. IQR: interquartile range. nr: not reported. DDR: DNA damage response. IHC: immunohistochemistry. IF: immunofluorescence. PCR: polymerase chain reaction. FC: flow cytometry. WB: Western blot. Y: young age group. M: middle age group. O: old age group.

[a]: Includes fetal/newborn/infant (≤1 year) tissue.

[b]: 18 subjects without dysplasia or carcinoma

[c]: All donors <25 years.

[d]: Tissue types: brain, spinal cord/peripheral nerves, heart, lung, liver, spleen, kidney, bladder, uterus, ovary, breast, testis, epididymis, prostate, oesophagus, stomach, intestines, pancreas, pituitary, adrenal, thyroid, parathyroid and salivary glands, skin, tonsil, lymph node and bone marrow.

[e]: Mix of normal and tumor tissue. Tissue types: breast, lung, colon-rectum, kidney, larynx, stomach, hematopoietic system, skin, soft tissue, bone.

Table 2 shows the multiple associations (N=78) between senescence and chronological age that were tested in the cohorts. Thirty-four out of the 78 (44%) reported associations showed a positive statistically significant association of cellular senescence and age, and six out of 78 (8%) associations showed a positive trend. Twenty-seven out of 78 (35%) inconclusive associations were reported. One negative statistically significant association of senescence with age was found. Ten out of 78 (13%) associations reported an association with age but provided too little quantification or did not report on a statistical test to solidify their findings.

Table 3 summarizes the associations of senescence with age per tissue. Kidney, blood and skin were used most. Out of 27 associations based on kidney tissue, nine (33%) were positive significant associations, three (11%) were positive trends, and 14 associations (52%) were inconclusive. One (4%) negative significant association of senescence with age was seen with matrix metalloproteinase (MMP-1). The outcomes of the 16 associations in blood samples were differently distributed: nine (56%) were positive significant associations, two (13%) were positive trends, four (25%) associations were inconclusive, and for one association (6%) insufficient information was supplied. In the skin 13 associations were studied, and results were diverse: four (31%) were positive significant associations, four (31%) associations were inconclusive, and insufficient information was supplied for five associations (38%).

Table 4 summarizes the reported associations for the various markers used. The most frequently used marker was p16 with 29 reported associations, though in some cases multiple samples of the same biopsy were stained for p16. With p16 as a marker, 14 (48%) positive significant associations were found, another four (14%) were positive trends, and nine (31%) associations were inconclusive. Two (7%) associations with p16 were reported without sufficient information. SAβ-gal was reported in eight associations, of which four (50%) were inconclusive and for the other four (50%) reported associations insufficient information was supplied. For the marker p21, seven associations were reported: one (14%) was a positive significant association and the other six (86%) associations were inconclusive.

Discussion

We have presented an extensive overview of the associations between senescence markers and chronological age in the literature. Overall, mostly significant positive associations of senescence with chronological age were found in different tissues.

The distribution of reported associations between senescence and chronological age favors positive associations, with only one reported significant negative association. This may be

Table 2. Assocations of senescence markers with age ordered by tissue type.

Tissue type	No. associa-tions tested	Association with age	Specification	Comments	First author	Year of publication
Artery						
	2	±; ±	FC O/M: 1.1 for both p21 and cyclin D		Marchand	2011
	4	+*;+;+*;+*	FC O/Y: 1.9 for p21; 1.7 for IL-6; 7.5 for IL-8; 2.1 for MCP-1		Morgan	2013
Blood						
	2	+*;+*	ΔOY: 13.73% for CD45RA+CD27+/CD4+; 27.82% for CD45RA+CD27+/CD8+	a	Ferrando-Martinez	2011
	4	+;+*;±; ±	r: -0.27 with MFI CD8+CD28+; -0.37 with MFI CD8+CD27+; -0.02 with MFI CD4+CD28+; -0.07 with MFI CD4+CD27+	a	Gelson	2010
	2	+*;±	Slope per year: -0.41% CD45RA+CD31+CD4+; 0.09% CD45RA+CD31-CD4+	a	Kilpatrick	2008
	2	+*;+*	r: 0.618 with % CD28-CD8+; 0.507 with % CD28-CD4+		Lemster	2008
	1	+*	r: 0.729 with %CD28-CD57+		Mondal	2013
	1	+*	ΔOY: 5.45 no. CD28-CD8+		Nociari	1999
	1	+*	Slope: 0.06 log2 expression of p16 per 1 year		Sanoff a	2014
	1	±	ΔOY: -0.23 log2 expression of p16		Sanoff b	2014
	1	nr	Slope: 0.0167 % Ki67 positive per year		Schonland	2003
	1	+*	FC O/Y: 2.16 p53		Werner	2011
Brain						
	1	+*	ΔOY: 43% p16 positive		Bhat	2012
Eye						
	1	+*	ΔOY: 0.56 rel. exp. of bmi1	a	Abdouh	2012
	1	+*	ΔOY: 0.833 stained area of IL-1RA		Cao	2013
	3	+*;±; ±	ΔOY: 0.365 rel.exp. for p16; -0.541 for p21; 0.063 for p53		Song	2008
	1	+*	r: 0.560 with rel. exp. p16		Wang	2012
Gastro-intestinal						

Table 2. (continued)

Tissue type	No. associations tested	Association with age	Specification	Comments	First author	Year of publication
	1	nr	No relation between SAβgal activity and age	b	Going	2002
Heart						
	1	+*	r: 0.83 with % p16 positive		Kajstura	2010
Kidney						
	1	+*	r: 0.27 with % cyclin d positive		Berkenkamp	2014
	6	+;+*;+;+*;+;±	r: 0.299-0.726 with p16	c	Chkhotua	2003
	1	+*	r: 0.597 with rel. exp. p16		Gingell-Littlejohn	2013
	2	±;+*	r: -0.01 with rel. exp. p21; 0.30 with rel. exp. p16		Koppelstaetter	2008
	3	±; ±; ±	r: 0.12 with % SAβgal positive; 0.25 with % p16 positive; 0.11 with % p21 positive		Liu	2012
	1	+*	r: 0.325 with rel. exp. p16		McGlynn	2009
	6	+*;±; ±;−*; ±; ±	Slope rel. exp. per year: 0.016 for p16 (cortex); 0.0003 for p53; 0.0028 for p21; -0.0128 for MMP1; 0.0019 for TGFβ1. R2: 0.03 for rel. exp. p16 (medulla)		Melk	2004
	4	+*;±; ±;+	R^2: 0.044-0.07 with % p16 positive	c, d	Sis	2007
	3	±; ±; ±	r: -0.02 with % p16 positive (glomerulus); 0.02 with % p16 positive (tubule); 0.38 with % SAβgal positive (tubule)		Verzola	2008
Lung						
	2	+*;+*	ΔOY: 2.273 rel. exp. p16; 0.408 rel. exp. mH2A		Shivshankar	2011
Prostate						
	1	nr	ΔOY: 0.31 SAβgal activity		Castro	2003
	1	±	Mean age of SAβgal negative tissue (N=26) 62.0 (SD 7.1) versus mean age of SAβgal positive tissue (N=17) mean age 60.4 (SD 5.9)		Choi	2000
Skin						

Table 2. (continued)

Tissue type	No. associa-tions tested	Association with age	Specification	Comments	First author	Year of publication
	2	nr;nr	Semi-quantative SAβgal positivity per biopsy: Y: 4 -, 3 ±, 2 +, 1 ++ (epidermis); O: 2 ±, 2++, 6 +++ (epidermis); Y: 10 - (dermis); O: 1 -, 4 ++, 5 +++ (dermis)		Dimri	1995
	2	nr;nr	"Robust levels of LMNB1 .. in the majority of young epidermal kerationocytes" " .. in skin from old donors, LMNB1.. were reduced" ".. the number of Ki-67–positive cells in the basal layer was dramatically reduced in aged skin"	a	Dreesen	2013
	2	+*;±	Slope p53 positivity+intensity score per year: 0.06 (facial skin); 0.001 (abdominal skin)		El-Domyati	2003
	1	+*	ΔOY: 13.2 % Ki67 positive	a	Klement	2012
	1	nr	"P16 stained cells were not detected well in Age 1 and Age 10 and numerous p16 stained cells were observed in Age 86"		Lee	2010
	2	±; ±	r: -0.385 with rel. exp. 16; -0.517 with rel. exp. p21		Marcoux	2013
	1	+*	ΔOY: 6 no. p16 positive x staining intensity		Ressler	2006
	1	±	r: 0.09 with no. of SAβgal positive		Severino	2000
	1	+*	ΔOY: 22.32 % 53BP1 positive		Spandau	2012
Testis						
	1	nr	Adult testes: ".. strong staining for γH2AX in spermatocytes.." Foetal testes: "..evident γH2AX staining that is characterized by numerous fine foci"	b	Bartkova	2011
Thymus						
	2	+*;nr	ΔOY: 62.6% Ki67 positive; increase p16 positive cells with age	a, b	Kanavaros	2001
Several tissues						
	several	nr	".. p16 expression in newborns was present only in Hassall's corpuscles, scattered thymic lymphocytes, and rare epithelial cells of the pancreas."	e	Nielsen	1999
	several	±	" .. there is no significant association between individual activated DDR markers and age, .."	b, e	Nuciforo	2007

Legend - table 2. continued
Rel. exp.: relative expression. FC: fold change. Δ: difference. r: correlation coefficient. R^2: coefficient of determination. nr: data not shown/no statistical testing. MFI: mean fluorescence intensity. Y: young age group. M: middle age group. O: old age group.
Direction of association: a positive association is defined as higher senescence (measured with a higher expression of a positive marker, or a lower expression of a negative marker for senescence) at higher ages. A negative association is defined as lower senescence at higher ages.
+*: positive significant association ($p<0.05$). +: positive trend ($0.05<p<0.10$), ±: inconclusive ($p>0.10$ or termed 'ns' in source report). −: negative trend ($0.05<p<0.10$). −*: negative significant association ($p<0.05$).
Comments: a: Negative marker of senescence: absence or low expression expected in senescence. b: Data not shown. c: Measured in several areas of kidney. d: p-value from multivariate model. e: cohort that used several, but less well-defined tissue-markers combinations, therefore unable to count within total number of associations tested.

Table 3. Statistical significance of associations between senescence and chronological age – ordered by type of tissue.

		Significance of associations with age (no., %)					
Tissue	**No.**	**Positive – significant**	**Positive – trend**	**inconclusive**	**Negative – trend**	**Negative – significant**	**Insufficient information reported**
All tissues	78	34 (44)	6 (8)	27 (35)	0 (0)	1 (1)	10 (13)
Kidney	27	9 (33)	3 (11)	14 (52)	0 (0)	1 (4)	0 (0)
Blood	16	9 (56)	2 (13)	4 (25)	0 (0)	0 (0)	1 (6)
Skin	13	4 (31)	0 (0)	4 (31)	0 (0)	0 (0)	5 (38)
Artery	6	3 (50)	1 (17)	2 (33)	0 (0)	0 (0)	0 (0)
Eye	6	4 (67)	0 (0)	2 (33)	0 (0)	0 (0)	0 (0)
Lung	2	2 (100)	0 (0)	0 (0)	0 (0)	0 (0)	0 (0)
Prostate	2	0 (0)	0 (0)	1 (50)	0 (0)	0 (0)	1 (50)
Thymus	2	1 (50)	0 (0)	0 (0)	0 (0)	0 (0)	1 (50)
Brain	1	1 (100)	0 (0)	0 (0)	0 (0)	0 (0)	0 (0)
Gastro-intestinal	1	0 (0)	0 (0)	0 (0)	0 (0)	0 (0)	1 (100)
Heart	1	1 (100)	0 (0)	0 (0)	0 (0)	0 (0)	0 (0)
Testis	1	0 (0)	0 (0)	0 (0)	0 (0)	0 (0)	1 (100)

No.: number of reported associations. Tissues are sorted on number of reported associations per tissue type. Direction of association: a positive association is defined as higher senescence (measured with a higher expression of a positive marker, or a lower expression of a negative marker for senescence) at higher ages. A negative association is defined as lower senescence at higher ages. Statistically significant: $p<0.05$; a trend: $0.05<p<0.10$; inconclusive: $p>0.10$ or reported as 'ns – not significant' by the source report.

Table 4. Statistical significance of associations between senescence and chronological age – ordered by senescence marker.

Marker	No.	Significance of associations with age (no., %)					
		Positive – significant	Positive – trend	Inconclusive	Negative – trend	Negative – significant	Insufficient information reported
All markers	78	34 (44)	6 (8)	27 (35)	0 (0)	1 (1)	10 (13)
p16	29	14 (48)	4 (14)	9 (31)	0 (0)	0 (0)	2 (7)
SAβ-gal	8	0 (0)	0 (0)	4 (50)	0 (0)	0 (0)	4 (50)
Markers naïve T-cells*	8	4 (50)	1 (13)	3 (38)	0 (0)	0 (0)	0 (0)
p21	7	1 (14)	0 (0)	6 (86)	0 (0)	0 (0)	0 (0)
SASP factors*	6	3 (50)	1 (17)	1 (17)	0 (0)	1 (17)	0 (0)
p53	5	2 (40)	0 (0)	3 (60)	0 (0)	0 (0)	0 (0)
Markers differentiated/ senescent T-cells*	4	4 (100)	0 (0)	0 (0)	0 (0)	0 (0)	0 (0)
Ki-67	4	2 (50)	0 (0)	0 (0)	0 (0)	0 (0)	2 (50)
Cyclin D	2	1 (50)	0 (0)	1 (50)	0 (0)	0 (0)	0 (0)
DNA damage markers*	2	1 (50)	0 (0)	0 (0)	0 (0)	0 (0)	1 (50)
Bmi-1	1	1 (100)	0 (0)	0 (0)	0 (0)	0 (0)	0 (0)
LMNB1	1	0 (0)	0 (0)	0 (0)	0 (0)	0 (0)	1 (100)
SAHF	1	1 (100)	0 (0)	0 (0)	0 (0)	0 (0)	0 (0)

N.: number of reported associations. Tissues are sorted on number of reported associations per marker. * Contains a set of markers. Direction of association: a positive association is defined as higher senescence (measured with a higher expression of a positive marker, or a lower expression of a negative marker for senescence) at higher ages. A negative association is defined as lower senescence at higher ages. Statistically significant: $p<0.05$; a trend: $p<0.10$; inconclusive: $p>0.10$ or reported as 'ns – not significant' by the source report.

the result of a real, strong association of senescent cells with chronological age or it may be partly explained by publication bias. Studies with large, significant and expected effects tend to get published more often (positive result bias) and cited more often (citation bias). Studies with small sample sizes are more prone to these types of biases than larger studies as the latter tend to be published and cited irrespective of the outcome [26-28]. Publication bias occurs in all scientific fields, and biogerontological research is no exemption. For example, when replicative capacity of fibroblasts *in vitro* was related dependent on the chronological age of the donor, the earliest but smaller studies predominantly found negative significant associations whereas more recent and larger studies did not confirm this association [29]. In the same area, a meta-analysis on the relation between DNA damage and age in animal tissue also provided arguments that publication and citation bias is at play [30].

The presence of senescent cells at older age has been postulated to be a result of an ongoing induction of this cellular phenotype via the exposure of various triggers (e.g. increased DNA damage or oncogenic signaling, reviewed in [31;32]), or indirectly via induction of senescence in neighboring cells of senescent cells [33]. An alternative interpretation of the presence is a reduced clearance of senescent cells. Some mouse studies have implicated the role of immune cells in the removal of senescent cells in premalignant lesions [34;35]. The precise mechanisms how senescent cell are cleared in non-malignant tissue have yet to be established, but an impaired balance between generation and clearance of senescent cells provides an another plausible hypothesis for the positive associations of senescence and chronological age. Only one negative significant association in this systematic review was found, namely a significant decrease of MMP-1 with age in the kidney. Although SASP is diverse, most SASP factors including MMP-1 are upregulated in senescent fibroblasts [36].

The different patterns of the associations in the various tissues might be the result of biological differences, such as tissue renewal rate or sensitivity to senescence triggers. The cell turnover rate of tissue varies widely[37;38]. Moreover homeostasis of the various tissues might be differently affected during aging [39]. Tissue-specificity of (unknown) environmental exposures are another explanation for the findings. Mice exposed to cigarette smoke show locally increased senescence in the nasal epithelium, whereas UV exposure induces senescence in the skin [40], indicating that environmental triggers can affect specific tissues more extensively than others. To the best of our knowledge information is lacking in humans on whether associations between senescence and age vary throughout the body, or whether they are linked intra-individually. Future studies on cellular senescence in several tissue types of the same individual should help to shed light on this question.

The various markers show different patterns of associations with age, and this is most prominent for the expression patterns of p16 and SAβ-gal. Associations using p16 are more frequently positive significant whereas reported associations with SAβ-gal were more often inconclusive. Moreover, for more than half of the associations sufficient information on statistical testing was missing. This might be explained by the fact that SAβ-gal was the marker of choice in the initial (more explorative) studies into senescence in human tissue [41], and results were more often not or semi-quantified compared to later studies. Taken together, the available senescence markers all have their caveats and restrictions in their use; and there is not yet an universal marker of senescent cells, which was addressed in a recent review [23].

Among the strengths of this study are the broad search strategy designed to capture many articles and extensive evaluation of articles for inclusion in the systematic review. We did not exclude any tissues and thus provide an overview of senescence in human aging in different organs. There are some limitations of this systematic review. First, while we aimed to design an inclusive broad search strategy, some studies might have still been missed. For example, we did not specifically add markers of immunosenescence in the search strategy, which might have led to an underrepresentation of those studies. Second, we only included articles in English, possibly biasing the results. Lastly we did not exclude any age ranges, thus associations between senescent cells with age also include data from foetuses to young adults. The associations between senescent cells with age might be different in the development phase versus reproductive and post-reproductive phases of life.

In conclusion, mainly positive associations of senescence with chronological age were found, which could be a real effect but can also to be due to an influence of publication bias. On a critical note, studies should more precisely report on the strength and variances of the associations using appropriate statistical testing, and to better describe the characteristics of patients/subjects from whom the tissues were sampled. This quantification can aid future systematic reviews and meta-analysis in the field and help to fairly judge the relevance of cellular senescence to the aging process in humans.

Acknowledgements

We are grateful for the excellent support of J.M. Langenhoff, information specialist of the Leiden University Medical Center's library, in designing the search strategy. We would like to posthumously thank dr. A.J.M. de Craen for his helpful advice on the process of conducting this systematic review.

Search strategy

PubMed

(“senescent”[all fields] OR “senescence”[all fields]) AND (“Tissues”[Mesh] OR “tissues”[all fields] OR “tissue”[all fields] OR “cell”[tiab] OR “cells”[tiab] OR “Biopsy”[Mesh] OR “Biopsy”[all fields] OR “Autopsy”[Mesh] OR “Autopsy”[all fields] OR “Histology”[Mesh] OR “Histology”[all fields] OR “histologic”[all fields]) AND (“Brain”[Mesh] OR “brain”[tiab] OR “Eye”[Mesh] OR “eye”[tiab] OR “eyes”[tiab] OR “cornea”[tiab] OR “lens”[tiab] OR “retina”[tiab] OR “retinal”[tiab] OR “Endocrine Glands”[Mesh] OR “thyroid”[tiab] OR “parathyroid”[tiab] OR “Cardiovascular System”[Mesh] OR “heart”[tiab] OR “myocard”[tiab] OR “myocardial”[tiab] OR “cardiovascular”[tiab] OR “artery”[tiab] OR “arteries”[tiab] OR “arterial”[tiab] OR “vein”[tiab] OR “venous”[tiab] OR “endothelial”[tiab] OR “Skin”[Mesh] OR “skin”[tiab] OR “dermis”[tiab] OR “dermal”[tiab] OR “epidermis”[tiab] OR “epidermal” OR “adipose”[tiab] OR “Lung”[Mesh] OR “lung”[tiab] OR “Lymphoid Tissue”[Mesh] OR “thymus”[tiab] OR “Breast”[Mesh] OR “breast”[tiab] OR “mammae”[tiab] OR “Digestive System”[Mesh] OR “intestinal”[tiab] OR “esophagus”[tiab] OR “esophagal”[tiab] OR “gastric”[tiab] OR “liver”[tiab] OR “pancreas”[tiab] OR “pancreatic”[tiab] OR “Urogenital System”[Mesh] OR “bladder”[tiab] OR “kidney”[tiab] OR “renal”[tiab] OR “adrenal”[tiab] OR “spleen”[tiab] OR “prostate”[tiab] OR “prostatic”[tiab] OR “uterus”[tiab] OR “uterine”[tiab] OR “ovaries”[tiab] OR “ovarian”[tiab] OR “testes”[tiab] OR “testicular”[tiab] OR “Muscles”[Mesh] OR “muscle”[tiab] OR “muscular”[tiab]) AND (“p16INK4a”[all fields] OR “Cyclin-Dependent Kinase Inhibitor p16”[Mesh] OR “Cyclin-Dependent Kinase Inhibitor p21”[Mesh] OR “p21”[all fields] OR “p21cip1”[all fields] OR “p21:MIB-1”[all fields] OR “p21WAF1/Cip”[all fields] OR “Tumor Suppressor Protein p53”[Mesh] OR “p53”[all fields] OR “GLB1 protein, human” [Supplementary Concept] OR “beta-galactosidase”[all fields] OR “SA-βgal”[all fields] OR “SA-betagal”[all fields] OR “H2AFX protein, human” [Supplementary Concept] OR “γH2AX”[all fields] OR “phospho-Histone H2A.X”[all fields] OR “γH2A.X”[all fields] OR “senescence-associated secretory phenotype”[all fields] OR “SASP”[all fields] OR “Ki-67 Antigen”[Mesh] OR “proliferation arrest”[all fields] OR “Ki-67”[all fields] OR “phospho-checkpoint 2 kinase”[all fields] OR “phospho-Chk2”[all fields] OR “Chromatin Assembly and Disassembly”[Mesh] OR “chromatin remodelling”[all fields] OR “ senescence associated heterochromatic foci”[all fields] OR “senescence associated heterochromatic foci”[all fields] OR “SAHF”[all fields] OR “DNA damage response”[all fields] OR “DDR”[tiab] OR “DNA damage foci”[all fields] OR “DNA damage focus”[all fields] OR “Telomere”[Mesh] OR “Telomere Shortening”[Mesh] OR “Telomere Homeostasis”[Mesh] OR “telomere”[all fields] OR “telomeres”[all fields])

EMBASE

(“senescent”.ti,ab. OR “senescence”.ti,ab.) AND (exp *tissues/ OR “tissues”.ti,ab. OR “tissue”.ti,ab. OR “cell”.ti,ab. OR “cells”.ti,ab. OR exp *biopsy/ OR “Biopsy”.ti,ab. OR *autopsy/ OR “Autopsy”.ti,ab. OR exp *histology/ OR “Histology”.ti,ab. OR “histologic”.ti,ab.) AND (exp *Brain/ OR “brain”.ti,ab. OR exp *Eye/ OR “eye”.ti,ab. OR “eyes”.ti,ab. OR “cornea”.ti,ab. OR “lens”.ti,ab. OR “retina”.ti,ab. OR “retinal”.ti,ab. OR exp *endocrine system/ OR “thyroid”.ti,ab. OR “parathyroid”.ti,ab. OR exp *Cardiovascular System/ OR “heart”.ti,ab. OR “myocard”.ti,ab. OR “myocardial”.ti,ab. OR “cardiovascular”.ti,ab. OR “artery”.ti,ab. OR “arteries”.ti,ab. OR “arterial”.ti,ab. OR “vein”.ti,ab. OR “venous”.ti,ab. OR “endothelial”.ti,ab. OR exp *Skin/ OR “skin”.ti,ab. OR “dermis”.ti,ab. OR “dermal”.ti,ab. OR “epidermis”.ti,ab. OR “epidermal” OR “adipose”.ti,ab. OR exp *Lung/ OR “lung”.ti,ab. OR exp *Lymphoid Tissue/ OR “thymus”.ti,ab. OR exp *Breast/ OR “breast”.ti,ab. OR “mammae”.ti,ab. OR exp *Digestive System/ OR “intestinal”.ti,ab. OR “esophagus”.ti,ab. OR “esophagal”.ti,ab. OR “gastric”.ti,ab. OR “liver”.ti,ab. OR “pancreas”.ti,ab. OR “pancreatic”.ti,ab. OR exp *Urogenital System/ OR “bladder”.ti,ab. OR “kidney”.ti,ab. OR “renal”.ti,ab. OR “adrenal”.ti,ab. OR “spleen”.ti,ab. OR “prostate”.ti,ab. OR “prostatic”.ti,ab. OR “uterus”.ti,ab. OR “uterine”.ti,ab. OR “ovaries”.ti,ab. OR “ovarian”.ti,ab. OR “testes”.ti,ab. OR “testicular”.ti,ab. OR exp *Muscle/ OR “muscle”.ti,ab. OR “muscular”.ti,ab.) AND (“p16INK4a”.ti,ab. OR *cyclin dependent kinase inhibitor 2A/ OR “Cyclin-Dependent Kinase Inhibitor p16”.ti,ab. OR *cyclin dependent kinase inhibitor 1A/ OR “p21”.ti,ab. OR “p21cip1”.ti,ab. OR “p21:MIB-1”.ti,ab. OR “p21WAF1/Cip”.ti,ab. OR Protein p53/ OR “p53”.ti,ab. OR *beta galactosidase/ OR “beta-galactosidase”.ti,ab. OR “SA-βgal”.ti,ab. OR “SA-betagal”.ti,ab. OR “γH2AX”.ti,ab. OR “phospho-Histone H2A.X”.ti,ab. OR “γH2A.X”.ti,ab. OR “senescence-associated secretory phenotype”.ti,ab. OR “SASP”.ti,ab. OR *Ki-67 Antigen/ OR “proliferation arrest”.ti,ab. OR “Ki-67”.ti,ab. OR “phospho-checkpoint 2 kinase”.ti,ab. OR “phospho-Chk2”.ti,ab. OR exp *”Chromatin Assembly and Disassembly”/ OR “chromatin remodelling”.ti,ab. OR “senescence associated heterochromatic foci”.ti,ab. OR “senescence associated heterochromatic foci”.ti,ab. OR “SAHF”.ti,ab. OR “DNA damage response”.ti,ab. OR “DDR”.ti,ab OR “DNA damage foci”.ti,ab. OR “DNA damage focus”.ti,ab. OR *Telomere/ OR *Telomere Shortening/ OR *Telomere Homeostasis/ OR “telomere”.ti,ab. OR “telomeres”.ti,ab.)

Web of Science

TS= (senescent OR senescence) AND TS=(tissues OR tissue OR cell OR cells OR Biopsy OR Autopsy OR Histology OR histologic) AND TI=(brain OR eye OR eyes OR cornea OR lens OR retina OR retinal OR thyroid OR parathyroid OR heart OR myocard OR myocardial OR cardiovascular OR artery OR arteries OR arterial OR vein OR venous OR endothelial OR skin OR dermis OR dermal OR epidermis OR epidermal OR adipose OR lung OR Lymphoid OR thymus OR breast OR mammae OR intestinal OR esophagus OR esophagal OR gastric OR liver OR pancreas OR pancreatic OR bladder OR kidney OR renal OR adrenal OR spleen OR prostate OR prostatic OR uterus OR uterine OR ovaries OR ovarian OR testes OR testicular OR muscle OR muscular) AND TS= (p16INK4a OR cyclin dependent kinase inhibitor 2A OR Cyclin-Dependent Kinase Inhibitor p16 OR cyclin dependent kinase inhibitor 1A OR p21 OR p21cip1 OR p21:MIB-1 OR p21WAF1/Cip OR p53 OR beta-galactosidase OR SA-βgal OR SA-betagal OR γH2AX OR phospho-Histone H2A.X OR γH2A.X OR senescence-associated secretory phenotype OR SASP OR proliferation arrest OR Ki-67 OR phospho-checkpoint 2 kinase OR phospho-Chk2 OR chromatin remodelling OR senescence associated heterochromatic OR SAHF OR DNA damage response OR DDR OR DNA damage foci OR DNA damage focus OR telomere OR telomeres)

References

(1) van Deursen JM. The role of senescent cells in ageing. *Nature* 2014;509:439-446.

(2) Coppe JP, Patil CK, Rodier F et al. Senescence-associated secretory phenotypes reveal cell-nonautonomous functions of oncogenic RAS and the p53 tumor suppressor. *PLoS Biol* 2008;6:2853-2868.

(3) Parrinello S, Coppe JP, Krtolica A, Campisi J. Stromal-epithelial interactions in aging and cancer: senescent fibroblasts alter epithelial cell differentiation. *J Cell Sci* 2005;118:485-496.

(4) Kuilman T, Peeper DS. Senescence-messaging secretome: SMS-ing cellular stress. *Nat Rev Cancer* 2009;9:81-94.

(5) Krtolica A, Parrinello S, Lockett S, Desprez PY, Campisi J. Senescent fibroblasts promote epithelial cell growth and tumorigenesis: a link between cancer and aging. *Proc Natl Acad Sci U S A* 2001;98:12072-12077.

(6) Schnabl B, Purbeck CA, Choi YH, Hagedorn CH, Brenner D. Replicative senescence of activated human hepatic stellate cells is accompanied by a pronounced inflammatory but less fibrogenic phenotype. *Hepatology* 2003;37:653-664.

(7) Csiszar A, Ungvari Z, Koller A, Edwards JG, Kaley G. Aging-induced proinflammatory shift in cytokine expression profile in coronary arteries. *FASEB J* 2003;17:1183-1185.

(8) Wang C, Jurk D, Maddick M, Nelson G, Martin-Ruiz C, von ZT. DNA damage response and cellular senescence in tissues of aging mice. *Aging Cell* 2009;8:311-323.

(9) Krishnamurthy J, Torrice C, Ramsey MR et al. Ink4a/Arf expression is a biomarker of aging. *J Clin Invest* 2004;114:1299-1307.

(10) Herbig U, Ferreira M, Condel L, Carey D, Sedivy JM. Cellular senescence in aging primates. *Science* 2006;311:1257.

(11) Jeyapalan JC, Ferreira M, Sedivy JM, Herbig U. Accumulation of senescent cells in mitotic tissue of aging primates. *Mech Ageing Dev* 2007;128:36-44.

(12) Melk A, Kittikowit W, Sandhu I et al. Cell senescence in rat kidneys in vivo increases with growth and age despite lack of telomere shortening. *Kidney Int* 2003;63:2134-2143.

(13) Tchkonia T, Zhu Y, van DJ, Campisi J, Kirkland JL. Cellular senescence and the senescent secretory phenotype: therapeutic opportunities. *J Clin Invest* 2013;123:966-972.

(14) Zhu Y, Tchkonia T, Pirtskhalava T et al. The Achilles' heel of senescent cells: from transcriptome to senolytic drugs. *Aging Cell* 2015;14:644-658.

(15) Baker DJ, Wijshake T, Tchkonia T et al. Clearance of p16Ink4a-positive senescent cells delays ageing-associated disorders. *Nature* 2011;479:232-236.

(16) Baker DJ, Childs BG, Durik M et al. Naturally occurring p16(Ink4a)-positive cells shorten healthy lifespan. *Nature* 2016;530:184-189.

(17) Dekker P, Maier AB, van HD et al. Stress-induced responses of human skin fibroblasts in vitro reflect human longevity. *Aging Cell* 2009;8:595-603.

(18) Waldera Lupa DM, Kalfalah F, Safferling K et al. Characterization of Skin Aging-Associated Secreted Proteins (SAASP) Produced by Dermal Fibroblasts Isolated from Intrinsically Aged Human Skin. *J Invest Dermatol* 2015;135:1954-1968.

(19) Quan T, Qin Z, Robichaud P, Voorhees JJ, Fisher GJ. CCN1 contributes to skin connective tissue aging by inducing age-associated secretory phenotype in human skin dermal fibroblasts. *J Cell Commun Signal* 2011;5:201-207.

(20) Sedelnikova OA, Horikawa I, Zimonjic DB, Popescu NC, Bonner WM, Barrett JC. Senescing human cells and ageing mice accumulate DNA lesions with unrepairable double-strand breaks. *Nat Cell Biol* 2004;6:168-170.

(21) Hewitt G, Jurk D, Marques FD et al. Telomeres are favoured targets of a persistent DNA damage response in ageing and stress-induced senescence. *Nat Commun* 2012;3:708.

(22) Aubert G, Hills M, Lansdorp PM. Telomere length measurement-caveats and a critical assessment of the available technologies and tools. *Mutat Res* 2012;730:59-67.

(23) Sharpless NE, Sherr CJ. Forging a signature of in vivo senescence. *Nat Rev Cancer* 2015;15:397-408.

(24) Cristofalo VJ, Lorenzini A, Allen RG, Torres C, Tresini M. Replicative senescence: a critical review. *Mech Ageing Dev* 2004;125:827-848.

(25) Sharpless NE, Sherr CJ. Forging a signature of in vivo senescence. *Nat Rev Cancer* 2015;15:397-408.
(26) Song F, Eastwood AJ, Gilbody S, Duley L, Sutton AJ. Publication and related biases. *Health Technol Assess* 2000;4:1-115.
(27) Sterne JA, Gavaghan D, Egger M. Publication and related bias in meta-analysis: power of statistical tests and prevalence in the literature. *J Clin Epidemiol* 2000;53:1119-1129.
(28) Thornton A, Lee P. Publication bias in meta-analysis: its causes and consequences. *J Clin Epidemiol* 2000;53:207-216.
(29) Maier AB, Westendorp RG. Relation between replicative senescence of human fibroblasts and life history characteristics. *Ageing Res Rev* 2009;8:237-243.
(30) Moller P, Lohr M, Folkmann JK, Mikkelsen L, Loft S. Aging and oxidatively damaged nuclear DNA in animal organs. *Free Radic Biol Med* 2010;48:1275-1285.
(31) Burton DG, Krizhanovsky V. Physiological and pathological consequences of cellular senescence. *Cell Mol Life Sci* 2014;71:4373-4386.
(32) Rodier F, Campisi J. Four faces of cellular senescence. *J Cell Biol* 2011;192:547-556.
(33) Nelson G, Wordsworth J, Wang C et al. A senescent cell bystander effect: senescence-induced senescence. *Aging Cell* 2012;11:345-349.
(34) Kang TW, Yevsa T, Woller N et al. Senescence surveillance of pre-malignant hepatocytes limits liver cancer development. *Nature* 2011;479:547-551.
(35) Xue W, Zender L, Miething C et al. Senescence and tumour clearance is triggered by p53 restoration in murine liver carcinomas. *Nature* 2007;445:656-660.
(36) Coppe JP, Desprez PY, Krtolica A, Campisi J. The senescence-associated secretory phenotype: the dark side of tumor suppression. *Annu Rev Pathol* 2010;5:99-118.
(37) Pelc S. Labelling of DNA and cell division in so called non-dividing tissues. *J Cell Biol* 1964;22:21-28.
(38) Gerber G, Berger G, Altman K. The catabolism of tissue nucleic acid in the rat. I. The replacement time of deoxribonucleic acid. *J Biol Chem* 1960;235:1433-1436.
(39) Tower J. Programmed cell death in aging. *Ageing Res Rev* 2015;23:90-100.
(40) Sorrentino JA, Krishnamurthy J, Tilley S, Alb JG, Jr., Burd CE, Sharpless NE. p16INK4a reporter mice reveal age-promoting effects of environmental toxicants. *J Clin Invest* 2014;124:169-173.
(41) Dimri GP, Lee X, Basile G et al. A biomarker that identifies senescent human cells in culture and in aging skin in vivo. *Proceedings of the National Academy of Sciences of the United States of America* 1995;92:9363-9367.
(42) Nociari MM, Telford W, Russo C. Postthymic development of CD28-CD8+ T cell subset: Age-associated expansion and shift from memory to naive phenotype. *Journal of Immunology* 1999;162:3327-3335.
(43) Nielsen GP, Stemmer-Rachamimov AO, Shaw J, Roy JE, Koh J, Louis DN. Immunohistochemical survey of p16INK4A expression in normal human adult and infant tissues. *Lab Invest* 1999;79:1137-1143.
(44) Choi J, Shendrik I, Peacocke M et al. Expression of senescence-associated beta-galactosidase in enlarged prostates from men with benign prostatic hyperplasia. *Urology* 2000;56:160-166.
(45) Severino J, Allen RG, Balin S, Balin A, Cristofalo VJ. Is beta-galactosidase staining a marker of senescence in vitro and in vivo? *Experimental Cell Research* 2000;257:162-171.
(46) Kanavaros P, Stefanaki K, Rontogianni D et al. Immunohistochemical expression of p53, p21/waf1, Rb, p16, cyclin D1, p27, Ki67, cyclin A, cyclin B1, bcl2, bax and bak proteins and apoptotic index in normal thymus. *Histology and Histopathology* 2001;16:1005-1012.
(47) Going JJ, Stuart RC, Downie M, Fletcher-Monaghan AJ, Nicol KW. 'Senescence-associated' beta-galactosidase activity in the upper gastrointestinal tract. *Journal of Pathology* 2002;196:394-400.
(48) Castro P, Giri D, Lamb D, Ittmann M. Cellular senescence in the pathogenesis of benign prostatic hyperplasia. *Prostate* 2003;55:30-38.
(49) El-Domyati MB, Attia S, Saleh F et al. Expression of p53 in normal sun-exposed and protected skin (type IV-V) in different decades of age. *Acta Dermato-Venereologica* 2003;83:98-104.
(50) Chkhotua AB, Gabusi E, Altimari A et al. Increased expression of p16((INK4a)) and p27((Kip1)) cyclin-dependent kinase inhibitor genes in aging human kidney and

chronic allograft nephropathy. *American Journal of Kidney Diseases* 2003;41:1303-1313.

(51) Schonland SO, Lopez C, Widmann T et al. Premature telomeric loss in rheumatoid arthritis is genetically determined and involves both myeloid and lymphoid cell lineages. *Proceedings of the National Academy of Sciences of the United States of America* 2003;100:13471-13476.

(52) Melk A, Schmidt BMW, Takeuchi O, Sawitzki B, Rayner DC, Halloran PF. Expression of p16INK4a and other cell cycle regulator and senescence associated genes in aging human kidney. *Kidney international* 2004;65:510-520.

(53) Ressler S, Bartkova J, Niederegger H et al. p16INK4A is a robust in vivo biomarker of cellular aging in human skin. *Aging Cell* 2006;5:379-389.

(54) Nuciforo PG, Luise C, Capra M, Pelosi G, Di Fagagna FD. Complex engagement of DNA damage response pathways in human cancer and in lung tumor progression. *Carcinogenesis* 2007;28:2082-2088.

(55) Sis B, Tasanarong A, Khoshjou F, Dadras F, Solez K, Halloran PF. Accelerated expression of senescence associated cell cycle inhibitor p16(INK4A) in kidneys with glomerular disease. *Kidney international* 2007;71:218-226.

(56) Koppelstaetter C, Schratzberger G, Perco P et al. Markers of cellular senescence in zero hour biopsies predict outcome in renal transplantation. *Aging Cell* 2008;7:491-497.

(57) Lemster BH, Michel JJ, Montag DT et al. Induction of CD56 and TCR-independent activation of T cells with aging. *Journal of Immunology* 2008;180:1979-1990.

(58) Song Z, Yang Y, Xie L, Zang X, Yin H. Expression of senescence-related genes in human corneal endothelial cells. *Molecular Vision* 2008;14:161-170.

(59) Verzola D, Gandolfo MT, Gaetani G et al. Accelerated senescence in the kidneys of patients with type 2 diabetic nephropathy. *American Journal of Physiology - Renal Physiology* 2008;295:F1563-F1573.

(60) Kilpatrick RD, Rickabaugh T, Hultin LE et al. Homeostasis of the naive CD4+ T cell compartment during aging. *J Immunol* 2008;180:1499-1507.

(61) Werner C, Furster T, Widmann T et al. Physical exercise prevents cellular senescence in circulating leukocytes and in the vessel wall. *Circulation* 2009;120:2438-2447.

(62) McGlynn LM, Stevenson K, Lamb K et al. Cellular senescence in pretransplant renal biopsies predicts postoperative organ function. *Aging Cell* 2009;8:45-51.

(63) Lee JH, Yoo JH, Oh SH, Lee K-Y, Lee KH. Knockdown of moesin expression accelerates cellular senescence of human dermal microvascular endothelial cells. *Yonsei Medical Journal* 2010;51:438-447.

(64) Gelson W, Hoare M, Vowler S et al. Features of immune senescence in liver transplant recipients with established grafts. *Liver Transplantation* 2010;16:577-587.

(65) Kajstura J, Gurusamy N, Ogorek B et al. Myocyte turnover in the aging human heart. *Circulation Research* 2010;107:1374-1386.

(66) Bartkova J, Moudry P, Hodny Z, Lukas J, Rajpert-De ME, Bartek J. Heterochromatin marks HP1, HP1alpha and H3K9me3, and DNA damage response activation in human testis development and germ cell tumours. *International Journal of Andrology* 2011;34:e103-e113.

(67) Shivshankar P, Boyd AR, Le Saux CJ, Yeh I-T, Orihuela CJ. Cellular senescence increases expression of bacterial ligands in the lungs and is positively correlated with increased susceptibility to pneumococcal pneumonia. *Aging Cell* 2011;10:798-806.

(68) Ferrando-Martinez S, Ruiz-Mateos E, Hernandez A et al. Age-related deregulation of naive T cell homeostasis in elderly humans. *Age* 2011;33:197-207.

(69) Marchand A, Atassi F, Gaaya A et al. The Wnt/beta-catenin pathway is activated during advanced arterial aging in humans. *Aging Cell* 2011;10:220-232.

(70) Bhat R, Crowe EP, Bitto A et al. Astrocyte Senescence as a Component of Alzheimer's Disease. *PLoS ONE* 2012;7.

(71) Klement K, Melle C, Murzik U, Diekmann S, Norgauer J, Hemmerich P. Accumulation of annexin A5 at the nuclear envelope is a biomarker of cellular aging. *Mechanisms of Ageing and Development* 2012;133:508-522.

(72) Zang X, Wang Y, Chen P. High expression of p16INK4a and low expression of Bmi1 are associated with endothelial cellular senescence in the human cornea. *Molecular Vision* 2012;18:803-815.

(73) Liu J, Yang J-R, He Y-N et al. Accelerated senescence of renal tubular epithelial cells is

associated with disease progression of patients with immunoglobulin A (IgA) nephropathy. *Translational Research* 2012;159:454-463.
(74) Abdouh M, Chatoo W, El HJ, David J, Ferreira J, Bernier G. Bmi1 is down-regulated in the aging brain and displays antioxidant and protective activities in neurons. *PLoS ONE* 2012;7.
(75) Spandau DF, Lewis DA, Somani AK, Travers JB. Fractionated Laser Resurfacing Corrects the Inappropriate UVB Response in Geriatric Skin. *Journal of Investigative Dermatology* 2012;132:1591-1596.
(76) Mondal AM, Horikawa I, Pine SR et al. P53 isoforms regulate aging- and tumor-associated replicative senescence in T lymphocytes. *Journal of Clinical Investigation* 2013;123:5247-5257.
(77) Marcoux S, Le ONL, Langlois-Pelletier C et al. Expression of the senescence marker p16INK4a in skin biopsies of acute lymphoblastic leukemia survivors: A pilot study. *Radiation Oncology* 2013;8.
(78) Morgan RG, Ives SJ, Lesniewski LA et al. Age-related telomere uncapping is associated with cellular senescence and inflammation independent of telomere shortening in human arteries. *American Journal of Physiology - Heart and Circulatory Physiology* 2013;305:H251-H258.
(79) Cao S, Walker GB, Wang X, Cui JZ, Matsubara JA. Altered cytokine profiles of human retinal pigment epithelium: Oxidant injury and replicative senescence. *Molecular Vision* 2013;19:718-728.
(80) Dreesen O, Chojnowski A, Ong PF et al. Lamin B1 fluctuations have differential effects on cellular proliferation and senescence. *Journal of Cell Biology* 2013;200:605-617.
(81) Gingell-Littlejohn M, McGuinness D, McGlynn LM et al. Pre-Transplant CDKN2A Expression in Kidney Biopsies Predicts Renal Function and Is a Future Component of Donor Scoring Criteria. *PLoS ONE* 2013;8.
(82) Sanoff HK, Deal AM, Krishnamurthy J et al. Effect of cytotoxic chemotherapy on markers of molecular age in patients with breast cancer. *Journal of the National Cancer Institute* 2014;106.
(83) Berkenkamp B, Susnik N, Baisantry A et al. In vivo and in vitro analysis of age-associated changes and somatic cellular senescence in renal epithelial cells. *PLoS ONE* 2014;9.

Chapter 8

Chapter 8

Assessment of health status by molecular measures in adults ranging from middle-aged to old: ready for clinical use?

M.E.C. Waaijer, R.G.J. Westendorp, D. Goldeck, D.A. Gunn, G. Pawelec, M. Stijntjes, P.E. Slagboom, A.B. Maier

Experimental Gerontology. 2016 Apr 2. pii: S0531-5565(16)30088-2

Abstract

In addition to measures already used in clinical practice, molecular measures have been proposed to assess health status, but these have not yet been introduced into clinical practice. We aimed to test the association of functional capacity measures used in current practice and molecular measures with age and health status.

The cohort consisted of 178 middle-aged to old participants of the Leiden Longevity Study (range 42-82 years). We tested associations between functional capacity measures (physical tests: grip strength, 4-meter walk, chair stand test; cognitive tests: Stroop test, digit symbol substitution test and 15-picture learning test) with age and with cardiovascular or metabolic disease as a measure of the health status. These associations with age and health status were also tested for molecular measures (C reactive protein (CRP), numbers of senescent p16INK4a positive cells in the epidermis and dermis and putative immunosenescence (presence of CD57+ T cells)).

All functional capacity measures were associated with age. CRP and epidermal p16INK4a positivity were also associated with age, but with smaller estimates. Grip strength and the Stroop test were associated with cardiovascular or metabolic disease, as was epidermal p16INK4a positivity. All associations with cardiovascular or metabolic disease attenuated when adjusting for age.

In conclusion, in middle-aged to old persons, the molecular measures tested here were more weakly associated with age and health status than functional capacity measures. Whether these molecular measures associate more closely with health status in the elderly or in specific groups of patients needs to be explored further.

Introduction

Markers that characterize the rate of aging in humans are important in an era of increasing lifespan and emerging novel opportunities for interventions to potentially prolong lifespan. Ideally, these measures should associate with age and with prevalence of age-related disease as a measure of an individual's health status. In clinical practice, functional capacity can be assessed by testing e.g. muscle strength, balance and walking speed. Performance on physical performance tests are associated with age [1-3], as well as health outcomes such as disability [4], disease [5] and mortality [6;7], even at middle age [2]. The cognitive domain is evaluated by making use of the Mini Mental State Examination (MMSE) assessing global cognitive functioning but also testing specific cognitive domains such as executive functioning, recall and attention. Performance on cognitive tests is associated with age [8], as well as disease [9;10] and mortality [11]. These functional capacity measures have proven their use in clinical practice.

Molecular mechanisms which are causally related to the aging process have also been reported to provide insights into an individual's health [12]. Molecular measures associated with age and health status include telomere length, transcriptomic and epigenetic parameters, inflammatory markers and cellular senescence [13-15]. Low grade systemic inflammation, measured by e.g. C-reactive protein (CRP) has been associated with age [16], disease [17;18] and mortality [17-19;19]. Cellular senescence, the phenomenon of permanent cell cycle arrest of somatic cells after a certain number of cell divisions or particular insults such as DNA damage, is found to be more prevalent at higher age in many tissues [20-23]. Immunosenescence, which may involve cellular senescence of T lymphocytes, has been linked to mortality [24;25]. Furthermore, cellular senescence has been related to many age-related diseases such as diabetes [26], glomerular disease [27] and chronic obstructive pulmonary disease [28], which strengthens the rationale to use senescence as a potential marker for the human aging process. A small number of studies has used such senescence measures to predict clinical outcome, but with inconsistent results [29-31]. Overall, molecular measures have not yet found their way into clinical practice.

We aimed to evaluate the associations between functional capacity measures and molecular measures (focussing specifically on t CRP, skin senescence and immunosenescence) from middle age onwards (age range 42-82 years), and to associate these with the presence of cardiovascular or metabolic disease as a measure for health status.

Methods

Study design and participants

In the Leiden Longevity Study, factors contributing to familial longevity are studied in long-lived families; the study design has been described previously [32]. Offspring of nonagenarian siblings as well as their partners, who act as environmentally-matched controls, participated in this study. Subjects were recruited from July 2002 to May 2006. Over several years (November 2006 to May 2008, and September 2009 to December 2010) data on functional capacity and molecular measures were acquired from these participants, many of which have been published previously [2;8;33-35]. The study was approved by the Medical Ethics Committee of Leiden University Medical Center and all participants gave their informed consent.

Medical history

Medical history on myocardial infarction, cerebrovascular accident, hypertension, diabetes mellitus, malignancy, chronic obstructive pulmonary disease and rheumatoid arthritis was obtained from general practitioners. Presence of any of these diseases was defined as one or more disease in the medical history. Presence of a cardiovascular or metabolic disease was defined as one or more of four cardiovascular or metabolic diseases (presence of myocardial infarction, cerebrovascular accident, hypertension or diabetes mellitus).

Functional capacity measures

Functional capacity measures were based on measures used in clinical practice, and included measures of physical and cognitive domains. Grip strength of the dominant hand was measured in the upright position with maximal force using a hand dynamometer (Jamar, Sammons Preston Inc., Bolingbrook, IL, USA) [33]. The best of three attempts, expressed in kilograms, was used for analysis. Four meter walking speed was measured twice across a 4-meter course starting from a standing position. Participants were asked to walk at usual pace. The fastest time in seconds was used for analyses. The time to stand up and sit down on a chair as fast as possible five times formed the chair stand test [2]. Cognition was assessed by neuropsychological testing [8]. For this study, part 3 of the Stroop test (time in seconds needed to read coloured words printed in an incongruous ink colour), the digit symbol substitution test (correct number of symbols) and delayed recall (correct number after 20 minutes) of the 15-picture learning test were used because of their known associations with age in larger cohorts [8].

Molecular measures

From the diverse set of existing molecular measures, we here studied specific measures of inflammation, skin senescence and immunosenescence.

High sensitive C-reactive protein (hsCRP) was measured in serum (Hitachi Modular P 800 from Roche, Almere, the Netherlands) [36]. Participants with a hsCRP>10 mg/L were excluded from the analyses due to possible acute infection.

Skin biopsies from the upper inner arm were taken and stained for senescence-associated p16INK4a expression by immunohistochemistry, as described previously [34]. p16INK4a-positive cells were counted separately in the epidermis (positive staining cells per mm length of the epidermal-dermal junction) and in the dermis (positive staining cells per $1mm^2$ dermis).

Peripheral blood mononuclear cells (PBMCs) were analysed by flow cytometry for T-cell differentiation phenotypes [35] to study immunosenescence. The frequency of T cells bearing the 'senescence-associated' marker CD57 was previously found to be higher in elderly than in young individuals [37;38]. In the present study, we therefore selected the proportion of CD4+CD57+ and CD8+CD57+ T-cells for analysis. Cytomegalovirus (CMV) serostatus was taken into account as a possible confounder, and measured by ELISA using the CMV-IgG-ELISA PKS assay (Medac GmbH, Wedel, Germany), as per the manufacturer's instructions [35].

Analyses - Datasets

Analysis of associations of the measures of the functional capacity and molecular measures with age and cardiovascular/ metabolic disease were conducted using data from 178 participants. The number of included participants was limited by the measure with the lowest number of available data (epidermal and dermal p16INK4a positivity). Not all measures were available in this exact same group of 178 participants, and therefore data from randomly selected participants of the cohort in whom the measures were available were added to complement the dataset (4-meter walk test and chair stand test random subset N=95, Stroop test, digit symbol substitution test and 15-picture learning test random subset N=57, CRP random subset N=15, proportion of CD8+CD57+ and CD4+CD57+ T-cells random subset N=98). The functional capacity and molecular measures were divided into tertiles of worst, average and best test results. Values of these tertiles are shown in Supplementary Table 1.

Analyses - Statistics

Statistical analyses were performed using IBM SPSS Statistics 20. Graphs were drawn with Prism Graphpad version 5. First we tested whether functional capacity and molecular measures were associated with age using linear regression (with estimated means via linear mixed models). The first model was adjusted for sex (grip strength analyses used sex-specific tertiles) and the immunosenescence associations for CMV serostatus. The second model additionally adjusted for the presence of one or more diseases. Next, we tested whether functional capacity and molecular measures associate with health status, determined by history of one or more cardiovascular or metabolic diseases using logistic regression. The first model was adjusted for sex (except grip strength analysis) and for CMV serostatus for immunosenescence associations. The second model additionally adjusted for age. Adjustment for membership of a long-lived family ('offspring') is not reported here as this did not change results. Lastly, we tested which measures were associated independently of other measures by using a multivariable model (linear regression for age and logistic regression for health status). Variables were included that were associated with age in the first analysis model (grip strength, 4-meter walk test, chair stand test, Stroop test, digit symbol substitution test, 15-picture learning test, CRP and epidermal p16INK4a positivity). For this analysis only those participants with data available on of all these measures were included (N=83). Within this group, we also used combined test results by computing the average tertile of functional capacity measures (grip strength, 4-meter walk test, chair stand test, Stroop test, digit symbol substitution test, 15-picture learning test) and the average tertile of molecular measures (CRP, epidermal p16INK4a positivity). These averaged test results were used as the independent variable in the linear regression with age, and logistic regression with health status analyses.

Results

Table 1 depicts the characteristics of the participants per functional capacity and molecular measure, including age, gender and diseases of participants.

Associations between functional capacity and molecular measures with age are shown in Supplementary Table 2. All functional capacity measures were significantly associated with age. Participants in the tertile of worst test results were older than those in the average and best test result tertiles. Except for the 4-meter walk test and the 15-picture learning test, all functional capacity measures were also significantly associated with age after further adjustment for disease. For the molecular measures, CRP and epidermal p16INK4a positivity were significantly associated with age. Participants in the tertile of worst test results were older than those in the average and best test result tertiles. CRP and epidermal p16INK4a positivity had smaller estimates and were less significantly associated with age than functional capacity measures. Dermal p16INK4a positivity and the proportion of CD57+ T cells within CD8+ and CD4+ T cells were not significantly associated with age. CRP was significantly associated with age independently of disease, whereas the association between epidermal p16INK4a positivity and age was attenuated upon further adjustment for disease. For visualisation purposes, measures that were most strongly associated with age are shown in Figure 1.

The associations between functional capacity and molecular measures with cardiovascular or metabolic disease are shown in Supplementary Table 3. Grip strength and the Stroop test as functional capacity measures were significantly associated with cardiovascular or metabolic

Table 1. Characteristics of study participants per functional capacity and molecular measure

	Functional capacity measures			Molecular measures		
	Grip strength	4-meter walk & chair stand test	Cognitive tests	CRP	Skin senescence	Immunosenescence
Participant overlap with skin senescence dataset, no.	178	83	121	163	178	80
Randomly selected participants, no.	0	95	57	15	0	98
Age, years, mean (SD)	63.4 (6.62)	62.7 (7.02)	63.3 (6.82)	62.9 (6.62)	63.4 (6.62)	61.9 (7.51)
Female, no. (%)	90 (50.6)	95 (53.4)	93 (52.2)	90 (50.6)	90 (50.6)	89 (50.0)
Offspring, no. (%)	90 (50.6)	91 (51.1)	95 (53.4)	90 (50.6)	90 (50.6)	87 (48.9)
≥1 disease, no. (%)	58 (35.4)	56 (31.5)	58 (38.4)	49 (31.8)	58 (35.4)	42 (28.0)
≥1 cardiovascular/metabolic disease, no. (%)	51 (31.1)	48 (30.6)	50 (32.1)	44 (27.7)	51 (31.1)	32 (21.1)

All subsets N=178. SD: standard deviation. No.: number. %: valid percentage. CRP: C-reactive protein. Missing data on diseases for 14-28 participants. ≥1 disease: presence of one or more of the following diseases: myocardial infarction, cerebrovascular accident, hypertension, diabetes mellitus, malignancy, chronic obstructive pulmonary disease or rheumatoid arthritis. ≥1 cardiovascular/metabolic disease: presence of one or more of the following diseases: myocardial infarction, cerebrovascular accident, hypertension or diabetes mellitus.

disease, whereas the other measures were not. Participants in the worst test result tertile of grip strength and of the Stroop test had a history of cardiovascular or metabolic disease more frequently than those in the average and best test result tertiles. Results did not remain statistically significant after further adjustment for age, although a trend remained for grip strength. Epidermal p16INK4a positivity was significantly associated with cardiovascular or metabolic disease, but did not remain significant after adjustment for age. Other molecular measures were not associated with cardiovascular or metabolic disease. Associations between the functional capacity and molecular measures and presence of cardiovascular or metabolic disease are shown in Figure 2.

Multivariable regression analyses of functional and molecular measures with age and health status demonstrated that grip strength, the Stroop test and digit symbol substitution test were significantly associated with age, independently of other measures, shown in Table 2. Grip strength and the 15-picture learning test were significantly associated with health status independently of the other measures.

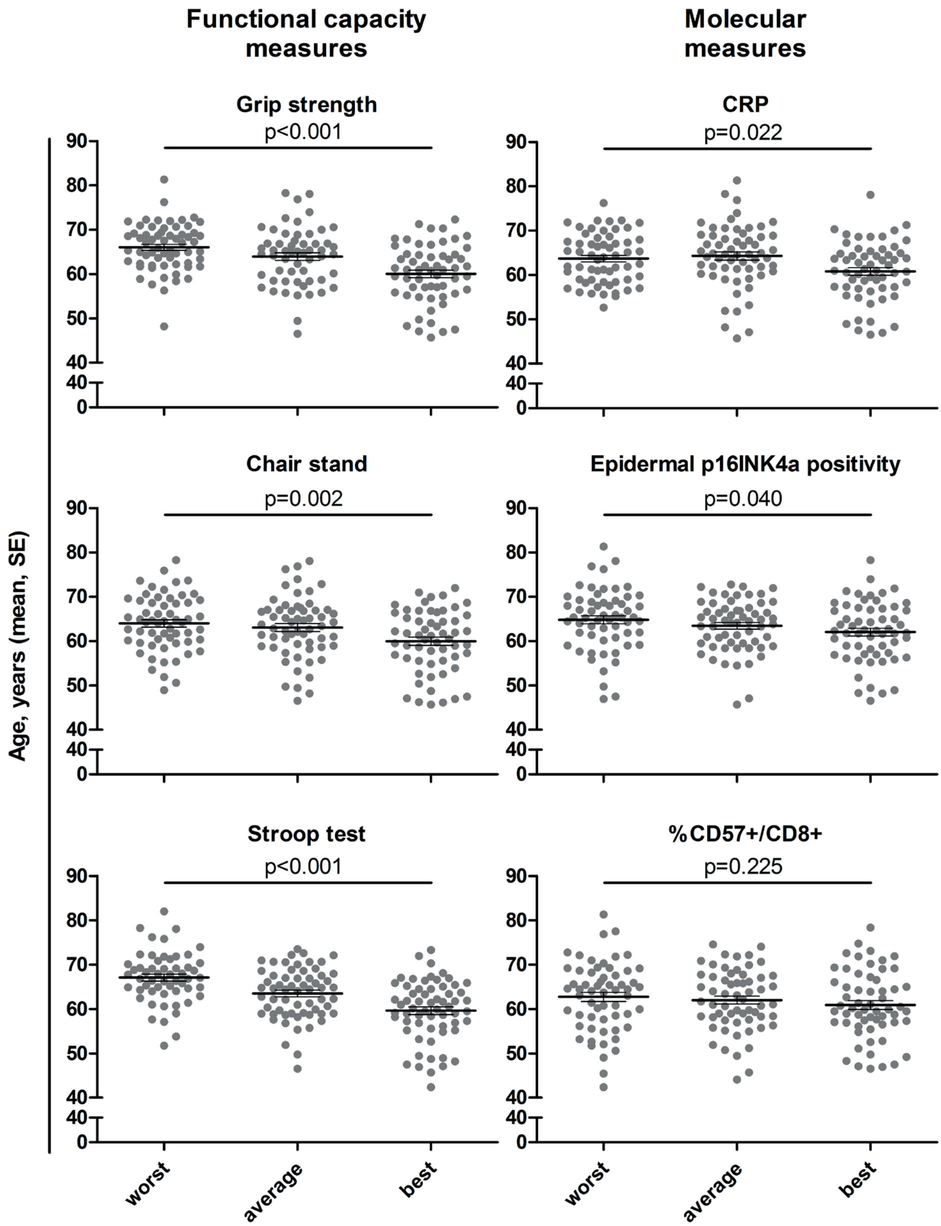

Figure 1. Age of participants dependent on functional capacity and molecular measures given in tertiles. SE: standard error. Single data points and the mean age per tertile of measure (worst, average, best test result) are given. P for trends are derived from linear mixed models, adjusted for sex (plus CMV serostatus in the CD57+/CD8+ association). N=178 for all measures.

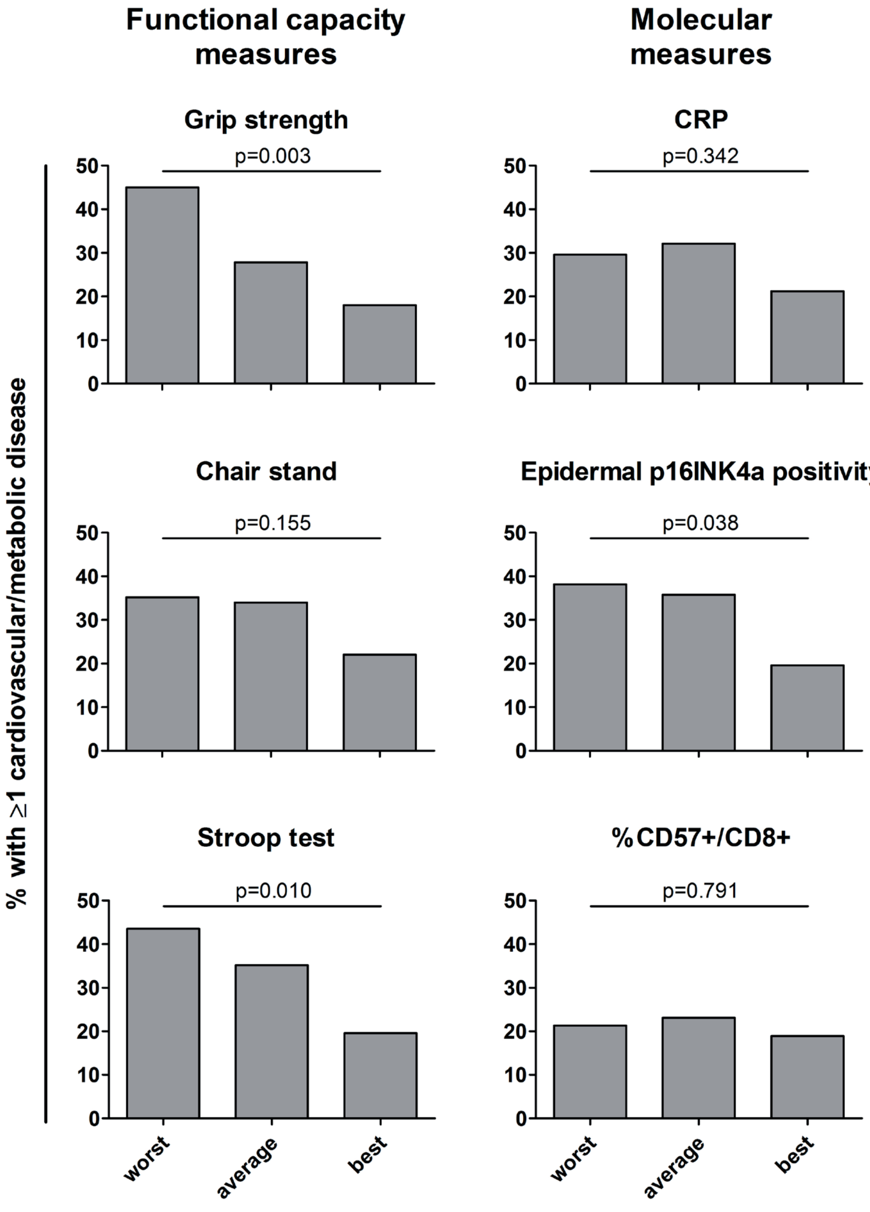

Figure 2. Presence of cardiovascular/ metabolic disease dependent on functional capacity and molecular measures given in tertiles.
Percentage of participants with one or more cardiovascular/metabolic diseases (myocardial infarction, cerebrovascular accident, hypertension or diabetes mellitus) are given per tertile of measure (worst, average, best test result). P-values were calculated with logistic regression; adjusted for sex (plus CMV serostatus in the CD57+/CD8+ association). N=178 for all measures.

Table 2. Associations between age and cardiovascular/metabolic disease with functional capacity and molecular measures

	Age		Cardiovascular/metabolic disease	
	β (SE)	P-value	β (SE)	P-value
a. Multivariable model				
Functional capacity measures				
Physical tests				
Grip strength	-3.17 (0.85)	<0.001	-1.28 (0.48)	0.008
4-meter walk test	0.79 (0.81)	0.333	0.53 (0.42)	0.208
Chair stand test	0.03 (0.83)	0.967	0.60 (0.43)	0.159
Cognitive tests				
Stroop test	-3.12 (0.90)	0.001	0.20 (0.47)	0.679
Digit symbol substitution test	-1.91 (0.95)	0.047	-0.34 (0.46)	0.460
15-picture learning test	-0.80 (0.86)	0.355	-1.09 (0.47)	0.019
Molecular measures				
CRP	-0.99 (0.79)	0.212	-0.16 (0.40)	0.689
Epidermal p16INK4a	-0.56 (0.82)	0.495	0.10 (0.40)	0.800
b. Univariate - combined measures				
Combined functional capacity measures	-8.88 (1.48)	<0.001	-1.04 (0.60)	0.085
Combined molecular measures	-2.86 (1.37)	0.039	-0.87 (0.50)	0.543

N=83 for all measures. SE: standard error. CRP: C-reactive protein. Multivariable model: tertiles of all measures were included as independent variable in a linear regression model for the association with chronological age; in a logistic regression model for the association with cardiovascular/metabolic disease. Univariate model: the average tertile of all functional capacity measures combined, and all molecular measures combined was used as the independent variable.

Discussion

In this study of middle-aged to old adults (range 42-82 years), functional capacity measures are associated with age, whereas molecular measures are inconsistently and weakly associated with age. Associations of all measures were stronger with age than with cardiovascular or metabolic disease as measure of health status.

These observed associations between different functional capacity measures and age are in line with the literature. Both physical and cognitive tests have been shown to be a reflection of the aging process through their links with mortality [6;7;11;39] and disability [4;40] in older people. Some measures of physical and cognitive performance are known to be different in men and women [41-46], which we therefore accounted for in our analyses. Even in this smaller group of

178 participants (to aid comparison to the molecular measure analyses) the associations were statistically significant, highlighting the strong links between these measures and aging in men and women.

Recently, several different measures of the underlying biological aging process have been studied, but here we have focussed on low-grade systemic inflammation and cellular senescence in the skin and in the immune system. We found low-grade systemic inflammation to be associated with age, similar to findings from other larger studies [19;47;48], but not to cardiovascular or metabolic disease within this study and sample size. Cellular senescence has been linked in the literature to both higher age [20-23] and to age-related pathologies [20;26-28], but most studies have a modest sample size and studies on disease rarely adjusted for age. Within the Leiden Longevity Study, epidermal but not dermal p16INK4a positivity also linked to age [49]. However, this association is not fully independent of disease, as estimates became smaller and the significance diminished after adjustment for disease. Epidermal p16INK4a is also linked to cardiovascular disease or metabolic disease in skin of middle-aged to old persons, but not independently of age. The associations of senescence measures (e.g. p16INK4a epidermal positivity) with age and health status were weaker than for the functional capacity measures (e.g. grip strength), indicating a need for large number of participants when using senescence measures, which are therefore in the current state less appropriate for clinical practice. Indeed, in a recent study p16INK4a positivity in T-cells was not predictive for length of stay in hospitalized middle-aged to old patients after a coronary artery bypass graft surgery [31]. In the present study, T cell CD57 positivity was not associated with either age or disease in these middle-aged to old persons. One of the reasons for this lack of association might be the more limited age range of these participants compared to other studies [37;38]. However, it is more likely that the history of pathogen exposures in these subjects over-rode any potential effects of age. When a multivariable model was performed, only grip strength was associated with both age and health status independently of all other measures. Thus, no clear added value of the molecular measures tested here was found when taking functional capacity measures into account.

More molecular markers have been proposed in the literature to capture the aging process. These markers are based on biomaterial, and are therefore more invasive than functional capacity measures. However, efforts should be made to measure molecular markers in a minimally-invasive manner in routinely clinically-obtained biomaterial such as blood, or other easily accessible material such as urine or saliva. Measurement of molecular markers has the potential to be optimized and routinized, whereas measurement of functional capacity measures is usually dependent on trained health care workers and is more time-consuming. With expanding knowledge of the biology of the aging process, more molecular markers are likely to be found in addition to current known markers which could better describe the pathophysiology of underlying systems. Within the Leiden Longevity Study markers like telomere length in leukocytes and expression levels of IL7R were shown to be markers of familial longevity and mortality [50;51], and several loci associated with longevity or familial longevity were identified [52;53]. When studying the value of markers for prediction of health status, most studies focus on older persons, or specific groups of patients. For example, various markers such as grip strength, vitamin D and brain natriuretic peptide were associated with health status in persons aged 85 years and above [54]. Sex-differences in molecular markers are rarely reported and should be more often considered in future studies. In addition to the search for single markers of the aging process, also multiple markers have been used to describe biological age [55;56]. This approach focusses on the correlated aging in multiple organs and might already be useful at a younger age [57]. However, the comparison of molecular measures with functional measures in terms of the strength of association with age and health status had not yet been performed.

A strength of the present study is that participants of the Leiden Longevity Study were uniquely phenotyped for both functional capacity and molecular measures. This allowed us to compare these measures dependent on both age and cardiovascular or metabolic disease (as a measure for health status). While not all participants had all phenotypes measured over the years of study participation, we ensured equally sized datasets by completing all datasets up to 178 participants by random selection. A limitation of this study its cross-sectional nature, which does not allow drawing firm conclusions on predictive properties of the measures on e.g. disease incidence, next to the limited sample size. In addition, only a limited number of molecular measures were tested, and the assessment of the numbers of senescent skin cells was done using only one marker of cellular senescence and in only a small section of sun-protected skin. It is still unclear whether senescence in a section can adequately reflect the whole organ. Another limitation is the use of middle-aged to old participants who were still relatively healthy.

In conclusion, currently used functional capacity measures show stronger associations with age and health status in middle-aged to old persons compared to tested molecular measures. Further studies are required to determine the value of other molecular measures of aging in addition to functional capacity measures, and in older persons or in specific groups of patients.

Acknowledgements

The Leiden Longevity Study was funded by the Innovation Oriented Research Program on Genomics (SenterNovem; IGE01014 and IGE5007), the Centre for Medical Systems Biology, and The Netherlands Genomics Initiative/Netherlands Organization for Scientific Research (05040202 and 050-060-810). The work was further funded by Unilever PLC, European Union-funded Network of Excellence LifeSpan FP6 036894, DFG-PA 361/14-1, DFG-PA 361/11-1, the seventh framework programme MYOAGE (HEALTH-2007-2.4.5-10), and Switchbox (FP7, Health-F2-2010-259772).

Supplementary Table 1. Values for tertiles of functional capacity and molecular measures.

	Tertiles of measures		
	Worst	Average	Best
Functional capacity measures			
Physical tests			
Grip strength (female), kg	<28	28-32	>32
Grip strength,(male), kg	<42	42-50	>50
4-meter walk test, s	>3.90	3.33-3.90	<3.33
Chair stand test, s	>13.4	11.4-13.4	<11.4
Cognitive tests			
Stroop test, trial 3, s	>54	42-54	<42
Digit symbol substitution test, no. correct	<40	40-49	>49
15-picture learning test, delayed recall, no. correct	<11	11-12	>12
Molecular measures			
Inflammation			
CRP, mg/L	>1.80	0.79-1.80	<0.79
Senescence – skin			
Epidermal p16INK4a, no./mm	>1.30	0.30-1.30	<0.30
Dermal p16INK4a, no./mm2	>2.05	0.72-2.05	<0.72
Senescence - immune system			
CD57+/CD8+, %	>32.4	18.5-32.4	<18.5
CD57+/CD4+, %	>1.82	0.64-1.82	<0.64

No.: number. CRP: C-reactive protein. Tertiles are given as worst, average and best test results.

Supplementary Table 2. Association of functional capacity and molecular measures with age.

	Age (years) per tertile of measures								
	worst		average		best				
	mean	SE	mean	SE	mean	SE	Stand. β[a]	P for trend[a]	P for trend[b]
Functional capacity measures									
Physical tests									
Grip strength	66.0	0.77	64.0	0.82	60.0	0.81	-0.372	<0.001	<0.001
4-meter walk test	65.1	0.87	61.2	0.86	62.3	0.87	-0.168	0.022	0.052
Chair stand test	64.2	0.87	64.0	0.86	60.3	0.87	-0.105	0.002	0.006
Cognitive tests									
Stroop test	67.0	0.82	63.6	0.78	59.7	0.78	-0.439	<0.001	<0.001
Digit symbol substitution test	65.7	0.76	64.7	0.84	59.2	0.81	-0.396	<0.001	<0.001
15-picture learning test	64.6	0.9	63.4	0.84	61.8	0.93	-0.163	0.035	0.068
Molecular measures									
Inflammation									
CRP	63.6	0.84	64.3	0.83	60.9	0.84	-0.170	0.022	0.037
Senescence – skin									
Epidermal p16	64.7	0.85	63.4	0.84	62.2	0.85	-0.154	0.040	0.133
Dermal p16	63.5	0.86	63.2	0.85	63.5	0.86	-0.006	0.992	0.822
Senescence - immune system									
%CD57+/CD8+	62.7	1.04	62.0	0.97	60.8	1.02	-0.103	0.225	0.285
%CD57+/CD4+	62.4	1.09	62.1	0.98	61.0	1.05	-0.077	0.375	0.165

N=178 for all measures. SE: standard error. Stand: standardized. Linear regression (estimated means via linear mixed models), age as dependent variable. Model 1: adjustment for sex (and CMV serostatus for immunosenescence). Model 2: as model 1 plus the presence of any disease. Estimated means from model 1 are given. P-value [a] for model 1, p-value [b] for model 2.

Supplementary Table 3. Association of functional capacity and molecular measures with presence of cardiovascular/metabolic disease.

	Percentage of disease per tertile of measures				
	worst	average	best	P-value[a]	P-value[b]
Functional capacity measures					
Physical tests					
Grip strength	45.0	27.8	18.0	0.003	0.057
4-meter walk test	29.4	26.8	36.0	0.466	0.797
Chair stand test	35.2	34.0	22.0	0.155	0.434
Cognitive tests					
Stroop test	43.5	35.2	19.6	0.010	0.203
Digit symbol substitution test	31.0	43.5	23.1	0.405	0.715
15-picture learning test	38.0	33.3	24.5	0.182	0.376
Molecular measures					
Inflammation					
CRP	29.6	32.1	21.2	0.342	0.660
Senescence – skin					
Epidermal p16INK4a	38.2	35.8	19.6	0.038	0.115
Dermal p16INK4a	32.7	33.3	27.3	0.537	0.603
Senescence - immune system					
%CD57+/CD8+	21.3	23.1	18.9	0.791	0.892
%CD57+/CD4+	15.1	26.0	22.4	0.436	0.851

N=178 for all measures. Number and valid percentages are given; P-values are derived from logistic regression, with measures as tertiles. The outcome is the presence of one or more of the following diseases: myocardial infarction, cerebrovascular accident, hypertension or diabetes mellitus. P-value [a] for model 1, p-value [b] for model 2 . Model 1 adjusted for sex (and CMV serostatus for immunosenescence), model 2 additionally for age.

References

(1) Beenakker KG, Ling CH, Meskers CG et al. Patterns of muscle strength loss with age in the general population and patients with a chronic inflammatory state. *Ageing Res Rev* 2010;9:431-436.

(2) Stijntjes M, Meskers CGM, de Craen AJM et al. Effect of calendar age on physical performance: a comparison of standard clinical measures with instrumented measures in middle-aged to older adults. *Gait & Posture*. In press.

(3) Verlinden VJ, van der Geest JN, Hoogendam YY, Hofman A, Breteler MM, Ikram MA. Gait patterns in a community-dwelling population aged 50 years and older. *Gait Posture* 2013;37:500-505.

(4) Guralnik JM, Ferrucci L, Simonsick EM, Salive ME, Wallace RB. Lower-extremity function in persons over the age of 70 years as a predictor of subsequent disability. *N Engl J Med* 1995;332:556-561.

(5) Abellan van KG, Rolland Y, Andrieu S et al. Gait speed at usual pace as a predictor of adverse outcomes in community-dwelling older people an International Academy on Nutrition and Aging (IANA) Task Force. *J Nutr Health Aging* 2009;13:881-889.

(6) Ling CH, Taekema D, de Craen AJ, Gussekloo J, Westendorp RG, Maier AB. Handgrip strength and mortality in the oldest old population: the Leiden 85-plus study. *CMAJ* 2010;182:429-435.

(7) Studenski S, Perera S, Patel K et al. Gait speed and survival in older adults. *JAMA* 2011;305:50-58.

(8) Stijntjes M, de Craen AJ, van HD et al. Familial longevity is marked by better cognitive performance at middle age: the Leiden Longevity Study. *PLoS One* 2013;8:e57962.

(9) Reis JP, Launer LJ, Terry JG et al. Subclinical atherosclerotic calcification and cognitive functioning in middle-aged adults: the CARDIA study. *Atherosclerosis* 2013;231:72-77.

(10) Lee M, Saver JL, Hong KS et al. Cognitive impairment and risk of future stroke: a systematic review and meta-analysis. *CMAJ* 2014;186:E536-E546.

(11) Gussekloo J, Westendorp RG, Remarque EJ, Lagaay AM, Heeren TJ, Knook DL. Impact of mild cognitive impairment on survival in very elderly people: cohort study. *BMJ* 1997;315:1053-1054.

(12) Lopez-Otin C, Blasco MA, Partridge L, Serrano M, Kroemer G. The hallmarks of aging. *Cell* 2013;153:1194-1217.

(13) Pallis AG, Hatse S, Brouwers B et al. Evaluating the physiological reserves of older patients with cancer: the value of potential biomarkers of aging? *J Geriatr Oncol* 2014;5:204-218.

(14) Peters MJ, Joehanes R, Pilling LC et al. The transcriptional landscape of age in human peripheral blood. *Nat Commun* 2015;6:8570.

(15) Horvath S, Pirazzini C, Bacalini MG et al. Decreased epigenetic age of PBMCs from Italian semi-supercentenarians and their offspring. *Aging (Albany NY)* 2015.

(16) Bruunsgaard H. The clinical impact of systemic low-level inflammation in elderly populations. With special reference to cardiovascular disease, dementia and mortality. *Dan Med Bull* 2006;53:285-309.

(17) De MM, Franceschi C, Monti D, Ginaldi L. Inflammation markers predicting frailty and mortality in the elderly. *Exp Mol Pathol* 2006;80:219-227.

(18) Akbaraly TN, Hamer M, Ferrie JE et al. Chronic inflammation as a determinant of future aging phenotypes. *CMAJ* 2013;185:E763-E770.

(19) Bruunsgaard H, Ladelund S, Pedersen AN, Schroll M, Jorgensen T, Pedersen BK. Predicting death from tumour necrosis factor-alpha and interleukin-6 in 80-year-old people. *Clin Exp Immunol* 2003;132:24-31.

(20) Bhat R, Crowe EP, Bitto A et al. Astrocyte senescence as a component of Alzheimer's disease. *PLoS One* 2012;7:e45069.

(21) Liu Y, Sanoff HK, Cho H et al. Expression of p16(INK4a) in peripheral blood T-cells is a biomarker of human aging. *Aging Cell* 2009;8:439-448.

(22) Melk A, Schmidt BM, Takeuchi O, Sawitzki B, Rayner DC, Halloran PF. Expression of p16INK4a and other cell cycle regulator and senescence associated genes in aging human kidney. *Kidney Int* 2004;65:510-520.

(23) Ressler S, Bartkova J, Niederegger H et al. p16INK4A is a robust in vivo biomarker of cellular aging in human skin. *Aging Cell* 2006;5:379-389.

(24) Wikby A, Johansson B, Ferguson F, Olsson J. Age-related changes in immune parameters in a very old population of Swedish people: a longitudinal study. *Exp Gerontol* 1994;29:531-541.
(25) Ferguson FG, Wikby A, Maxson P, Olsson J, Johansson B. Immune parameters in a longitudinal study of a very old population of Swedish people: a comparison between survivors and nonsurvivors. *J Gerontol A Biol Sci Med Sci* 1995;50:B378-B382.
(26) Verzola D, Gandolfo MT, Gaetani G et al. Accelerated senescence in the kidneys of patients with type 2 diabetic nephropathy. *Am J Physiol Renal Physiol* 2008;295:F1563-F1573.
(27) Sis B, Tasanarong A, Khoshjou F, Dadras F, Solez K, Halloran PF. Accelerated expression of senescence associated cell cycle inhibitor p16INK4A in kidneys with glomerular disease. *Kidney Int* 2007;71:218-226.
(28) Tsuji T, Aoshiba K, Nagai A. Alveolar cell senescence in patients with pulmonary emphysema. *Am J Respir Crit Care Med* 2006;174:886-893.
(29) Koppelstaetter C, Schratzberger G, Perco P et al. Markers of cellular senescence in zero hour biopsies predict outcome in renal transplantation. *Aging Cell* 2008;7:491-497.
(30) Gingell-Littlejohn M, McGuinness D, McGlynn LM et al. Pre-transplant CDKN2A expression in kidney biopsies predicts renal function and is a future component of donor scoring criteria. *PLoS One* 2013;8:e68133.
(31) Pustavoitau A, Barodka V, Sharpless NE et al. Role of senescence marker p16INK4a measured in peripheral blood T-lymphocytes in predicting length of hospital stay after coronary artery bypass surgery in older adults. *Experimental Gerontology*. In press.
(32) Schoenmaker M, de Craen AJ, de Meijer PH et al. Evidence of genetic enrichment for exceptional survival using a family approach: the Leiden Longevity Study. *Eur J Hum Genet* 2006;14:79-84.
(33) Ling CH, de Craen AJ, Slagboom PE, Westendorp RG, Maier AB. Handgrip strength at midlife and familial longevity : The Leiden Longevity Study. *Age (Dordr)* 2012;34:1261-1268.
(34) Waaijer ME, Parish WE, Strongitharm BH et al. The number of p16INK4a positive cells in human skin reflects biological age. *Aging Cell* 2012;11:722-725.
(35) Derhovanessian E, Maier AB, Beck R et al. Hallmark features of immunosenescence are absent in familial longevity. *J Immunol* 2010;185:4618-4624.
(36) Rozing MP, Mooijaart SP, Beekman M et al. C-reactive protein and glucose regulation in familial longevity. *Age (Dordr)* 2011;33:623-630.
(37) McNerlan SE, Rea IM, Alexander HD, Morris TC. Changes in natural killer cells, the CD57CD8 subset, and related cytokines in healthy aging. *J Clin Immunol* 1998;18:31-38.
(38) Di Benedetto S, Derhovanessian E, Steinhagen-Thiessen E, Goldeck D, Muller L, Pawelec G. Impact of age, sex and CMV-infection on peripheral T cell phenotypes: results from the Berlin BASE-II Study. *Biogerontology* 2015;16:631-643.
(39) Bohannon RW. Hand-grip dynamometry predicts future outcomes in aging adults. *J Geriatr Phys Ther* 2008;31:3-10.
(40) Taekema DG, Gussekloo J, Maier AB, Westendorp RG, de Craen AJ. Handgrip strength as a predictor of functional, psychological and social health. A prospective population-based study among the oldest old. *Age Ageing* 2010;39:331-337.
(41) Guralnik JM, Simonsick EM, Ferrucci L et al. A short physical performance battery assessing lower extremity function: association with self-reported disability and prediction of mortality and nursing home admission. *J Gerontol* 1994;49:M85-M94.
(42) Guralnik JM, Ferrucci L, Pieper CF et al. Lower extremity function and subsequent disability: consistency across studies, predictive models, and value of gait speed alone compared with the short physical performance battery. *J Gerontol A Biol Sci Med Sci* 2000;55:M221-M231.
(43) Vereeck L, Wuyts F, Truijen S, Van de Heyning P. Clinical assessment of balance: normative data, and gender and age effects. *Int J Audiol* 2008;47:67-75.
(44) Callisaya ML, Blizzard L, Schmidt MD, McGinley JL, Srikanth VK. Sex modifies the relationship between age and gait: a population-based study of older adults. *J Gerontol A Biol Sci Med Sci* 2008;63:165-170.
(45) Hardy R, Cooper R, Aihie SA et al. Body mass index, muscle strength and physical performance in older adults from eight cohort studies: the HALCyon programme. *PLoS One* 2013;8:e56483.

(46) Matthews F, Marioni R, Brayne C. Examining the influence of gender, education, social class and birth cohort on MMSE tracking over time: a population-based prospective cohort study. *BMC Geriatr* 2012;12:45.

(47) Rumley A, Emberson JR, Wannamethee SG, Lennon L, Whincup PH, Lowe GD. Effects of older age on fibrin D-dimer, C-reactive protein, and other hemostatic and inflammatory variables in men aged 60-79 years. *J Thromb Haemost* 2006;4:982-987.

(48) Ballou SP, Lozanski FB, Hodder S et al. Quantitative and qualitative alterations of acute-phase proteins in healthy elderly persons. *Age Ageing* 1996;25:224-230.

(49) Waaijer ME, Gunn DA, Adams PD et al. P16INK4a Positive Cells in Human Skin Are Indicative of Local Elastic Fiber Morphology, Facial Wrinkling, and Perceived Age. *J Gerontol A Biol Sci Med Sci* 2015.

(50) Deelen J, Beekman M, Codd V et al. Leukocyte telomere length associates with prospective mortality independent of immune-related parameters and known genetic markers. *Int J Epidemiol* 2014;43:878-886.

(51) Passtoors WM, van den Akker EB, Deelen J et al. IL7R gene expression network associates with human healthy ageing. *Immun Ageing* 2015;12:21.

(52) Deelen J, Beekman M, Uh HW et al. Genome-wide association meta-analysis of human longevity identifies a novel locus conferring survival beyond 90 years of age. *Hum Mol Genet* 2014;23:4420-4432.

(53) Beekman M, Blanche H, Perola M et al. Genome-wide linkage analysis for human longevity: Genetics of Healthy Aging Study. *Aging Cell* 2013;12:184-193.

(54) Martin-Ruiz C, Jagger C, Kingston A et al. Assessment of a large panel of candidate biomarkers of ageing in the Newcastle 85+ study. *Mech Ageing Dev* 2011;132:496-502.

(55) Li Q, Wang S, Milot E et al. Homeostatic dysregulation proceeds in parallel in multiple physiological systems. *Aging Cell* 2015.

(56) Arbeev KG, Ukraintseva SV, Akushevich I et al. Age trajectories of physiological indices in relation to healthy life course. *Mech Ageing Dev* 2011;132:93-102.

(57) Belsky DW, Caspi A, Houts R et al. Quantification of biological aging in young adults. *Proc Natl Acad Sci U S A* 2015;112:E4104-E4110.

Summary and discussion

Nederlandse samenvatting

List of publications

Dankwoord / Acknowledgements

Curriculum Vitae

Summary and discussion

Description of the findings

This thesis describes to which extent the skin reflects the aging process, with a specific focus on cellular senescence. Since the first descriptions of the growth arrested state of fibroblasts upon multiple replication rounds [1;2], cellular senescence has now emerged as a promising target to regulate the aging process in vivo as well.

Part I of this thesis covers the question **if skin fibroblasts in vitro mirror the aging process.** For this purpose cultured skin fibroblasts from young and old donors were studied, aged on average 22 and 90 years respectively. We further aimed to describe differences based on membership of a long-lived family and health status. Comparisons were made between middle-aged to old offspring from long-lived families (members of a long-lived family) and their age and environmentally matched partners. As a measure for health status those persons with a history of none versus one or more cardiovascular/metabolic diseases (myocardial infarction, cerebrovascular accident, diabetes mellitus or hypertension) were compared.

First we described in **Chapter 1** whether microRNA-663 (miR-663), which has been shown to be differentially expressed in senescent cells in vitro, was differentially expressed in young versus old donors. We found that under non-stressed conditions fibroblasts from young and old donors did not differ in their miR-663 levels. However, when fibroblasts in culture were stressed with rotenone for three days, the fibroblasts from old donors showed higher levels of miR-663. We found no association between miR-663 levels in fibroblast cultures and membership of a long-lived family, or in donors with a different health status.

In **Chapter 2** we extend the comparison of senescent phenotypes of cultured human dermal fibroblasts dependent on age of the donor, membership of a long-lived family and health status to DNA damage markers. DNA damage foci were shown to be markers of senescent cells in culture as well as in situ. Here we compared the numbers of whole-nuclear DNA damage foci measured with 53BP1, DNA damage foci localized at telomeres (or TAF – telomere-associated foci) and micronuclei as measure of unresolved DNA damage and chromosomal instability. The numbers of 53BP1 foci and TAF in cultured fibroblasts, but not the number of micronuclei, were positively associated with the age of the donor. We did not find associations between DNA damage markers and membership of a long-lived family, or in donors with a different health status.

After finding an association between senescence-associated features in cultured cells and the age of the donor, we extrapolated these in vitro findings to markers of cellular senescence in situ. Using skin biopsies of the same donors, we compared several senescence markers as measured in vitro with the presence of the senescence marker p16INK4a in situ.

In **Chapter 3** we show that the same *in vitro* the senescence markers reactive oxygen species, telomere-associated foci, p16INK4a, senescence-associated β-gal, and telomere shortening, are reasonably correlated between duplicate cultures and between cultures in short-term versus long-term experiments. The different markers were correlated amongst each other to a lesser extent. However, when correlating the various senescence markers as obtained from *in vitro* cultures versus dermal p16INK4a positivity *in situ*, there was no correlation.

The findings above mark the next part of this thesis, where we have studied several age related phenotypes within the skin biopsies from participants of the Leiden Longevity Study, **Part II - Does skin tissue mirror the aging process?**

In **Chapter 4** we describe age-dependent epidermal and dermal skin characteristics. We observed reduced epidermal thickness, a flatter epidermal-dermal junction and higher amount of elastic fibres in the reticular dermis in donors of higher ages. We did not observe any significant differences in morphological skin characteristics that were dependent on membership of a long-lived family.

In **Chapter 5** we show that the senescence associated marker p16INK4a is less frequently present in the skin of offspring from long-lived families when compared to the skin of their partners. We also observed a higher number of epidermal p16INK4a positive cells in skin from donors with cardiovascular or metabolic disease, and with a higher number of medications used. This findings indicate that cellular senescence is not only related to age, but may also be a marker of health status.

Chapter 6 describes the association between p16INK4a positive cells in the skin and elastic fibre characteristics, facial wrinkles and perceived facial age. We show that the number of p16INK4a positive cells in both epidermis and dermis are linked to age-associated changes in elastic fibre morphology. Also, the number of p16INK4a positive cells in the epidermis is positively associated with facial wrinkling and perceived age.

Our observations show that markers of cellular senescence in human skin biopsies reflect some aspects of the aging process in middle-aged and old individuals. We aimed to place our findings amidst earlier literature reports and in a clinical context, as described in **Part III-Does skin senescence mirror aging in vivo?**

The overview on markers in **Chapter 7** was written to place our work in human skin in context to that in various other human tissues. We performed a systematic review of the literature on prevalence of senescence markers dependent on chronological age in several human tissues. In general higher numbers of senescent cells are found in all tissues sampled from older donors. The scarcity of reports that find negative associations give rise to the question if also publication bias is at play.

In **Chapter 8** we show the cross-sectional associations between age, the presence of cardiovascular/metabolic disease as a marker of health status with functional capacity measures (physical and cognitive tests), and a series of molecular measures (C-reactive protein (CRP) as inflammation marker, senescence-associated p16INK4a positivity in the skin, and CD57 in T-cells as putative marker for immunosenescence). All functional capacity measures associated with age, as well as CRP and epidermal p16INK4a positivity from the molecular measures but the latter were not as robustly associated. The associations of the functional capacity and molecular measures with cardiovascular or metabolic disease were less apparent when compared to those with age. Overall, in middle-aged to old persons the molecular measures were more weakly associated with age and health status than functional capacity measures.

Based on these findings, we conclude that several skin phenotypes are linked to chronological aging, familial propensity for longevity and/or health status, and thus reflect the aging process in humans. Residual questions remain however; (1) whether cellular senescence is a good marker of the aging process, (2) whether senescence is causally related to aging, and (3) whether senescence opens a therapeutic window to slow the aging process.

Cellular senescence as marker of the aging process

Using markers of cellular senescence to predict clinical phenotypes has been rarely studied so far, but p16INK4a positivity has been shown to successfully predict renal graft function in transplant patients better than age [3;4]. Others have studied whether p16INK4a levels in peripheral blood T-lymphocytes associated with the frailty status of middle-aged to old patients and also with the length of hospital stay after a coronary artery bypass operation, and did not find any clear association [5]. Our findings line up with these reports as we did find links between cellular senescence in skin and age and health status, but these links were not more robust than measures of functional capacity already used in the clinic. It seems too early to use senescence markers for identifying detrimental clinical phenotypes as the predictive value is still limited. New prospective studies are needed to assess the value of senescence markers (in addition to or in combination with other biomarkers) to identify those who age fast and are at a higher risk for adverse health outcomes.

Questions of causality

While causality is not a prerequisite for the use senescence as a marker of the aging process, it is an important issue to address as manifold scholars and entrepreneurs are venturing into therapeutically targeting senescent cells in an attempt to delay the aging process. The associations that we describe in this thesis between higher numbers of senescent cells and age-related disease might be explained by confounders such as smoking. This lifestyle factor was shown to induce senescence in mice [6] but is also a well-known risk factor of many age-related diseases. Another way of explaining the data is by reversed causation: an age-related disease such as type II diabetes is characterized by high glucose levels, which has also been shown to drive senescence in cultured cells [7]. Thus, the higher numbers of senescent cells in biopsies from diabetic patients might be result rather than a contributing cause of diabetes as an age associated disease. Lastly, we found indications of publication bias in our systematic review. Publication bias, with an overrepresentation of small, positive studies, could lead to overestimating the association between senescent markers and aging. The actual contribution of cellular senescence to the aging process in humans would then be smaller than it appears to be.

Therapeutic potential

In contrast, there is important emerging evidence from experimental work in mice showing that senescent cells contribute to age-related disease, and that selective removal of these senescent cells improves health and life span of the animals. Prevention or attenuation of the detrimental effects of senescent cells (without losing the tumour-suppressive features) could therefore be a novel therapeutic target for various age-related diseases. For example, induction of p16INK4a resulted in several aging phenotypes in transgenic mice with conditional expression of p16INK4a, which were largely reversible upon de-induction [8]. In transgenic progeroid mice clearance of naturally occurring p16INK4a positive cells delayed age-related pathology, and increased the health span of these animals [9]. This study was recently extended to normally aged mice rather than progeroid mice. It was shown that removing accumulated senescent cells positively affected health and lifespan and removal attenuated age-related histological changes in several organs [10]. Positive effects of senescent cell removal are also seen in adipose tissue of mice, where upon removal fat mass and expression of mRNA's related to insulin sensitivity was preserved [11]. An approach that uses orally administered drugs that target senescent cells and evoke apoptosis ('senolytics') rather than using transgenic mice also showed promising results. In normally aged mice these drugs (dasatinib and quercetin) improved cardiac and vascular function, as well as improving the healthspan of progeroid mice [12]. The positive effects of this senolytic therapy on vasomotor were later confirmed in normally aged and in hypercholesterolemic mice [13]. Another variant of senolytic drugs, JAK inhibitors, prevented age-related fat loss in naturally aged mice, as well as preserving insulin sensitivity [11]. These studies show promising potential future applications of cellular senescence in the clinic, as also described in some reviews [14;15]. However some tissues seem to be less prone to the effects of removal of senescent cells than others. In addition, while attenuation of age-related disease is found histologically, more clinically relevant, functional measures such as grip strength, balance and memory were not affected [10]. These questions will undoubtedly be studied further in the coming years, and help clarify therapeutic benefits from senescent cell removal.

Of course, while promising, the beneficial results of removing senescent cells on healthspan extension in mice are not guaranteed to extrapolate to humans. Firstly, senescence mechanisms might differ between mouse and man; e.g. mouse and human fibroblasts differ in telomerase expression [16]. Secondly, discrepancies between different animals have emerged for other methods for lifespan extension. For example the benefits of caloric restriction seem to differ across and even within animals species and are thus still highly debated [17-19]. In regard to cellular senescence in vivo we are still on the verge of studying these interspecies differences. However, senescent cells do accumulate in humans with age [20-23], and are linked to age-related pathology [20;24-26], so the target is present in humans. Future studies will have to determine whether targeting senescent cells in humans can actually slow down the aging process and ameliorate the burden of age-related diseases.

References

(1) Hayflick L, Moorhead PS. The serial cultivation of human diploid cell strains. *Exp Cell Res* 1961;25:585-621.

(2) Hayflick L. The limited in vitro lifetime of human diploid cell strains. *Exp Cell Res* 1965;37:614-636.

(3) Koppelstaetter C, Schratzberger G, Perco P et al. Markers of cellular senescence in zero hour biopsies predict outcome in renal transplantation. *Aging Cell* 2008;7:491-497.

(4) Gingell-Littlejohn M, McGuinness D, McGlynn LM et al. Pre-transplant CDKN2A expression in kidney biopsies predicts renal function and is a future component of donor scoring criteria. *PLoS One* 2013;8:e68133.

(5) Pustavoitau A, Barodka V, Sharpless NE et al. Role of senescence marker p16INK4a measured in peripheral blood T-lymphocytes in predicting length of hospital stay after coronary artery bypass surgery in older adults. *Experimental Gerontology*. In press.

(6) Sorrentino JA, Krishnamurthy J, Tilley S, Alb JG, Jr., Burd CE, Sharpless NE. p16INK4a reporter mice reveal age-promoting effects of environmental toxicants. *J Clin Invest* 2014;124:169-173.

(7) Dekker P, Maier AB, van HD et al. Stress-induced responses of human skin fibroblasts in vitro reflect human longevity. *Aging Cell* 2009;8:595-603.

(8) Boquoi A, Arora S, Chen T, Litwin S, Koh J, Enders GH. Reversible cell cycle inhibition and premature aging features imposed by conditional expression of p16Ink4a. *Aging Cell* 2015;14:139-147.

(9) Baker DJ, Wijshake T, Tchkonia T et al. Clearance of p16Ink4a-positive senescent cells delays ageing-associated disorders. *Nature* 2011;479:232-236.

(10) Baker DJ, Childs BG, Durik M et al. Naturally occurring p16-positive cells shorten healthy lifespan. *Nature* 2016.

(11) Xu M, Palmer AK, Ding H et al. Targeting senescent cells enhances adipogenesis and metabolic function in old age. *Elife* 2015;4.

(12) Zhu Y, Tchkonia T, Pirtskhalava T et al. The Achilles' heel of senescent cells: from transcriptome to senolytic drugs. *Aging Cell* 2015;14:644-658.

(13) Roos CM, Zhang B, Palmer AK et al. Chronic senolytic treatment alleviates established vasomotor dysfunction in aged or atherosclerotic mice. *Aging Cell* 2016.

(14) Tchkonia T, Zhu Y, van DJ, Campisi J, Kirkland JL. Cellular senescence and the senescent secretory phenotype: therapeutic opportunities. *J Clin Invest* 2013;123:966-972.

(15) Kirkland JL, Tchkonia T. Clinical strategies and animal models for developing senolytic agents. *Exp Gerontol* 2015;68:19-25.

(16) Itahana K, Campisi J, Dimri GP. Mechanisms of cellular senescence in human and mouse cells. *Biogerontology* 2004;5:1-10.

(17) Demetrius L. Aging in mouse and human systems: a comparative study. *Ann N Y Acad Sci* 2006;1067:66-82.

(18) Demetrius L. Of mice and men. When it comes to studying ageing and the means to slow it down, mice are not just small humans. *EMBO Rep* 2005;6 Spec No:S39-S44.

(19) Sohal RS, Forster MJ. Caloric restriction and the aging process: a critique. *Free Radic Biol Med* 2014;73:366-382.

(20) Bhat R, Crowe EP, Bitto A et al. Astrocyte senescence as a component of Alzheimer's disease. *PLoS One* 2012;7:e45069.

(21) Liu Y, Sanoff HK, Cho H et al. Expression of p16(INK4a) in peripheral blood T-cells is a biomarker of human aging. *Aging Cell* 2009;8:439-448.

(22) Melk A, Schmidt BM, Takeuchi O, Sawitzki B, Rayner DC, Halloran PF. Expression of p16INK4a and other cell cycle regulator and senescence associated genes in aging human kidney. *Kidney Int* 2004;65:510-520.

(23) Ressler S, Bartkova J, Niederegger H et al. p16INK4A is a robust in vivo biomarker of cellular aging in human skin. *Aging Cell* 2006;5:379-389.

(24) Tsuji T, Aoshiba K, Nagai A. Alveolar cell senescence in patients with pulmonary emphysema. *Am J Respir Crit Care Med* 2006;174:886-893.

(25) Sis B, Tasanarong A, Khoshjou F, Dadras F, Solez K, Halloran PF. Accelerated expression of senescence associated cell cycle inhibitor p16INK4A in kidneys with glomerular disease. *Kidney Int* 2007;71:218-226.

(26) Verzola D, Gandolfo MT, Gaetani G et al. Accelerated senescence in the kidneys of patients with type 2 diabetic nephropathy. *Am J Physiol Renal Physiol* 2008;295:F1563-F1573.

Nederlandse samenvatting

Overzicht van de bevindingen

In dit proefschrift wordt beschreven in welke mate de huid het verouderingsproces weerspiegelt, waarbij de nadruk ligt op cellulaire 'senescence'. Hieronder wordt een situatie waarin cellen zich niet meer delen na een aantal vermeerderingen verstaan. Sinds de eerste beschrijving van dit fenomeen, [1,2], blijkt cellulaire 'senescence' inmiddels een veelbelovend aangrijpingspunt waarmee het verouderingsproces gereguleerd kan worden.

Deel I van dit proefschrift behandelt de vraag of **fibroblasten uit de huid het verouderingsproces kunnen weerspiegelen**. Hiertoe zijn gekweekte fibroblasten uit de huid van jonge (gemiddeld 22 jaar) en oudere donoren (gemiddeld 90 jaar) bestudeerd. Tevens bestudeerden we of er verschillen waren in deze fibroblasten berustend op familiaire langlevendheid of gezondheidsstatus. Er werden daarom vergelijkingen gemaakt tussen middelbare tot oudere nakomelingen van langlevende families en hun levenspartners, die een vergelijkbare leeftijd hebben en in een vergelijkbare leefomgeving verkeren. Als maatstaf voor de gezondheidsstatus werd gekeken naar de mensen zonder en die met een ziektegeschiedenis van één of meer cardiovasculaire en/of metabole ziekten (myocardinfarct, herseninfarct, diabetes mellitus of hypertensie).

In **Hoofdstuk 1** beschrijven we het verschil in de expressie van microRNA-663 (miR-663) in fibroblasten tussen jonge en oudere donoren, aangezien eerder aangetoond is dat de expressie van miR-663 hoger is in gekweekte 'senescent' cellen. We hebben aangetoond dat onder normale, niet-gestresste condities er geen verschil is in miR-663 expressie tussen jonge en oudere donoren. Echter, onder gestresste condities (na een behandeling van drie dagen met de stof rotenon) is de miR-663 expressie hoger in de fibroblasten van oudere donoren dan in die van de jongere donoren. Er werd geen associatie gevonden tussen miR-663 en familiaire langlevendheid of gezondheidsstatus.

In **Hoofdstuk 2** vervolgen we deze vergelijkingen tussen leeftijdsgroepen, nakomelingen van langlevende families en hun partners, en mensen met een verschillende gezondheidsstatus, waarbij we ditmaal markers van DNA-schade in de gekweekte fibroblasten bestuderen. Deze markers van DNA-schade zijn zowel in gekweekte cellen ('in vitro') als in cellen in weefselbiopten ('in situ') een marker voor cellulaire 'senescence'. Hiertoe werden de aantallen van DNA-schade foci (gemeten met het eiwit 53BP1) in de hele celkern, DNA-schade foci op telomeren (ook wel 'TAF' genoemd) en micronuclei gemeten. Er werd een positieve associatie waargenomen tussen de aantallen DNA-schade foci in de hele celkern en TAF met de leeftijd van de donor, maar dit werd niet waargenomen voor micronuclei. Er werden geen associaties gevonden tussen een van deze DNA-schade markers en familiaire langlevendheid of gezondheidsstatus.

Gezien deze bevindingen over de samenhang tussen 'senescente' kenmerken in gekweekte fibroblasten ('in vitro') en de leeftijd van de donoren hebben we deze 'in vitro senescence' kenmerken hierna tevens gerelateerd aan een 'senescence' marker in huidbiopten ('in situ').
In **Hoofdstuk 3** bestuderen we de onderlinge correlaties tussen meerdere markers van cellulaire 'senescence' in vitro: zuurstofradicalen ('ROS'), DNA-schade foci op telomeren ('TAF'), p16INK4a (een celcyclusremmer), 'senescence associated-β-galactosidase' ('SAβ-gal') en telomeerverkorting. Dezelfde markers zijn redelijk gecorreleerd in herhaalde experimenten, en ook tussen de korte versus lange stresscondities. De verschillende markers zijn onderling in mindere mate gecorreleerd. Wanneer de in vitro markers binnen de individuele donors worden vergeleken met het aantal p16INK4a positieve fibroblasten in situ, blijken er geen correlaties te zijn.

Deze bevindingen leiden tot het volgende deel van dit proefschrift, waarin we een aantal verouderingsgerelateerde huidkenmerken bestuderen in de biopten van deelnemers uit de Leiden Langleven Studie: **Deel II – Kan huidweefsel het verouderingsproces weerspiegelen?**
In **Hoofdstuk 4** beschrijven we verouderingsgerelateerde kenmerken in de epidermis en dermis. Bij onze deelnemers zagen wij bij hogere leeftijden een dunnere epidermis, een verminderde welving van de scheiding tussen epidermis en dermis, en meer elastische vezels. Deze huidkenmerken verschilden niet tussen nakomelingen van langlevende families en hun partners.
In **Hoofdstuk 5** tonen we aan dat bij nakomelingen van langlevenden de cellen in de huid minder frequent positief aankleuren voor de 'senescence' marker p16INK4a dan bij hun partners. Tevens zagen we dat de mensen met meer cardiovasculaire en metabole ziekten, en de mensen die meer medicatie gebruiken, ook een hoog aantal p16INK4a positieve epidermale cellen hebben. De bevindingen wijzen erop dat cellulaire 'senescence' niet alleen gerelateerd is aan een hogere kalenderleeftijd, maar ook een marker kan zijn voor een slechtere gezondheid.
Hoofdstuk 6 beschrijft de associaties tussen p16INK4a positieve cellen in de huid en elastische vezelkenmerken, gezichtsrimpels en de geschatte leeftijd (iemands leeftijd geschat door externe beoordelaars). Het aantal p16INK4a positieve cellen in de epidermis en dermis is geassocieerd met verouderingsgerelateerde kenmerken van elastische vezels. Tevens is een hoger aantal p16INK4a positieve epidermale cellen geassocieerd met gezichtsrimpels en de geschatte leeftijd.
Deze observaties tonen aan dat cellulaire ´senescence´ in menselijke huidbiopten enkele aspecten van het verouderingsproces kan weerspiegelen. In **Deel III- Kan 'senescence' in de huid het verouderingsproces van de mens weerspiegelen?** trachten we deze bevindingen te positioneren binnen de bestaande literatuur en in een klinische context.
In **Hoofdstuk 7** wordt een overzicht gegeven van verschillende 'senescence' markers in diverse menselijke weefselsoorten. In een systematische review worden studies samengevat die een

verband tussen 'senescence' markers en leeftijd beschrijven. Over het algemeen worden er meer 'senescent' cellen gevonden in weefsel van oudere donoren. De zeldzaamheid van studies die negatieve associaties rapporteren doet de vraag rijzen of er sprake is van publicatie bias.
In **Hoofdstuk 8** tonen we de cross-sectionele associaties van leeftijd en gezondheidsstatus met zowel testen van functionaliteit (fysieke en cognitieve functionaliteit) als met enkele moleculaire markers (C-reactief proteïne (CRP) als maat voor ontsteking, p16INK4a in de huid als 'senescence' marker en CD57 in T-cellen als vermeende 'immunosenescence' marker). De testen voor functionele capaciteit zijn geassocieerd met leeftijd, evenals met CRP en p16INK4a, hoewel deze laatste minder robuust geassocieerd zijn. De associaties tussen gezondheidsstatus en functionele capaciteit en moleculaire markers zijn minder evident in vergelijking tot die met leeftijd. Globaal gezien kunnen we concluderen dat bij middelbare tot oudere mensen de hier geteste moleculaire markers zwakker geassocieerd zijn met leeftijd en gezondheidsstatus dan de testen van functionele capaciteit.
Gebaseerd op bovenstaande bevindingen kunnen we concluderen dat meerdere huidkenmerken gerelateerd zijn aan kalenderleeftijd, familiaire langlevendheid en/of gezondheidsstatus, en dus het verouderingsproces in mensen kunnen weerspiegelen. Echter, een aantal vragen resteert, te weten: (1) is cellulaire 'senescence' een goede marker voor het verouderingsproces, (2) leidt cellulaire 'senescence' tot veroudering (oftewel: is er sprake van causaliteit) en (3) biedt 'senescence' therapeutische mogelijkheden om het verouderingsproces te vertragen?

Cellulaire 'senescence' als marker voor het verouderingsproces

Het gebruik van cellulaire 'senescence' markers om klinische uitkomsten te voorspellen is nog zelden bestudeerd. P16INK4a blijkt echter het functioneren van een niertransplantaat beter te kunnen voorspellen dan alleen leeftijd van de donor [3,4]. In een andere studie is onderzocht of p16INK4a in bloedcellen geassocieerd is met kwetsbaarheid en tevens met opnameduur na een coronaire bypassoperatie bij middelbare tot oudere patiënten. Deze associatie kon niet worden aangetoond [5]. Onze bevindingen zijn hiermee in overeenstemming, aangezien wij wel associaties vonden tussen cellulaire 'senescence' in de huid en leeftijd en gezondheidsstatus, maar deze associaties niet zo robuust waren als de testen van functionele capaciteit die reeds gebruikt worden in de praktijk. Nieuwe prospectieve onderzoeken zijn nodig om de waarde van 'senescence' markers (in toevoeging op, of in combinatie met andere biomarkers) te kunnen bepalen bij het identificeren van diegenen die snel verouderen en een hoger risico hebben op nadelige uitkomsten van ziekte.

Causaliteit

Causaliteit is geen vereiste om cellulaire 'senescence' te gebruiken als marker voor het verouderingsproces, maar het is een belangrijke vraag om te beantwoorden nu wetenschappers en ondernemers zich begeven in het gebied van therapeutische opties om 'senescent' cellen te verwijderen om zo het verouderingsproces te vertragen. De associaties tussen 'senescent' cellen en ouderdomsgerelateerde ziekten, die in dit proefschrift worden beschreven, kunnen mogelijk verklaard worden verstorende ('confounding') effecten van bijvoorbeeld roken. Deze leefstijlfactor kan 'senescence' induceren in muizen[6] en is tevens een bekende risicofactor voor verscheidene ouderdomsgerelateerde ziekten. De bevindingen zouden ook verklaard kunnen worden door omgekeerde causaliteit: een ouderdomsziekte zoals type II diabetes wordt gekenmerkt door hoge glucosewaarden, hetgeen tevens 'senescence' kan aandrijven in gekweekte cellen [7]. De hogere aantallen 'senescent' cellen in nierbiopten van patiënten met diabetes zouden dus het resultaat en niet een (bijdragende) oorzaak zijn van deze ouderdomsziekte. We hebben verder aanwijzingen gevonden voor publicatiebias in de verrichte systematische review. Publicatiebias, waarbij er een oververtegenwoordiging is van kleine studies met een positieve uitkomst, zou kunnen leiden tot een overschatting van de associatie tussen 'senescence' markers en veroudering. De feitelijke bijdrage van cellulaire 'senescence' aan het verouderingsproces in mensen zou dan kleiner zijn dan deze lijkt op basis van de huidige gegevens.

Cellulaire 'senescence' – therapie

Hier tegenover staan de recente belangrijke bevindingen uit experimentele onderzoeken in muizen. Deze tonen aan dat 'senescent' cellen inderdaad bijdragen aan ouderdomsgerelateerde ziekten en dat het selectief verwijderen van deze cellen de levensduur en de gezondheid van deze dieren kan verbeteren. Het voorkomen of vertragen van de schadelijke gevolgen van 'senescent' cellen (zonder hierbij de tumoronderdrukkende effecten te verliezen) kan daarom een vernieuwende manier zijn om ouderdomsgerelateerde ziekten te behandelen. Zo is eerder aangetoond dat het induceren van p16INK4a in transgene muizen leidt tot velerlei lichamelijke uitingen van veroudering, wat grotendeels reversibel blijkt na de-inductie [8]. In transgene muizen met vormen van progeria (syndromen waarbij sprake is van versnelde veroudering) vertraagt het verwijderen van (natuurlijk voorkomende) p16INK4a positieve cellen het ontstaan van ouderdomsgerelateerde ziekten, en verhoogt hiermee de gezonde levensduur van deze muizen [9]. Dit type onderzoek is recent uitgebreid naar muizen die normaal verouderd zijn, in tegenstelling tot de versneld verouderde progeria muizen. Het verwijderen van in het leven opgestapelde 'senescent' cellen blijkt ook hier de (gezonde) levensduur positief te beïnvloeden, en het verwijderen dempt tevens histologische tekenen van veroudering in meerdere organen [10]. Deze goede effecten van verwijdering van 'senescent' cellen worden ook gezien in vetweefsel van muizen, aangezien na verwijdering de vetmassa en expressie van mRNA's die met insulinegevoeligheid samenhangen behouden bleven [11]. Een andere aanpak is om gebruik te maken van oraal toegediende medicijnen die specifiek 'senescent' cellen aanzetten tot apoptose ('senolytica'), hetgeen ook veelbelovend lijkt. In normaal verouderde muizen verbeteren deze medicijnen (dasatinib en quercetine) de hartfunctie en de functie van de vaten, en verbeteren tevens de gezonde levensduur in muizen met progeria [12]. De gunstige effecten van deze senolytica op vasomotorfunctie zijn daarnaast bevestigd in normaal verouderde muizen en muizen met hypercholesterolemie [13]. Een andere variant van senolytica, JAK remmers, draagt bij aan het voorkomen vetverlies bij veroudering en het behoud van insulinegevoeligheid in normaal verouderde muizen [11]. Deze studies tonen veelbelovende mogelijkheden om cellulaire 'senescence' therapieën toe te passen in de kliniek, zoals tevens in enkele reviewartikelen beschreven is [14;15]. Sommige weefselsoorten lijken echter minder vatbaar te zijn voor de effecten van 'senescent' celverwijdering dan anderen [10]. Tevens worden wel minder histologische tekenen van veroudering gezien, maar andere, waarschijnlijk klinisch relevantere uitkomsten zoals knijpkracht, balans en geheugen waren onveranderd [10]. Deze vragen zullen ongetwijfeld bestudeerd worden de komende jaren en de voordelen van therapeutische verwijdering van 'senescent' cellen verhelderen.

Hoe veelbelovend ook, de gunstige resultaten van het verwijderen van 'senescent' cellen op de gezonde levensduur in muizen zijn uiteraard niet met volledige zekerheid te extrapoleren naar mensen. Ten eerste kunnen mechanismen van 'senescence' verschillen tussen muizen en mensen, zoals bijvoorbeeld de telomerase expressie anders is in muizen dan in mensen [16]. Ten tweede zijn er verschillen tussen diersoorten gebleken in andere methoden voor levensduurverlenging. De voordelen van calorische restrictie lijken bijvoorbeeld te verschillen tussen verschillende diersoorten en zelfs binnen een diersoort, en deze methode blijft dus betwist [17-19]. Wat betreft cellulaire 'senescence' in levende organismen staan we nog aan het begin van het bestuderen van verschillen tussen diersoorten. Echter, 'senescent' cellen accumuleren ook in mensen met de leeftijd [20-23], en zijn geassocieerd met ouderdomsgerelateerde ziekten [20;24-26], dus dit biedt vooralsnog ook een onderzoeksdoel in mensen. Toekomstige onderzoeken zullen moeten uitwijzen of het verwijderen van 'senescent' cellen in mensen daadwerkelijk het verouderingsproces kan vertragen en de last van ouderdomsgerelateerde ziekten kan verlichten.

Referenties

(1) Hayflick L, Moorhead PS. The serial cultivation of human diploid cell strains. *Exp Cell Res* 1961;25:585-621.

(2) Hayflick L. The limited in vitro lifetime of human diploid cell strains. *Exp Cell Res* 1965;37:614-636.

(3) Koppelstaetter C, Schratzberger G, Perco P et al. Markers of cellular senescence in zero hour biopsies predict outcome in renal transplantation. *Aging Cell* 2008;7:491-497.

(4) Gingell-Littlejohn M, McGuinness D, McGlynn LM et al. Pre-transplant CDKN2A expression in kidney biopsies predicts renal function and is a future component of donor scoring criteria. *PLoS One* 2013;8:e68133.

(5) Pustavoitau A, Barodka V, Sharpless NE et al. Role of senescence marker p16INK4a measured in peripheral blood T-lymphocytes in predicting length of hospital stay after coronary artery bypass surgery in older adults. *Experimental Gerontology*. In press.

(6) Sorrentino JA, Krishnamurthy J, Tilley S, Alb JG, Jr., Burd CE, Sharpless NE. p16INK4a reporter mice reveal age-promoting effects of environmental toxicants. *J Clin Invest* 2014;124:169-173.

(7) Dekker P, Maier AB, van HD et al. Stress-induced responses of human skin fibroblasts in vitro reflect human longevity. *Aging Cell* 2009;8:595-603.

(8) Boquoi A, Arora S, Chen T, Litwin S, Koh J, Enders GH. Reversible cell cycle inhibition and premature aging features imposed by conditional expression of p16Ink4a. *Aging Cell* 2015;14:139-147.

(9) Baker DJ, Wijshake T, Tchkonia T et al. Clearance of p16Ink4a-positive senescent cells delays ageing-associated disorders. *Nature* 2011;479:232-236.

(10) Baker DJ, Childs BG, Durik M et al. Naturally occurring p16-positive cells shorten healthy lifespan. *Nature* 2016.

(11) Xu M, Palmer AK, Ding H et al. Targeting senescent cells enhances adipogenesis and metabolic function in old age. *Elife* 2015;4.

(12) Zhu Y, Tchkonia T, Pirtskhalava T et al. The Achilles' heel of senescent cells: from transcriptome to senolytic drugs. *Aging Cell* 2015;14:644-658.

(13) Roos CM, Zhang B, Palmer AK et al. Chronic senolytic treatment alleviates established vasomotor dysfunction in aged or atherosclerotic mice. *Aging Cell* 2016.

(14) Tchkonia T, Zhu Y, van DJ, Campisi J, Kirkland JL. Cellular senescence and the senescent secretory phenotype: therapeutic opportunities. *J Clin Invest* 2013;123:966-972.

(15) Kirkland JL, Tchkonia T. Clinical strategies and animal models for developing senolytic agents. *Exp Gerontol* 2015;68:19-25.

(16) Itahana K, Campisi J, Dimri GP. Mechanisms of cellular senescence in human and mouse cells. *Biogerontology* 2004;5:1-10.

(17) Demetrius L. Aging in mouse and human systems: a comparative study. *Ann N Y Acad Sci* 2006;1067:66-82.

(18) Demetrius L. Of mice and men. When it comes to studying ageing and the means to slow it down, mice are not just small humans. *EMBO Rep* 2005;6 Spec No:S39-S44.

(19) Sohal RS, Forster MJ. Caloric restriction and the aging process: a critique. *Free Radic Biol Med* 2014;73:366-382.

(20) Bhat R, Crowe EP, Bitto A et al. Astrocyte senescence as a component of Alzheimer's disease. *PLoS One* 2012;7:e45069.

(21) Liu Y, Sanoff HK, Cho H et al. Expression of p16(INK4a) in peripheral blood T-cells is a biomarker of human aging. *Aging Cell* 2009;8:439-448.

(22) Melk A, Schmidt BM, Takeuchi O, Sawitzki B, Rayner DC, Halloran PF. Expression of p16INK4a and other cell cycle regulator and senescence associated genes in aging human kidney. *Kidney Int* 2004;65:510-520.

(23) Ressler S, Bartkova J, Niederegger H et al. p16INK4A is a robust in vivo biomarker of cellular aging in human skin. *Aging Cell* 2006;5:379-389.

(24) Tsuji T, Aoshiba K, Nagai A. Alveolar cell senescence in patients with pulmonary emphysema. *Am J Respir Crit Care Med* 2006;174:886-893.

(25) Sis B, Tasanarong A, Khoshjou F, Dadras F, Solez K, Halloran PF. Accelerated expression of senescence associated cell cycle inhibitor p16INK4A in kidneys with glomerular disease. *Kidney Int* 2007;71:218-226.

(26) Verzola D, Gandolfo MT, Gaetani G et al. Accelerated senescence in the kidneys of patients with type 2 diabetic nephropathy. *Am J Physiol Renal Physiol* 2008;295:F1563-F1573.

List of publications

Waaijer MEC, Westendorp RGJ, Goldeck D, Gunn DA, Pawelec G, Stijntjes M, Slagboom PE, Maier AB. *Assessment of health status by molecular measures, ready for clinical use?* Experimental Gerontology, April 2016.

Waaijer MEC, Croco E, Westendorp RGJ, Slagboom PE, Sedivy JM, Lorenzini A, Maier AB. *DNA damage markers in dermal fibroblasts in vitro reflect chronological donor age.* Aging, January 2016.

Waaijer MEC*, Gunn DA*, Adams PD, Pawlikowski JS, Griffiths CEM, van Heemst D, Slagboom PE, Westendorp RGJ, Maier AB. *P16INK4a positive cells in human skin are indicative of local elastic fibre morphology, facial wrinkling and perceived age.* Journal of Gerontology: Biological Sciences, August 2015.

Waaijer MEC*, Wieser M*, Grillari-Voglauer R, van Heemst D, Grillari J, Maier AB. *MicroRNA-663 induction upon oxidative stress in cultured human fibroblasts depends on the chronological age of the donor.* Biogerontology, June 2014.

Waaijer MEC, Gunn DA, Catt SD, van Ginkel M, de Craen AJM, Hudson NM, van Heemst D, Slagboom PE, Westendorp RGJ, Maier AB. *Morphometric skin characteristics dependent on chronological and biological age: the Leiden Longevity Study.* Age (Dordr), December 2012.

Waaijer MEC, Parish WE, Strongitharm BH, van Heemst D, Slagboom PE, de Craen AJM, Sedivy JM, Westendorp RGJ, Gunn DA, Maier AB. *The number of p16INK4a positive cells in human skin reflects biological age.* Aging Cell, August 2012.

Dankwoord / Acknowledgements

Allereerst wil ik de deelnemers van de Leiden Langleven Studie en de Leiden 85-Plus Studie bedanken. Zonder hun bereidwilligheid om deel te nemen aan onderzoek was dit proefschrift nooit tot stand gekomen. Tevens wil ik alle collega's van het Ouderengeneeskunde lab bedanken; ik heb mogen voortbouwen op een onderwerp waar al veel energie en werk in was gestoken.

Een goede begeleiding is essentieel: Rudi, dank voor de enthousiaste introductie met 'the aging process' en de prikkelende discussies sindsdien. Andrea, jouw onvermoeibare drang om het verouderingsonderzoek verder te brengen inspireert, en ik waardeer dat jij ook tijdens mijn coschappen de tijd voor begeleiding nam. Met twee promotoren op afstand is de Leidse basis echter ook belangrijk. Diana, bedankt voor je input op mijn papers en presentaties die ik je altijd kon vragen, het heeft mijn werk veel goeds gebracht. Ik wil postuum Ton de Craen bedanken, voor de vele (eigen)wijze lessen die ik van hem heb mogen leren over diverse facetten van de wetenschap.

I would further like to thank everyone who has collaborated with me on the projects included in this thesis for their valuable input.

During my time at the department I've had the pleasure to work with many colleagues. I have enjoyed learning from all of you, with all our different topics but surprisingly similar issues we faced in our research. Those coffee runs were moments of good discussion and ideas. I can honestly say that I've spent a good deal of my PhD with a smile on my face, and I thank you for that!

Lieve vrienden, zoals jullie weten ben ik enthousiast over mijn werk, maar zit ik ook in mijn vrije tijd niet graag stil. Dankjulliewel voor alle steun tijdens het schrijven van dit proefschrift maar vooral voor alle leuke afleiding daarvan! Ik heb genoten van alle gezellige, artistieke en sportieve momenten samen.

Ik wil ook mijn familie bedanken, en in het bijzonder oma, die mij inspireert om oud te worden met een glimlach voor alle mensen om mij heen. Cath, jij staat vandaag naast mij zoals je praktisch je hele leven hebt gedaan. Een grote zus met wie ik kon optrekken in dit wetenschappelijke avontuur, en hopelijk volgend jaar in ons IJslandse avontuur. Lieve pap en mam, jullie steun is een vast gegeven voor mij, maar die vanzelfsprekendheid is eigenlijk heel bijzonder. Jullie hebben me geïnspireerd om mezelf uit te dagen en tegelijkertijd van het leven te genieten. Laten we dan ook samen deze feestelijke mijlpaal vieren!

Curriculum Vitae

Mariëtte Waaijer werd op 18 november 1988 geboren te Delft. Haar middelbare schooltijd aan het Erasmiaans Gymnasium te Rotterdam rondde zij in 2007 af met het cum laude behalen van haar diploma. Aansluitend heeft zij Geneeskunde gestudeerd aan de Universiteit Leiden/ het Leids Universitair Medisch Centrum (LUMC), waar zij tijdens een keuzevak geïnteresseerd raakte in het verouderingsproces. Na selectie voor het MD-PhD traject voor excellente studenten heeft zij zich dan ook verder verdiept in verouderingsonderzoek. Binnen de afdeling Ouderengeneeskunde van het LUMC is zij in 2010 naast haar studie begonnen met promotieonderzoek onder begeleiding van prof. dr. R.G.J. Westendorp en prof. dr. A.B. Maier. Haar wetenschapsstage verrichtte zij in het lab van dr. Grillari aan de Universität für Bodenkultur te Wenen, Oostenrijk. Na het behalen van het Masterdiploma Geneeskunde (cum laude) heeft zij een MD-PhD beurs verworven, beschikbaar gesteld door het LUMC. Hiermee heeft zij gedurende 2014-2016 haar promotieonderzoek op de afdeling Ouderengeneeskunde van het LUMC voortgezet. Per mei 2015 is zij werkzaam als ANIOS Interne Geneeskunde in het Alrijne Ziekenhuis te Leiderdorp.